



UNIVERSITI SAINS MALAYSIA

# **Laporan Akhir Projek Penyelidikan Jangka Pendek**

## **Development and Characterization of Platinum-Palladium Ceramic Membranes for Fuel Cell Application**

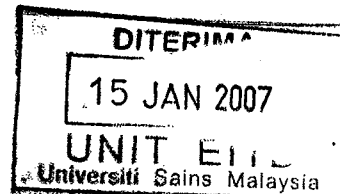
**by**

**Dr. Mohd Roslee Othman  
Prof. Dr. Hj. Abd. Latif Ahmad**

**2007**

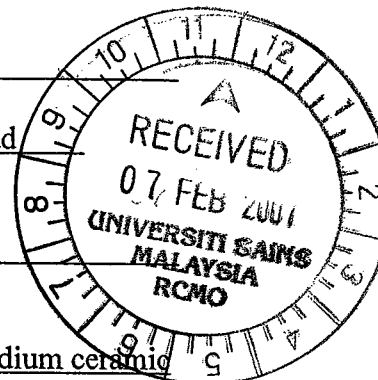
BAHAGIAN PENYELIDIKAN & PEMBANGUNAN CANSELORI

UNIVERSITI SAINS MALAYSIA



Laporan Akhir Projek Penyelidikan Jangka Pendek

- 1) Nama Penyelidik: Dr. Mohd Roslee Othman  
Nama Penyelidik-Penyelidik: Prof. Dr. Hj. Abd. Latif Ahmad  
Lain (Jika berkaitan)
- 2) Pusat Pengajian/Pusat/Unit: Kejuruteraan Kimia
- 3) Tajuk Projek: Development and characterization of platinum-palladium ceramic Membranes for fuel cell application
- 4) (a) **Penemuan Projek/Abstrak**  
*(Perlu disediakan maklumat di antara 100-200 perkataan di dalam Bahasa Malaysia dan Bahasa Inggeris. Ini kemudiannya akan dimuatkan di dalam Laporan Tahunan Bahagian Penyelidikan & Pembangunan sebagai satu cara untuk menyampaikan dapatan projek tuan/puan kepada pihak Universiti)*



**Bahasa Malaysia**

Membran pembaur hidrogen dan alumina terpilih semakin mendapat tempat dalam bidang pemisahan gas kerana hidrogen merupakan sumber industri bagi pembuatan bahan-api dan berbagai jenis bahan kimia. Alumina ialah bahan seramik yang mempunyai struktur kristal padat, ikatan kimia yang kuat dan stabil dari sifat kimia dan suhunya di samping menawarkan pembauran dan kepemilihan yang tinggi terhadap hidrogen. Paladium, platinum dan logam dari kumpulan 3 hingga 5 dalam Jadual Berkala mempunyai keafinitian terhadap hidrogen pada sesuatu tahap. Membran pd/alumina mempunyai kestabilan mekanikal dan keupayaan mendapatkan pembauran hidrogen yang tinggi, kesesuaian bahan kimia yang mengandungi hidrokarbon, dan kepemilihan tak terhingga dalam pemisahan hidrogen. Bahan ini sangat sesuai untuk kegunaan pemisahan hidrogen pada tekanan dan suhu tinggi. Oleh kerana ciri yang unik ini, pembangunan bahan palladium/ $\gamma$ - $Al_2O_3$  membran komposit yang stabil strukturnya diberi perhatian. Dalam kajian ini, paladium/ $\gamma$ - $Al_2O_3$  membran komposit diperolehi daripada proses sol-gel. Cecair paladium ( $PdCl_2$ +air suling) ditambah ke dalam cecair

permulaan semasa penyediaannya. Gel yang diperolehi daripada cecair permulaan yang mengandungi alumina butoxide sekunder dan paladium klorida dikeringkan pada suhu bilik selama 24 jam, dan disinter pada suhu berlainan (500-1100°C). Struktur dan morfologi membran komposit diukur menggunakan XRD, SEM dan penyerapan nitrogen, sementara analisis terma dilakukan menggunakan TG/DTA dan FTIR. Kesan sesetengah pembolehubah seperti kandungan logam, kepekatan PVA dan asid terhadap ciri-ciri struktur sampel yang dikalsin dipelajari. Sampel menunjukkan kestabilan terma dan keluasan permukaan BET yang tinggi apabila kandungan logam dan suhu pengkalsinan ditingkatkan. Logam yang lebih mahal seperti platinum juga digunakan untuk perbandingan.

### Bahasa Inggeris

Hydrogen permeable and selective alumina membranes have attracted much interest in the membrane gas separation field due to the importance of hydrogen as an industrial feedstock for the production of fuels and many chemicals. Alumina is a ceramic material and it has compact crystal structure, strong chemical bonding and is chemically and thermally stable while offering high permeability and selectivity for hydrogen. Palladium and its alloys, platinum and the metals in groups 3 to 5 of the periodic table are all permeable and have affinity for hydrogen to a certain extent. Pd/alumina membrane have the advantage of being mechanically more stable with ability to yield high hydrogen permeability, chemical compatibility with many hydrocarbon containing gas streams, and infinite high selectivity hydrogen separation. This material is very suitable for hydrogen separation application that operates in high pressure and temperature operating conditions. Because of the unique characteristic of this material the development of composite palladium/ $\gamma$ -Al<sub>2</sub>O<sub>3</sub> membrane that is structurally stable has been on focus. In this work, the palladium/ $\gamma$ -Al<sub>2</sub>O<sub>3</sub> composite membrane was prepared by sol-gel process. Palladium solution (PdCl<sub>2</sub> + deionized water) was added to the starting solution during preparation. The dried gel obtained from a starting solution containing alumina secondary butoxide and palladium chloride was dried in ambient temperature for 24 hours, and thermally treated at various temperatures (500-1100°C). The structural and morphological of composite membrane were measured by powder X-ray diffraction (XRD), scanning electron microscopy (SEM) and nitrogen adsorption, while thermal analysis was analyze by thermal gravimetric and differential thermal analyses (TG/DTA) and Fourier transform infrared analysis (FTIR). The influence of several parameters used in the synthesis including metal content, PVA concentration and acid concentration on the structural properties of the calcined samples was studied. The sample resulted high thermal stability and it was found that the BET surface area decreased with an increase in the palladium content and calcining temperature. More expensive metal i.e., platinum was also used in the preparation of pt-alumina membrane for comparison purpose.

**(b) Senarai kata kunci yang digunakan di dalam abstrak:**

Palladium

Platinum

Alumina

Sol-gel

Ceramic membrane

**(c) Ringkasan keputusan**

The texture of both Pd/Al and Pt/Al changed with the thermal treatment (500-1100°C). The surface area decreased as the temperature of treatment increased. The total pore volume also decreased (0.33-0.16 cc/g) with increasing the heating temperature but the pore sizes increased (26.6-98.5 Å) and broadened as the temperature of treatment was raised. The shape of the isotherms and hysteresis loops indicate that for Pd/Al and Pt/Al samples calcined at temperature 500, 700 and 900°C exhibited isotherm Type I and hysteresis loop Type A associated with microporosity and cylindrical pore shapes open at both ends. However, the isotherm progressively changed when thermally treated at 1000°C as the samples exhibited isotherm Type III and Type E hysteresis loop associated with bottle-neck pore structure. Alumina gel containing palladium and platinum exhibited lower degree of cracks compared to pure alumina, since both metals provide better adhesion to each other and support. From TEM analysis, palladium and platinum particles dispersed uniformly in alumina matrix with diameter ranging between 5-15 nm. By increasing the metal loading, however, the metal particles agglomerated to form bigger clusters encapsulated within the alumina network. XRD analysis indicated that the crystalline phase was mainly  $\gamma$ -Al<sub>2</sub>O<sub>3</sub> when the sample was calcined at 500°C.  $\alpha$ -Al<sub>2</sub>O<sub>3</sub> phase began to appear when the temperature was increased to 1100°C. Since the use of palladium in pd-alumina membrane synthesis yielded almost similar characteristics to that of more expensive platinum metal, it is hypothesized that palladium could be used to substitute platinum in order to produce more cost effective and efficient product from this project.

**5) Output dan Faedah Projek**

- (a) Penerbitan (*termasuk laporan/kertas seminar*)  
(*Sila nyatakan jenis, tajuk, pengarang, tahun terbitan dan di mana telah diterbit/dibentangkan*)

Penerbitan di Jurnal Antarabangsa

1. M.R Othman and I.S. Sahadan. On the Characteristics and Hydrogen Adsorption Properties of a Pd/ $\gamma$ -Al<sub>2</sub>O<sub>3</sub> Prepared by Sol-Gel Method. *Journal of Microporous and Materials*. 2006. Vol. 91, 145-150.
2. M.R Othman, N.N.N Mustafa and A.L Ahmad. Effect of thermal treatment on the microstructure of sol-gel derived porous alumina modified platinum. *Journal of Microporous and Materials*. 2006. Vol. 91, 268-275.
3. A.L Ahmad and N.N.N Mustafa. Pore surface fractal analysis of palladium-alumina ceramic membrane using Frenkel-Halsey-Hill (FHH) model. *Journal of Colloid and Interface Science*. 2006. Vol. 301, 575-584
4. A.L Ahmad and N.N.N Mustafa. Sol-gel synthesized of nanocomposite palladium-alumina ceramic membrane for H<sub>2</sub> permeability: Preparation and characterization. 2006 (in press).

Pembentangan/Prosiding Antarabangsa dan Kebangsaan

1. M.R. Othman, N.N.N. Mustafa and A.L. Ahmad. Contemporary Technologies for CO Reduction from Mobile and Stationary Sources. Seminar on Environment. February 2003. Pulau Pinang
2. N.N.N Mustafa, M.R Othman and A.L Ahmad. Development of palladium-alumina membrane using sol-gel technique. The National Postgraduate Colloquium 2004. 8-9<sup>th</sup> December 2004. Pulau Pinang, p. 424-430.

- (b) **Faedah-Faedah Lain Seperti Perkembangan Produk, Prospek Komersialisasi dan Pendaftaran Paten.**  
(Jika ada dan jika perlu, sila gunakan kertas berasingan)

Hasilan daripada projek ini masih lagi dalam peringkat penyelidikan makmal walaupun ada prospek untuk pengkomersialan dan pendaftaran paten. Ini kerana produk yang terbit daripada kajian ini perlu menjalani ujian pembauran (permeation test) untuk mengenalpasti tahap atau kebolehan sebenar produk ini memisahkan gas hydrogen daripada gas-gas lain. Projek ini memerlukan pelantar eksperimen bagi tujuan tersebut. Sumber untuk membangunkan pelantar berkenaan akan diperolehi daripada projek jangka pendek/panjang yang akan dipohon pada waktu terdekat.

- (c) **Latihan Gunatenaga Manusia**

i) *Pelajar Siswazah:*

Kajian ini telah dijalankan oleh seorang pelajar siswazah sebagai rancangan ijazah tinggi.

Nama: Nik Norfauziah Bt. Nik Mustafa (P-JM 0070)

ii) *Pelajar Prasiswazah:*

Kajian ini juga telah dijalankan oleh 2 orang pelajar pra-siswazah

Nama: Chiu Nai Yu  
Intan Sari Binti Sahadan

iii) *Lain-lain: -*

6) **Peralatan Yang Telah Dibeli:**

Sumber kewangan daripada projek ini digunakan untuk membeli bahan pakai habis seperti logam platinum dalam bentuk kompleks, penyokong membran alumina berliang 200nm, dan juga bahan-bahan kimia yang lain. Juga, sumber kewangan dari projek ini digunakan bagi membiayai kos penyampelan seperti XRD, XRF, FTIR, Autosorb, TGA, SEM dan TEM, utility, dan persidangan.

Tiada alatan/aset yang dibeli.

Disediakan oleh:

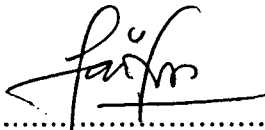


.....  
Dr. Mohd. Roslee Othman

UNTUK KEGUNAAN JAWATANKUASA PENYELIDIKAN UNIVERSITI

Projek telahpun dijalankan dengan jayanya.  
Objektif penyelidikan telah pun  
tercapai semuanya

b/p



.....  
TANDATANGAN PENERUSI  
JAWATANKUASA PENYELIDIKAN  
PUSAT PENGAJIAN

PROFESOR ABDUL LATIF AHMAD, CEng FICHEM  
Dekan  
Pusat Pengajian Kejuruteraan Kimia  
Kampus Kejuruteraan  
Universiti Sains Malaysia, Seri Ampangan  
14300 Nibong Tebal, Seberang Perai Selatan  
Pulau Pinang.



## Sol–gel synthesized of nanocomposite palladium–alumina ceramic membrane for H<sub>2</sub> permeability: Preparation and characterization

A.L. Ahmad\*, N.N.N. Mustafa

*School of Chemical Engineering, Engineering Campus, Universiti Sains Malaysia, Seri Ampangan, 14300 Nibong Tebal, Penang, Malaysia*

Received 27 June 2006; received in revised form 2 August 2006; accepted 2 August 2006

### Abstract

Palladium–alumina membrane with mesopore and narrow pore size distribution was prepared by the sol–gel method. Effect of the finely dispersed metal on the microstructure and the characteristic properties of the palladium–alumina membrane were investigated. Observations were made on membrane weight loss, morphology, pore structure, pore size, surface area, pore surface fractal and membrane's crystal structure. Autosorb analysis, X-ray Diffraction (XRD), Scanning Electron Microscopy (SEM) and Fourier Transform Infrared (FTIR) analysis were employed in the membrane characterization. Autosorb analysis found that, BET surface area decreased and pore size of the membrane increased with the increasing of calcinations temperature (500–1100 °C) and with the increasing of palladium amount in the membrane. FTIR and TG/DTA analysis show that the suitable temperature for calcinations of palladium–alumina membrane is at 700 °C. Palladium metals are highly dispersed at calcinations temperature of 700 °C as observed by TEM analysis. The fine crystallinity of the palladium and  $\gamma$ -alumina phase was obtained after calcined at 700 °C. The SEM morphology shows a smooth and free crack layer of palladium–alumina membrane after repeating the process of dipping, drying and calcinations at temperature of 700 °C. The membrane also successfully coated with a good adhesion on support. The thickness of the final membrane layer was estimated as 9  $\mu$ m.

© 2006 International Association for Hydrogen Energy. Published by Elsevier Ltd. All rights reserved.

**Keywords:** Palladium membrane; Alumina membrane; Sol–gel; Surface morphology; Pore structure

### 1. Introduction

Nanocomposites are usually involved noble or transition metals incorporated in such oxide matrices such as alumina, silica and titania by various process whether as a catalyst or membrane [1–3]. It has been found that among the dispersed metals used as the guest phase, palladium creates the greatest variety of applications ranging from catalysis to electronics. Catalytic activity is attributed to the surface of the fine metal particles [4]. These composites have attracted considerable interests in recent years due to their important industrial applications. They are widely used in industrial practice such as hydrogenation, hydrocracking, oxidation reactions and abatement of motor vehicle emissions but the most used is in hydrogen separation application [5]. Hydrogen is a clean energy

resource and it is an important raw material and product in chemical industries [6].

Membranes can be classified in two main groups, porous and non-porous membranes. The definition of porous membranes is more in agreement with the definitions adopted by the International Union of Pure and Applied Chemistry (IUPAC); the pore size classification given is referred to pore diameter:

- (i) Macropores > 50 nm.
- (ii) Mesopores 2 nm < pore size < 50 nm.
- (iii) Micropores < 2 nm.

Transport occurs through the pores in porous membranes rather than the dense matrix and ideal gas separation membranes possess a high flux and a high selectivity [7].

Palladium, platinum, nickel and the metals in groups 3–5 of the periodic table are all permeable to hydrogen gas. Palladium has long been recognized to possess the characteristics

\* Corresponding author. Tel.: +604 5941012; fax: +604 5941013.

E-mail address: [chlatif@eng.usm.my](mailto:chlatif@eng.usm.my) (A.L. Ahmad).



of a membrane. Palladiums have high hydrogen permeability, chemical compatibility with many hydrocarbon containing gas streams and infinite hydrogen selectivity [8]. Palladium is a steel-white metal which is lustrous, malleable and ductile and it does not tarnish in air. Palladium has no known biological role, and is non-toxic. It also has a unique resistance to surface oxidation [9]. In 1866, Thomas Graham first discovered the metallic palladium absorbs a large amount of hydrogen and it is permeable only to hydrogen [10]. Hydrogen easily diffuses through heated palladium and this provides a way of purifying the gas. Palladium resists corrosion and at room temperature the metal has the unusual property of absorbing up to 900 times its own volume of hydrogen [9]. While, alumina (ceramic material) has compact crystal structure, strong chemical bonding, high hydrogen permeability, have an advantage of thermal, chemical and mechanical stability and low cost [11,12]. This material also plays an important role in the adsorption properties of the catalyst, due to both its relatively large surface area and the presence of active sites on the alumina surface (such as Lewis and/or Brønsted acid sites). These features lead to a good activity and selectivity of the supported catalyst [13].

$\gamma$ - $\text{Al}_2\text{O}_3$  phase was chosen in this work because it has a large specific surface area, well-defined pore size distribution, and stability in a wide temperature range [14]. It is also able to stabilize and disperse the active phase adequately [13]. An increase in the heating temperature generates transformation to the other transitional-phase aluminas such as  $\delta$ -,  $\theta$ - and  $\alpha$ - $\text{Al}_2\text{O}_3$  with changes in the pore structure to accommodate densification [3,15]. It is important to note that these phase transformation accompany a microstructural change, because the first criterion in selectivity of membrane filtration processes is a narrow pore size distribution. Microstructure of the transformed  $\alpha$ - $\text{Al}_2\text{O}_3$  is composed of pores, grains, and pore channels [15]. A novel porous Pd/ $\gamma$ - $\text{Al}_2\text{O}_3$  membrane synthesized by sol-gel method can produce membrane with higher permselectivity to hydrogen due to its surface diffusion or hydrogen spillover on palladium metals and a very high permeability due to its porous properties.

Currently, in hydrogen separation, commonly used membranes are a dense palladium metal membrane which is only selective to hydrogen and a porous ceramic membrane which has high hydrogen permeability. The commercial applications of these two kinds of membranes in catalysis are generally limited either by the extremely low permeability of the dense metal membrane, or by the very poor permselectivity of a porous ceramic membrane [16]. Thus the preparation of inorganic membranes which can exhibit both higher permselectivity and permeability is urgently needed for industrial applications. Palladium-alumina membrane has the advantage of being mechanically more stable with higher permeability than dense metal membranes while maintaining good selectivity to hydrogen. Owing to the excellent hydrogen permeability and selectivity, the membrane are the most promising media for hydrogen purification and separation [6,17].

Sol-gel method has many advantages and it is the most practical method in preparation porous ceramic membrane. The

porous structure also allows for the sol-gel material to be useful as membranes with catalytic properties [16]. Previous work done by Ahmad et al. [18] has successfully separated hydrogen from binary gas mixture using coated alumina-titania membrane by sol-gel technique. Therefore, this shows that a useful catalytic membrane must have small enough pores to achieve separation of gases while maintaining a high dispersion of metal to avoid pore plugging. This method is possible to prepare nanocomposites containing finely dispersed metal particles within ceramic matrices at relatively low temperatures [16,17,19]. The other advantages include the preparation of materials with superior homogeneity and purity, higher BET surface areas, well-defined pore size distribution and a better control over the microstructural properties of the metallic particles [16].

It is necessary to obtain a better understanding of the effect of the metal used on the microstructure of the alumina membrane by sol-gel method. The properties of dispersed palladium metal on the membrane and the structure of the membrane by introducing a palladium metals to alumina sol have to be investigated. Most studied have been reported on the preparation and the characterization of the composite metal/ceramic membrane by other method such as wetness-impregnation method and electroless plating method [6,8,20], though for method of metal introduces to sol by sol-gel method has not received sufficient investigation. Palladium commonly used as a dense metal membrane. However, in this study palladium was doped with ceramic alumina membrane to perform a porous ceramic membrane which is believed can increase the gas permeability in separation process.

In the current manuscript, palladium-alumina nanocomposites membranes prepared by sol-gel synthesis and the effect of finely dispersed palladium particles on the microstructure of alumina ( $\gamma$ - $\text{Al}_2\text{O}_3$ ) membrane were investigated. The objective of the study is to improve the performance of alumina membrane for application in  $\text{H}_2$  separation process by addition of palladium as an additive. The purpose of palladium addition in alumina ceramic membrane is to improve the structure and stability of membrane at elevated temperature. The effect of PVA, aging sol and thermal treatment on the membrane structure was also studied. The discussion includes the characteristic of the sol, membrane surface area and pore characteristic, pore surface fractal, crystal structure of the membrane sample, weight loss and thermal evolution of membrane during heat treatment, functional groups of the membrane before and after calcined and membrane morphology. Membrane characterization is important in order to establish stability and uniformity of the thin membrane layer.

## 2. Experimental

### 2.1. Preparation of unsupported and supported palladium/ $\gamma$ - $\text{Al}_2\text{O}_3$ membranes

The membrane sol containing alumina and palladium precursor solution was prepared by sol-gel synthesis. Aluminum secondary butoxide ( $\text{AlO}_3\text{C}_{12}\text{H}_{27}$ ) was used as alumina

precursor and palladium chloride ( $\text{PdCl}_2$ ) as palladium precursor. In this work, nitric acid ( $\text{HNO}_3$ ) was used as peptizing agent. The alkoxide: water: butanol: nitric acid molar ratio used in this work was 1:100:5.5:0.07. Butanol ( $\text{C}_4\text{H}_9\text{OH}$ ) was added in sol-gel processing as they allow to control the reaction of alkoxide precursors with water, and hence to direct with more flexibility of the structure of sol-gel products [8]. The addition of butanol would enhance the adhesion of coating layer to the support and was used to slow the hydrolysis rates and thus to stabilize the alkoxides to the formation of clear gel [21,22]. If the hydrolysis was faster, it will lead to the precipitation of the sol [21]. Polyvinyl alcohol (PVA) was used as a binder. An appropriate amount of PVA was added to sol in preventing crack formation on the membrane layer during drying process. The metal precursor which was first dissolved in hot deionized water was then added directly to the alumina sol. The metal concentration used in this work was 0.5 and 2 g metal in 100 ml deionized water. The sol was stirred vigorously in a closed container at temperature of  $90^\circ\text{C}$  for 30 min to dissolve the mixture before undergoing reflux process for 24 h at  $90^\circ\text{C}$ . Then the sol was allowed to dry in ambient temperature to form a dried gel through evaporation on Petri dish. A part of the sol was used to dip coat onto the alumina support. After drying, the dried gel without support and coated gel were calcined at  $500\text{--}1100^\circ\text{C}$  to form unsupported and supported composite palladium-alumina membranes.

## 2.2. Characterization of membranes

Nitrogen adsorption analysis using an Autosorb I (Quantachrome, Nova 1200) was used to determine pore characteristic of the membrane. XRD analysis was used to determine the crystallinity and to identify the alumina phase of the membrane after calcinations using Philips PW 1729 X-ray generator, Philips PW 1820 diffractometer (Cu-K $\alpha$  radiation and graphite monochromator) and Philips PW 1710 diffraction controller. The morphology of membrane was examined by Scanning Electron Microscopy (SEM) instrument, Leo Supra 50 VP from Germany. Metal dispersion in alumina matrix was measured by Transmission Electron Microscopy (TEM) using CM12 (Philips) with an accelerator voltage of 80 kV. The images were captured with SIS Image Analysis System version 3.11. The weight loss and thermal evolution of membrane sample during heat treatment was measured by thermogravimetric and differential thermal analysis (TG/DTA) and this was carried out in a Shimadzu TG 50. FTIR analysis was used to identify the functional groups of the membrane and the chemical changes which occurred upon heating the membrane. The analysis was conducted by Perkin-Elmer FTIR 2000, USA.

## 3. Result and discussion

### 3.1. Sol characterization and the membrane formation

#### 3.1.1. Effect of PVA

The use of appropriate sol viscosity is important in order to successfully obtain the desired membrane layer on the support.

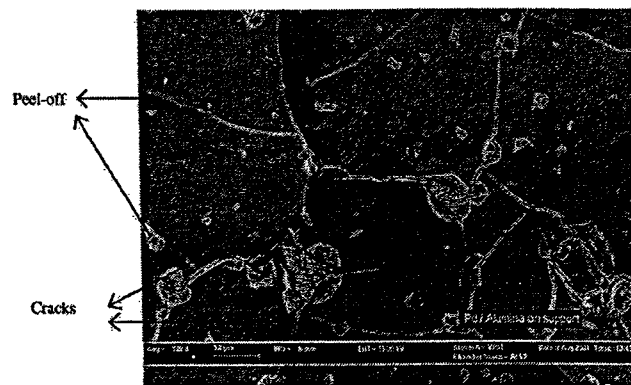


Fig. 1. SEM image of supported palladium-alumina membrane surface after coated with highly viscous sol and calcined at  $700^\circ\text{C}$  (100 $\times$  magnifications).

The use of the binder such as PVA was found to be very important in preparing coating sol. PVA addition into sol is important as it can: (i) changes the sol viscosity; (ii) improve the mechanical strength of the membrane by decreasing the brittleness; (iii) maintains its original shape until calcinations process takes place; (iv) prevent crack formation of the membrane and (v) give a good adhesion of the coated membrane layer on the support [19,21,23].

In this study, the palladium-alumina sol was prepared with palladium concentration of 2 g Pd/100 ml  $\text{H}_2\text{O}$  with a 6:100 volume ratio of palladium to sol. This ratio was chosen based on the preliminary study of the experiment. If the ratio of palladium is higher than 6, the porosity of membrane is less. From the results of experimental work, the optimum PVA concentration in producing a thin membrane layer with smooth and free of cracking is 4 g PVA in 100 ml  $\text{H}_2\text{O}$  with a 4:100 volume ratio of PVA to sol. The similar finding was reported by Ahmad et al [24]. PVA was added to sol during the peptization period. Lambert and Gonzalez [19] found that, PVA was much more effective in preventing crack formation, when it was added prior to the alumina precursor and present during the peptization step. The addition of PVA concentration greater than 4 g PVA/100 ml  $\text{H}_2\text{O}$  increased the sol viscosity and lead to a highly viscous sol. The highly viscous sol would produce a thick and non uniform membrane gel layer which tends to crack during drying process, furthermore adhesion of the thicker film was not good [25]. Higher viscosity enhanced the formation of aggregates, thus leading to easily detachable particles on the surface of the microstructure [26]. Fig. 1 shows the SEM image of palladium-alumina membrane layer surface that coated with highly viscous sol on alumina support after calcined at  $700^\circ\text{C}$ . The sol contains PVA concentration of 8 g PVA/100 ml  $\text{H}_2\text{O}$  with a 4:100 volume ratio of PVA to sol. It was found that, application of viscous sol resulted in high cracking and peeling-off of the membrane layer after calcined as can be seen in the Fig. 1.

Fig. 2(a) and (b) show the light microscope image of unsupported palladium-alumina dried gel membrane layer on Petri dish and supported palladium-alumina dried gel membrane

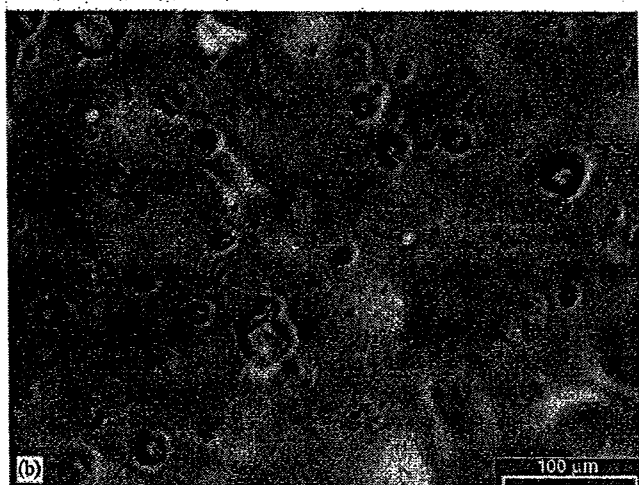
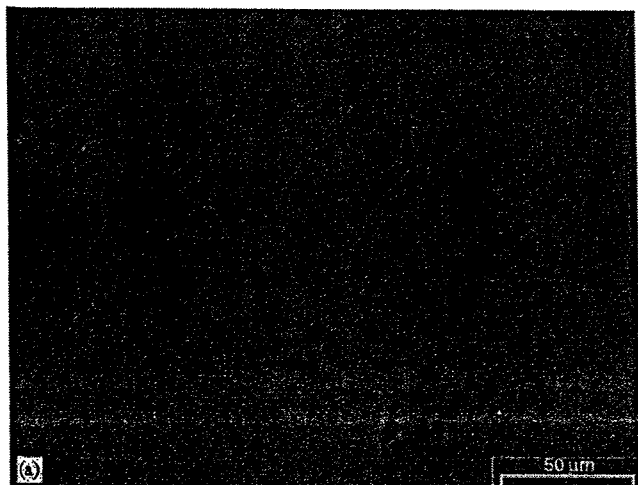


Fig. 2. Light Microscope image of the palladium–alumina dried gel membrane surface: (a) on Petri dish (10 000 × magnification) and (b) on alumina support (10 000 × magnification).

layer on alumina support containing 4 g PVA/100 ml H<sub>2</sub>O with 4:100 volume ratio of PVA to sol after dried at ambient temperature for 48 h. The dried gel layers for both unsupported and supported membrane present a smooth surface and did not show the formation of crack. Yeung et al. [26] discovered that alumina gel containing PVA and metal exhibit less cracks as compared to pure alumina. Palladium metal addition increases viscosity and leads to a slower drying rate of membrane gel [27].

Fig. 3 shows the light microscope image of unsupported palladium–alumina membrane surface containing 4 g PVA/100 ml H<sub>2</sub>O with 4:100 volume ratio of PVA to sol after dried for 48 h and calcined at 700 °C. It can be seen that, the membrane surface showed morphologically homogeneous, smooth and free of cracks even after calcined at 700 °C.

As mentioned earlier, PVA was added to sol as a surface additive to reduce stress on the membrane layer during drying process and in order to enhance the strength of the membrane [19]. However, PVA amount was found to change

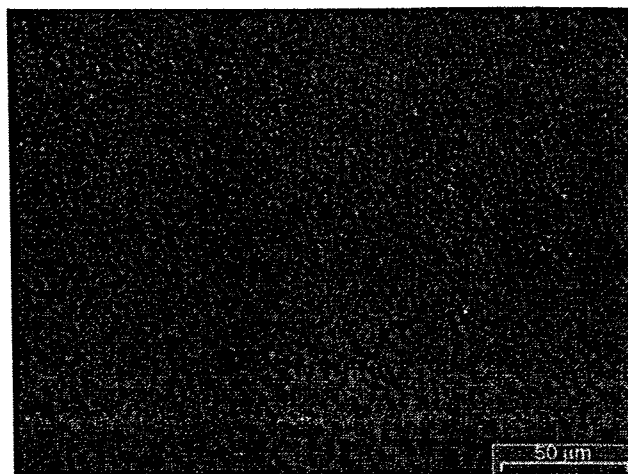


Fig. 3. Light Microscope image of the surface of unsupported palladium–alumina membrane after calcined at 700 °C (20 000 × magnifications).

the membrane morphology which is the addition of higher PVA concentration increased the sol viscosity and lead to a highly viscous sol that produce non uniform membrane layer with highly degree of cracks. Beside can change membrane morphology, it also has strong influence on the membrane characteristic properties such as pore size, pore volume and surface area that were measured by Quantachrome Autosorb analysis [28]. In this study, the effect of different volume ratio of PVA to sol with concentration of 4 g PVA/100 ml H<sub>2</sub>O followed by calcinations temperature of 700 °C on palladium–alumina membrane characteristic properties was studied.

Table 1 shows the effect of PVA amount on BET surface area, pore size and pore volume of palladium–alumina membrane after calcined at 700 °C. The volume ratio of PVA to sol was varied from 2:100 to 8:100. The table shows that the membrane pore size was increased from 7.02 to 9.36 nm, the BET surface area decreased from 201.4 to 135.4 m<sup>2</sup>/g and pore volume decreased from 0.37 to 0.28 cm<sup>3</sup>/g as the volume ratio of PVA in sol increased from 2:100 to 8:100. Similar trend of result was reported by Othman et al. [29].

The increasing amount of PVA increased the pore size of the membrane. Higher PVA amount promotes agglomeration of the ceramic particles, which on calcinations leads to wider pore size [30]. The agglomeration causes inhomogeneous grain growth and void formation. When the PVA concentration in the sol is fairly low, the sol is highly dispersed. Well-dispersed sol tends to produce small pore size and homogeneous product [31].

### 3.1.2. Effect of sol aging

The age of the sol was supposed to have influence on the viscosity of sol. With increasing reaction time, the condensation reaction continued, therefore the viscosity of the sol increase with the aging time. It is known that increasing viscosity of the sol produces thicker layers, thus leading to an enhanced risk of cracks and lower adhesion of the coating [25]. In this study,

Table 1

The effect of different volume ratio of PVA (4 g PVA/100 ml H<sub>2</sub>O) in sol on membrane microstructures properties

Volume ratio of PVA in sol	BET surface area (m <sup>2</sup> /g)	Pore size (nm)	Pore volume (cm <sup>3</sup> /g)
2:100	201.4	7.02	0.3684
4:100	189.5	7.45	0.3109
6:100	142.4	8.31	0.2953
8:100	135.4	9.36	0.2832

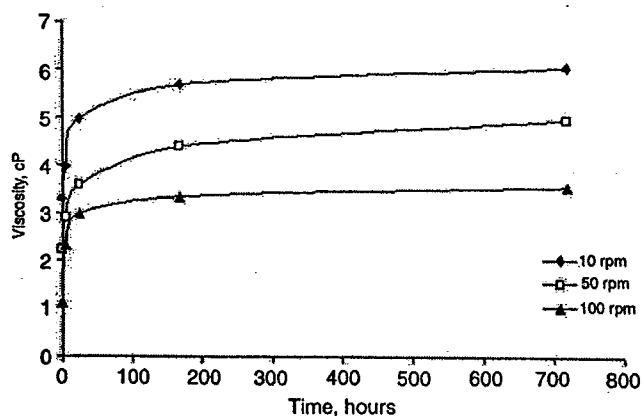


Fig. 4. The effect of aging times on palladium–alumina sol viscosity at different stirring speed.

6:100 volume ratio of palladium to sol with concentration of 2 g Pd/100 ml H<sub>2</sub>O and 4:100 volume ratio of PVA to sol with PVA concentration of 4 g PVA/100 ml H<sub>2</sub>O were used in sol preparation. The viscosity of the sol after 5, 24, 168, 336 and 720 h was studied. The sol was aged in a close beaker at ambient temperature.

Fig. 4 shows the plot of viscosity versus aging time for palladium–alumina sol at different spindle speed. On the shorter aging of up to 24 h, the sol viscosity increased rapidly. The rapid increase in sol viscosity is due to evaporation of water and butanol. For longer aging times to 720 h, the viscosity increased in a linear fashion, which is the viscosity only increase slightly. Viscosity is affected by the chain length and degree of molecular association. As aging proceeds, there is continued formation and condensation growth of aluminum clusters, along with agglomeration of the alumina clusters. The agglomerated will cause high viscosity of the sol. With continued aging process, condensation growth and agglomeration of aluminum clusters will results in the gel formation [21,32].

Effect of aging on membrane characteristics was also investigated. Three membrane samples were studied to determine the effect of aging on membrane characteristic. The samples are the fresh palladium–alumina sol, the sol aging for 720 h and the palladium–alumina dried gel aging for 720 h. For the sol aging sample, the sol was kept for 720 h in a close beaker then dried for 48 h and calcined; while the dried gel membrane sample, the sol was dried for 48 h in ambient temperature then was aged for 720 h before calcined to determine the

changes of the membrane structure. The membrane characteristic of the palladium–alumina membrane was characterized at calcinations temperature of 700 °C.

The effect of aging sol and dried membrane gel on membrane microstructures properties after calcined at 700 °C is shown in Table 2. The table shows that, the BET surface area, pore diameter and pore volume is almost identical for aged palladium–alumina sol and the fresh sol. These results indicate that, the surface area and the pore structure do not change remarkably with the aging time of palladium–alumina membrane sol. This suggests that, sol kept in close container in ambient temperature for 720 h still can be used for coating. However the aging of dried membrane gel for 720 h had affected membrane structure after calcined. BET surface area and pore volume highly decreased from 189.5–132.4 m<sup>2</sup>/g and 0.31–0.28 cm<sup>3</sup>/g, respectively. While, pore diameter increased from 7.45–10.72 nm. When dried membrane gel was kept for a long time without being calcined, little shrinkage occurred. Shrinkage often leads to the build up of stress that caused by capillary force which is relatively to the formation of pore. Further calcinations would increase more pore size of the membrane and this led to the decreasing of membrane surface area [22].

Aging of the dried membrane gel without calcinations is supposed to give an affect to the dried gel membrane and the calcined membrane morphological structure. As stated by Klein [23], gel calcined after long aging would be expected to have a denser and brittle structure. Fig. 5(a) and (b) shows the light microscope image and SEM image of dried palladium–alumina membrane gel before calcinations that were aged for 720 h, respectively. Light microscope only observed the major malformation of the gel membrane surface, while SEM enable to show the existence of small defects on the membrane surface that cannot be observed by light microscope.

Fig. 5(a) shows that, the surface of dried membrane gel exhibits rougher surface with cracks. The SEM image as shown in Fig. 5(b) shows the dried membrane gel surface is not smooth which is flaky in appearance and have a lot of chap. As mention earlier, this happens due to the gel network is under compression stress [22]. A wet gel formed from alkoxy-derived sol normally shrinks to some extent while being aged due to the removal of some of its internal alcohol and water (evaporation process). When the gel is continued to dry and being aged, it shrinks by a rather large amount, and this shrinkage often leads to the build up of a non-uniform stress which fractures the gel. Stress is caused by capillary force which is proportional to the evaporation rate and pore formation [22].

Table 2

The effect of sol aging on palladium–alumina membrane microstructures properties after calcined at 700 °C

Samples	BET surface area (m <sup>2</sup> /g)	Pore diameter (nm)	Pore volume (cm <sup>3</sup> /g)
Fresh palladium–alumina sol dried for 48 h	189.5	7.45	0.3109
Sol aging for 720 h and dried for 48 h	188.9	7.48	0.3100
Dried gel membrane aging for 720 h	132.4	10.72	0.2845

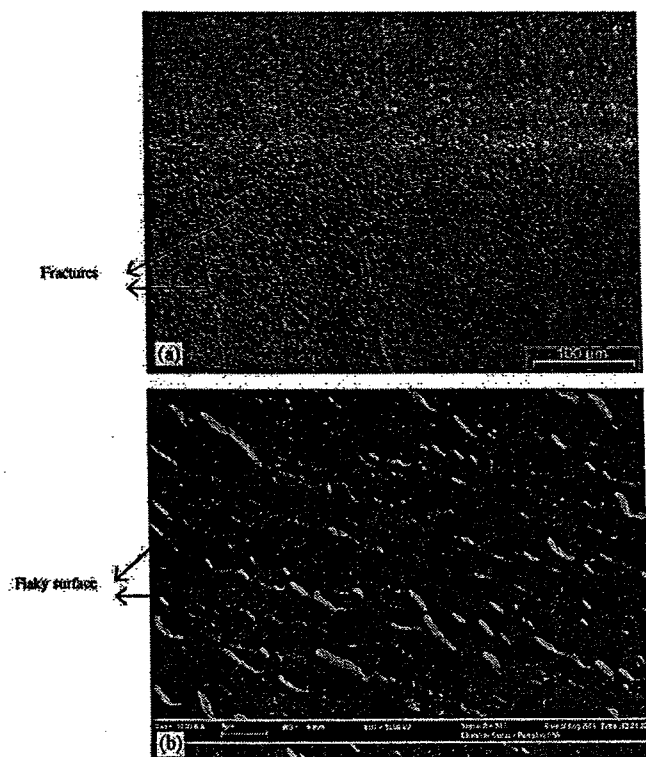


Fig. 5. Images of dried membrane gel surface without calcined and aged for 720 h by: (a) light microscope image (10 000 × magnification) and (b) SEM image (10 000 × magnification).

### 3.2. Characterization of unsupported membrane

#### 3.2.1. Fourier transform infrared (FTIR) analysis

FTIR analysis was used to identify the functional groups of the membrane and the chemical changes which occurred upon heating the membrane gel layer. In FTIR analysis, the membrane was deposited onto a KBr (IR-transparent substrate) and was compressed to form a disc shape before analysis. Fig. 6 shows the infrared (IR) absorption spectra of Pd/alumina gel at four different temperatures treatment. The Pd/alumina gel heated at 130 °C shows the wide and broad absorption peak at 3408 cm<sup>-1</sup>. This peak associated to the stretching vibrations of the O–H bonds adjoining the Al atoms (hydroxyl groups) and the O–H bonds, a functional group of water and butanol that contain in the sample [34]. It also associated with carbonaceous materials such as PVA [34]. The absorption peaks at 3084, 1072 and 614 cm<sup>-1</sup> is typical gelatinous boehmite,

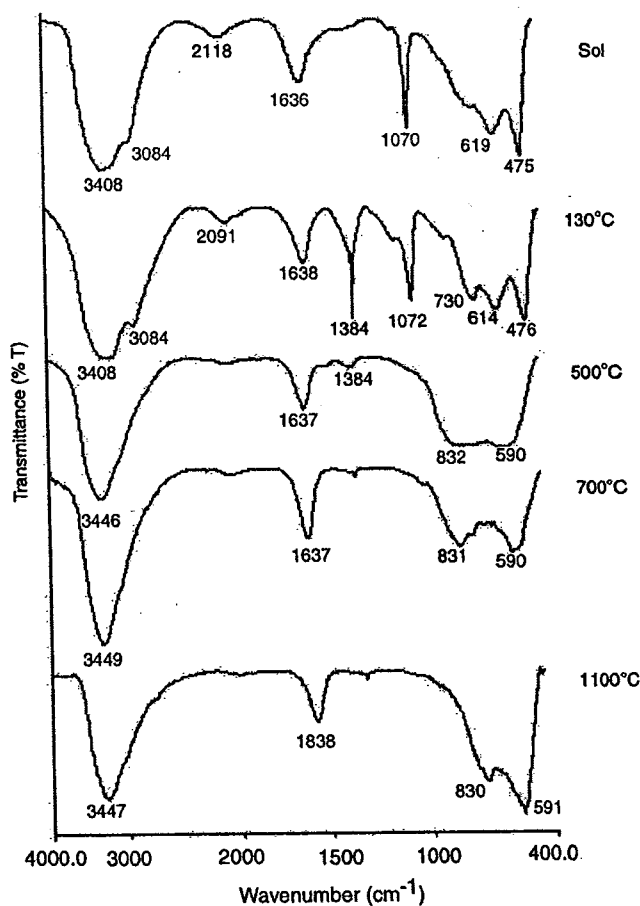


Fig. 6. FTIR spectra of palladium–alumina membrane at different stages of processing temperature.

a poorly crystallized modification of aluminum hydroxide (Al(OH)<sub>3</sub>) boehmite [35]. The absorption peak at 1384 cm<sup>-1</sup> related to nitrate (-NO<sub>2</sub>) group and at 730 cm<sup>-1</sup> was related to C–Cl bond that associated with nitrate and chlorine compound derived from nitric acid and PdCl<sub>2</sub> precursor solution [36]. However, these absorption peaks were no longer visible for samples calcined at 700 and 1100 °C, attributing to the burning reaction of organic compounds and water molecules in heating process.

The absorption peak around 3447–3449 cm<sup>-1</sup> and 1637–1638 cm<sup>-1</sup> that exists for entire sample associated to the functional group of water in crystallization phase (solid state spectra) due to trace amount of water in KBr disc [36]. The absorption peak corresponds to Al–O–Al bond is at

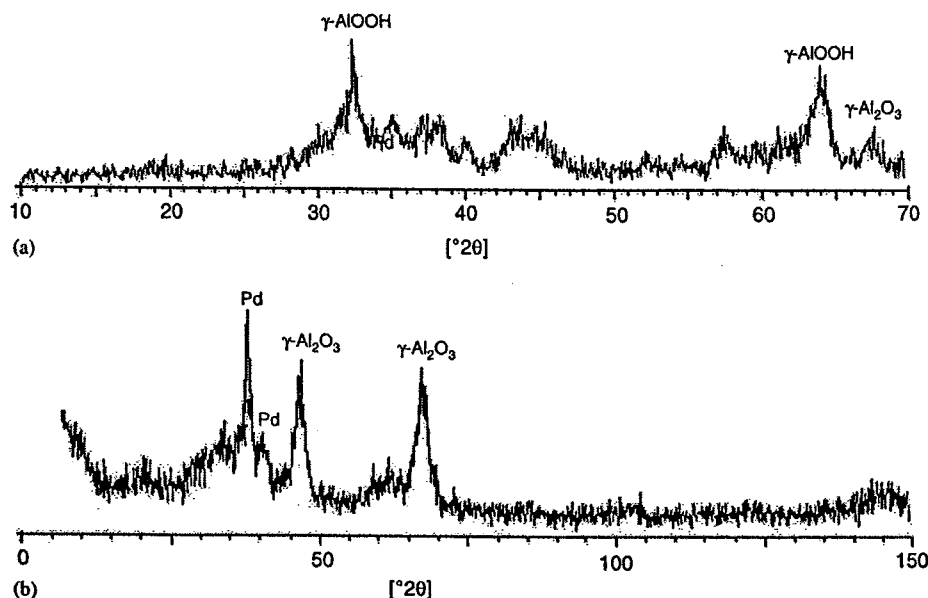


Fig. 7. X-ray diffraction patterns of the palladium–alumina membrane at calcinations temperature of: (a) 400 °C and (b) 700 °C.

around 830–832  $\text{cm}^{-1}$  and the broad absorption peak at 590–591  $\text{cm}^{-1}$  corresponds to the inorganic metal characteristic (Pd and Pt) [36]. The absorption peaks at around 590–591 and 830–832  $\text{cm}^{-1}$  became narrow with increased of heat treatment temperature. The sharper peak indicates strengthening of the bonds. In the same frequency range, the sharp peak suggests an increase in crystallization of alumina and palladium particles [21].

### 3.2.2. X-ray diffraction analysis (XRD)

XRD analysis was carried out to identify the alumina phase and to determine the crystal structure of the membrane. Fig. 7(a) and (b) show the XRD patterns of the membrane at two different calcinations temperature, 400 and 700 °C. At calcinations temperature of 400 °C (Fig. 7(a)), the crystallinity was poor for palladium–alumina membrane and boehmite ( $\gamma\text{-AlOOH}$ ) still exist in membrane sample which is less stable than gamma alumina ( $\gamma\text{-Al}_2\text{O}_3$ ). The observed peaks for  $\gamma\text{-Al}_2\text{O}_3$  and metallic palladium are broad, thereby implying that the crystallite size is small [3]. Fig. 7(b) shows the XRD pattern of palladium–alumina membrane at calcinations temperature of 700 °C. The XRD pattern of membrane shows a fine crystalline of the  $\gamma\text{-Al}_2\text{O}_3$  and metallic Pd whereas the intensity of  $\gamma\text{-Al}_2\text{O}_3$  and metallic Pd increased after calcined at 700 °C. At this calcinations temperature also,  $\gamma\text{-AlOOH}$  was disappeared. At temperature of 400 °C, the phase transformation of  $\gamma\text{-Al}_2\text{O}_3 \cdot 2[\text{AlOOH}] \rightarrow \gamma\text{-Al}_2\text{O}_3 + \text{H}_2\text{O}$  is not completely yet. The poorly crystalline AlOOH convert to  $\gamma\text{-Al}_2\text{O}_3$  at temperature as low as 450 °C. Similar finding was reported by Haas-Santo et al. [25]. The organic group of hydroxyl also not completely decomposes at this temperature. This group was completely removed after heating to 700 °C.

### 3.2.3. Effect of calcinations temperature on membrane structures

The effect of calcinations temperature on palladium–alumina membrane structures were examined and were measured by Quantachrome Autosorb analysis. Characterizations were carried out on unsupported membranes by assuming that their properties are similar to those of supported membrane layers [37,38]. Membrane with metal concentration of 0.5 g Pd/100 ml  $\text{H}_2\text{O}$  and 2 g Pd/100 ml  $\text{H}_2\text{O}$  with a 6:100 volume ratio of palladium to sol was used to study the effect of calcinations temperature on membrane structures, respectively. Characterization of the membranes was carried out at the temperature starting from 500 to 1100 °C. The effect of calcinations temperature on pore size, pore volume and surface area of the membrane is shown in Fig. 8(a)–(c), respectively. As can be seen from the Fig. 8(a), membrane pore size for palladium–alumina membranes increased; whereas pore volume and BET surface area (Fig. 8(b) and (c)) decreased with increased the calcinations temperature from 500 to 1100 °C. Membrane sample containing palladium concentration of 0.5 g Pd/100 ml  $\text{H}_2\text{O}$  resulted an increasing in pore size from 2.70–8.54 nm, pore volume decreased from 0.43–0.18  $\text{cm}^3/\text{g}$  and the surface area decreased from 471.8–102.73  $\text{m}^2/\text{g}$ . While for membrane sample containing palladium concentration of 2 g Pd/100 ml  $\text{H}_2\text{O}$ , the membrane pore size increased from 6.99–15.967 nm, pore volume decreased from 0.39–0.09  $\text{cm}^3/\text{g}$  and the surface area decreased from 249.5–46  $\text{m}^2/\text{g}$ .

As can be seen from the Fig. 8(a)–(c), the pore diameter of the membrane highly increased and pore volume and surface area decreased sharply at calcinations temperature of 1100 °C. At higher temperatures, the formation of larger grains due to the collapse of the pores with shrinkage (densification process) of the material structure resulted in a strong increase in crystallite



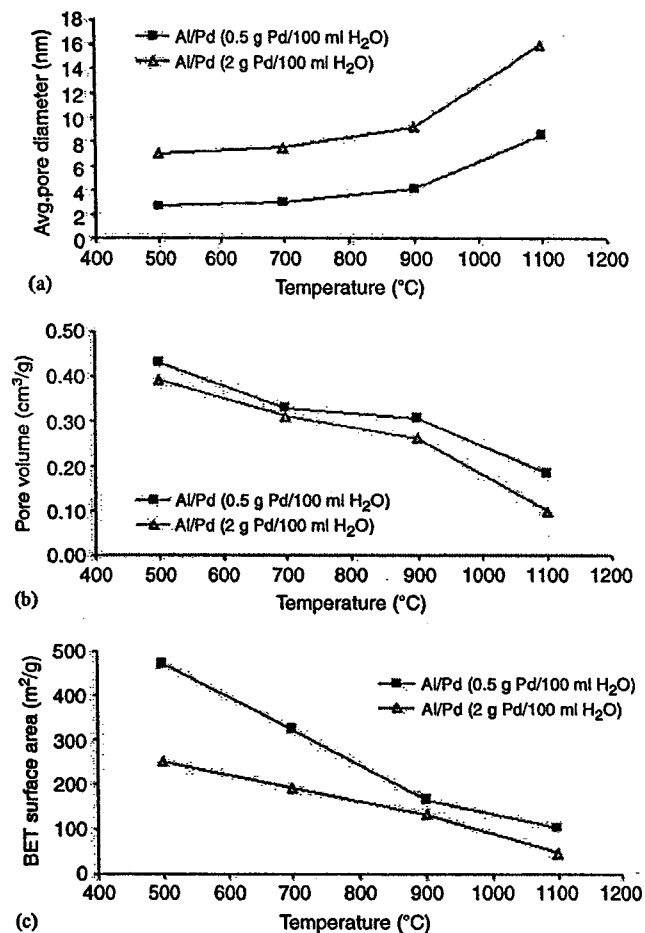


Fig. 8. The effect of calcinations temperatures on the: (a) average pore diameter; (b) pore volume and (c) BET surface area of membrane.

size and decrease of surface area and pore volume [16]. It indicates that, collapse of the pore structure started as conversion to the stable  $\alpha$ -Al<sub>2</sub>O<sub>3</sub> phase took place which is at temperature of 1100 °C. The transformation of  $\alpha$ -Al<sub>2</sub>O<sub>3</sub> occurred at calcinations temperature of higher than 1000 °C [25]. As state by Gestel et al. [39], after  $\alpha$ -Al<sub>2</sub>O<sub>3</sub> transformation grain size grew up which was accompanied by strong surface area reduction.

Good separation selectivity requires a narrow pore size distribution [21]. Pore size distribution gives more information on pore growth of the membrane with the increasing of calcinations temperature. Fig. 9 shows the pore size distribution profile of palladium–alumina membrane contains palladium concentration of 2 g Pd/100 ml H<sub>2</sub>O with 6:100 volume ratio of palladium to sol at different calcinations temperatures (500–1100 °C). As can be seen from the Fig. 9, the pore size distribution profile of membrane samples shows the pore volume was sharply decreased and the average pore diameter gradually increased as calcinations temperature increased from 500 to 900 °C. The pore size distributions profiles of the membrane at calcinations temperature of 500–900 °C showed narrow pore size distribution. This indicated that the membrane samples had relatively uniform pore sizes [40]. It reveals that the addition

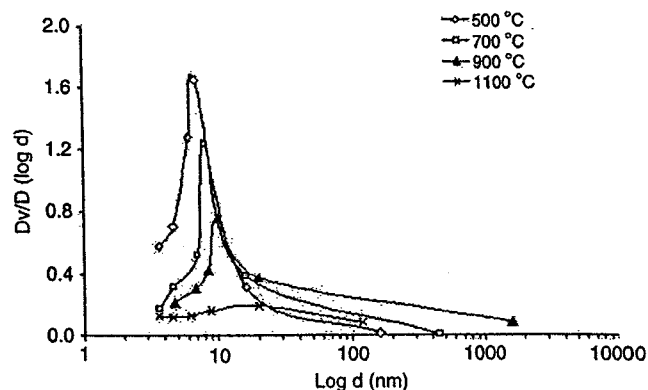


Fig. 9. Pore size distribution of palladium–alumina membrane at different calcinations temperature.

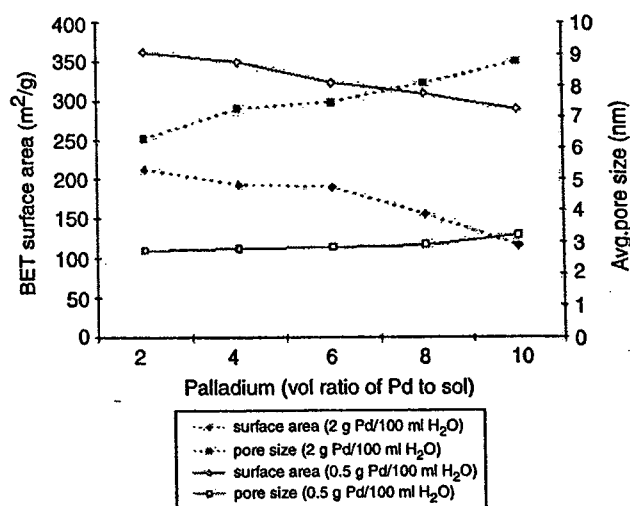


Fig. 10. The effect of palladium amounts on average pore size and BET surface area of the membrane.

of metals did not destroy the uniform membrane based on the narrow pore size distribution of the membrane. However, when calcinations temperature increased to 1100 °C, the pore size distribution profile for the membrane become wider, indicating that the membrane pore structure was almost collapse.

### 3.2.4. Effect of palladium amounts on membrane structures

Based on FTIR and XRD analysis, 700 °C was chosen for the calcinations temperatures for the following experiments. At this calcinations temperature the copolymer or the traces of the organic compounds is fully removed and fine crystalline of  $\gamma$ -Al<sub>2</sub>O<sub>3</sub> phase was observed. Palladium concentration of 0.5 g Pd/100 ml H<sub>2</sub>O and 2 g Pd/100 ml H<sub>2</sub>O were used to study the effect of palladium amounts on membrane microstructure using different volume ratio of palladium to sol. The mean pore size and BET surface area of the membrane at calcinations temperatures of 700 °C are shown in Fig. 10. It can be seen that, the pore diameter increased whereas the BET surface area decreased with increased the palladium concentration and volume

ratio of palladium in sol. Membrane sample with lower palladium concentration (0.5 g Pd/100 ml H<sub>2</sub>O) shows that the pore diameter increased slightly from 2.72–3.20 nm and BET surface area decreased from 362.3–289.3 m<sup>2</sup>/g as the volume ratio of palladium in sol increased from 2:100 to 10:100. While for membrane sample with higher palladium concentration (2 g Pd/100 ml H<sub>2</sub>O) the pore diameter increased from 6.29–8.75 nm and BET surface area decreased from 212.4–115.0 m<sup>2</sup>/g.

When the palladium amounts increased the palladium particles agglomerated and this would enlarge the palladium metal particle size [3,6]. The decreasing of surface area and increasing in pore size were due to the pore blocking effect caused by the metal particles that agglomerated and located along the pore channel that close some membrane smaller pores [9]. Based on the result observed in Fig. 10, the addition of palladium higher than 6:100 volume ratio of palladium in sol with concentration of 2 g Pd/100 ml H<sub>2</sub>O shows that, the BET surface area of palladium–alumina membrane was sharply decreased and with highly increased in pore size. If high BET surface areas are a major consideration, it appears reasonable to keep palladium concentration at 2 g Pd/100 ml H<sub>2</sub>O with volume ratio 6:100 of palladium to sol.

### 3.2.5. SEM analysis

SEM analysis was performed to investigate and to determine the surface morphology of unsupported palladium alumina membrane at calcinations temperature of 700 °C. 4:100 volume ratio of PVA to sol with concentration of 4 g PVA/100 ml H<sub>2</sub>O and 6:100 volume ratio of palladium to sol with concentration of 2 g Pd/100 ml H<sub>2</sub>O were used in membrane preparation. The same sample was used for supported membrane. Fig. 11(a) and (b) present the SEM image of unsupported palladium–alumina membrane surface after calcined at 700 °C at two different magnifications. It shows that, at the lower magnification (500×) and even at the higher magnification (10,000×) the membrane surface was morphologically homogeneous, smooth and free of cracks. The white dots that were observed in the SEM image in Fig. 11(b) representing the palladium particles were well dispersed.

### 3.3. Supported membrane analysis

#### 3.3.1. Effect of support structure on membrane morphology

In this study, an alumina powder was used as the support material with an average particle size of 20 μm. The alumina powder was pressed at pressure of 8–10 ton by hydraulic press equipment to form pellet (disks) shape with diameter of 20 and 2 mm thickness. The resulting pellet then was sintered up to 1000 °C. The structure and pore characteristic properties of the alumina support was characterized by SEM and Autosorb analysis. The microstructural properties of alumina support after calcined at 1000 °C are 9.84 nm in pore diameter and 83.78 m<sup>2</sup>/g of BET surface area with surface fractal of 2.483.

The surface of support has an important role in producing good membrane morphology. Poor membrane morphology such as cracks and holes will be observed due to rough surface

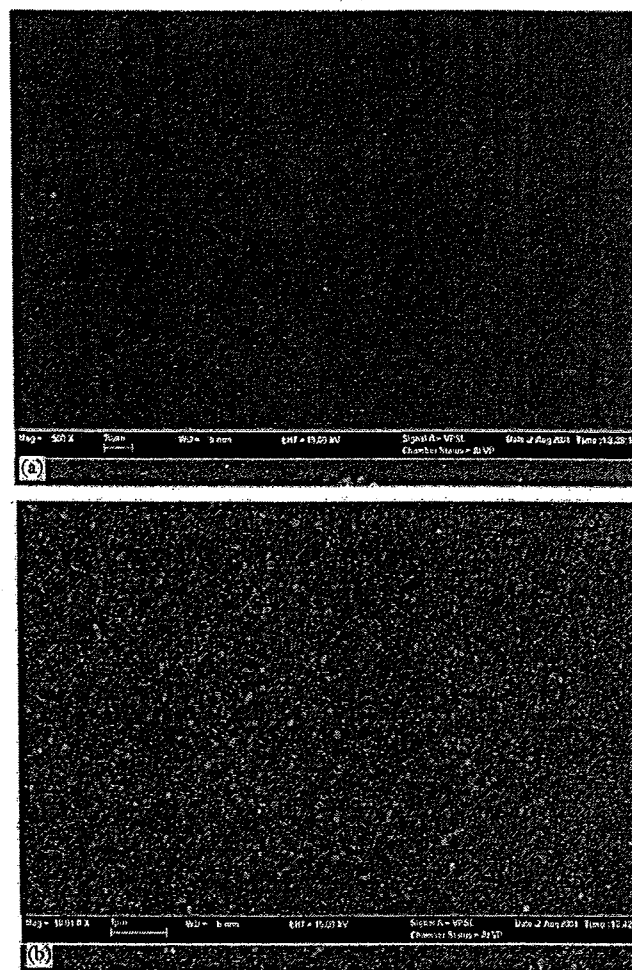


Fig. 11. SEM images of unsupported membrane surface after calcined at 700 °C at different magnification: (a) 500× and (b) 10000×.

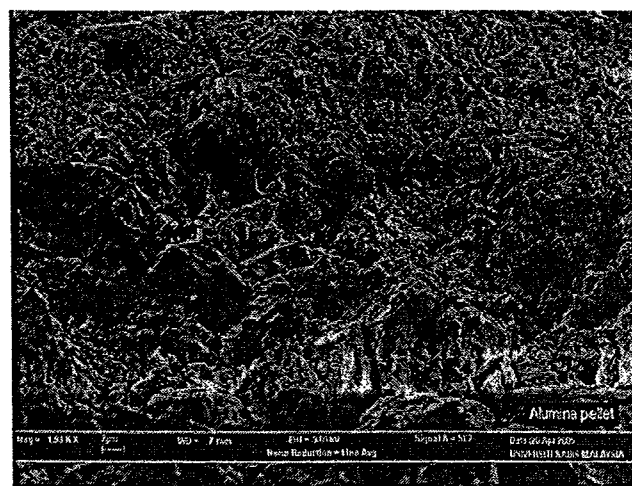


Fig. 12. SEM image of alumina support surface (500 × magnification).

of support and these defects will decrease the membrane performance. Fig. 12 shows the SEM image of alumina support surface. It can be seen that, the surface of the alumina support



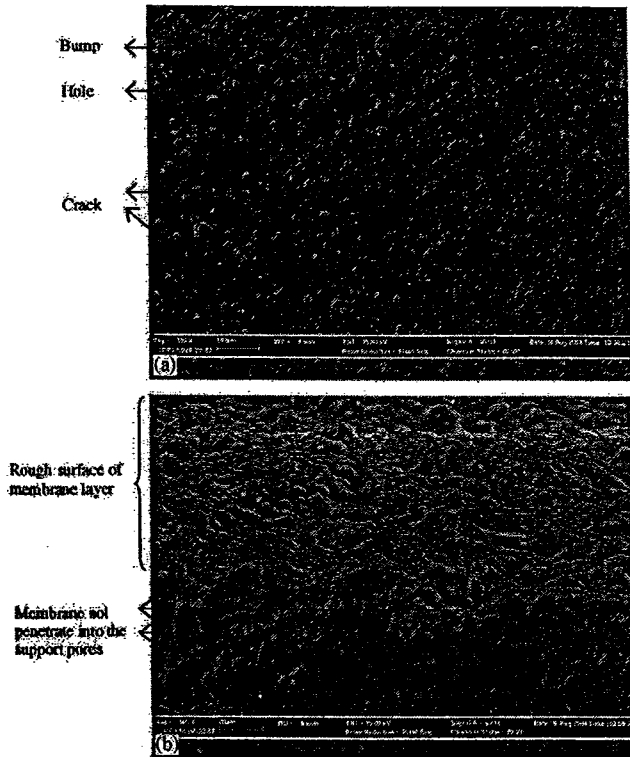


Fig. 13. SEM images of palladium–alumina membrane layer on untreated support after calcined at 700 °C: (a) membrane surface (100 × magnification) and (b) cross sectional view of the membrane on the top of alumina support (500 × magnification).

is very rough. This poor morphology of support surface must be treating in order to produce a smooth membrane layer. In this study, the support was treated by coated the alumina support with PVA (as a pore filling) before membrane coating.

The supported palladium–alumina membrane was prepared by coating the palladium–alumina sol on the top of alumina support and dried for 48 h at ambient temperature until dried gel formed before calcined at 700 °C. The membrane layer contains 6:100 volume ratio of Pd to sol with palladium concentration of 2 g Pd/100 ml H<sub>2</sub>O. The membrane layer on the untreated support (without coated with PVA) is shown in Fig. 13. Fig. 13(a) shows the SEM image of the membrane surface. The membrane surface that illustrated in the figure was structurally non-uniform and its surface morphology was very poor. The appearance of cracks, bumps and holes can be seen in the figure.

Fig. 13(b) shows the cross sectional image of the membrane. It shows that the part of the coating sol was penetrated into the support. This is due to the rough and irregular surface of the support. It clearly shows that the coarse support surface cause cracks, holes and bumps on the membrane layer. When holes or cracks are developed on the coated membrane, the hydrogen selectivity would greatly deteriorate [33].

### 3.3.2. Coating of palladium–alumina membrane

To produce a good morphology of membrane layer, the alumina support was treated by filling the support pores and

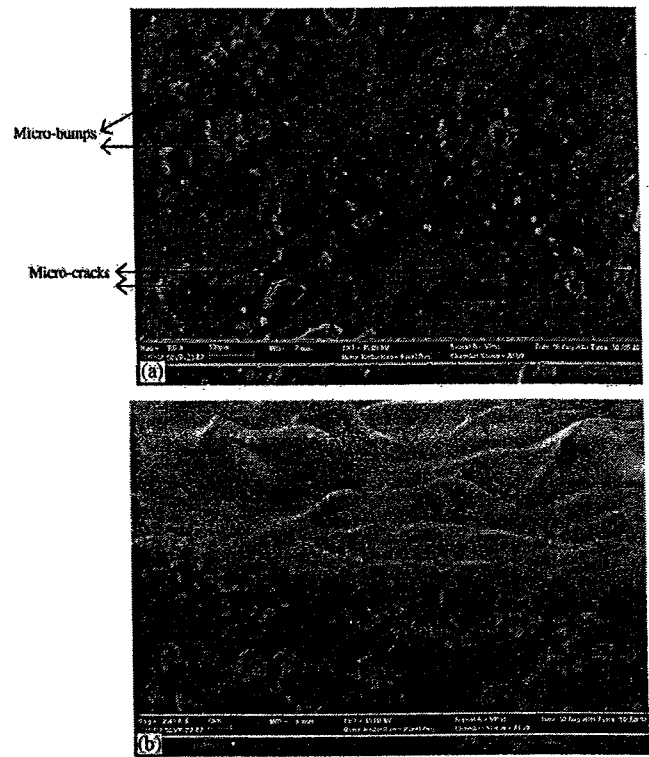


Fig. 14. SEM images of first coating palladium–alumina membrane layer on treated support after calcined at 700 °C: (a) membrane surface (100 × magnification) and (b) cross sectional view of membrane layer (2500 × magnification).

smoother the support surface with PVA before coating was applied. The alumina support was dipped in PVA for 5 h and dried before coating was applied. Fig. 14(a) and (b) show the surface and cross sectional SEM image of first-coating membrane layer on alumina support after treated or coated with PVA, respectively. As can be seen in the Fig. 14(a), membrane surface on the treated support was smoother than membrane surface on untreated support (Fig. 13(a)). However, some micro-cracks and micro-bumps still can be seen on the membrane layer. Fig. 14(b) shows good adhesion of membrane layer on the support and no sol was penetrated into the support. The observed thickness of the membrane is approximately 2 μm. The membrane layer on the alumina support which treated with PVA that acts as a pore filling substance and support surface smoother helps to prevent almost the cracks formation. It also improving more adhesion of membrane layer on the support and at the same time successfully prevent the coating solution from penetrate into the support.

The first coating membrane layer is not enough to cover the overall of the rough surface on the support which is the formation of defects such as micro-cracks, pinholes and bumps on membrane surface still can be observed. Second coating was done to cover the membrane surface irregularities and repair defects on membrane surface developed during first coating [26]. However, when the membrane was calcined after repeating the dipping-drying procedure more than twice the adhesiveness of

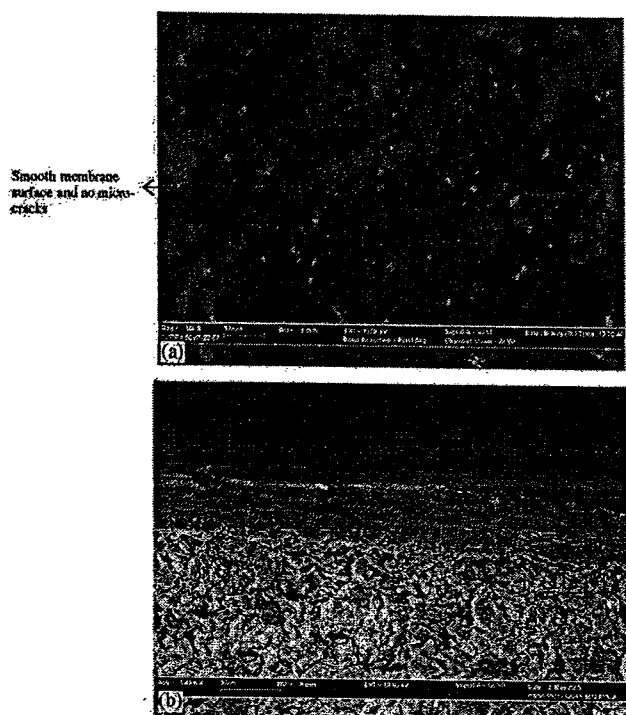


Fig. 15. SEM images of second coating palladium–alumina membrane layer on treated support after calcined at 700 °C; (a) membrane surface (100 × magnification) and (b) cross sectional view of membrane layer (1500 × magnification).

the membrane became poor and the formation of cracks was unavoidable [38].

Fig. 15(a) and (b) show SEM image of the surface and cross sectional image of the palladium–alumina second coating membrane on support, respectively. After second coating, no cracks, bumps or pinholes were observed. As can be seen in Fig. 15(a), the membrane surface is even, smooth and compact. The second coating step reduced almost the membrane surface roughness. The cross sectional image of supported membrane demonstrates that the upper palladium–alumina membrane layer was successfully coated and fused onto the alumina support and the thickness of the membrane layer was estimated as 9 μm (Fig. 15(b)). Some findings were reported that, membrane with thickness of approximately 10 μm has been developed for hydrogen gas separation [6,41,42].

#### 4. Conclusion

The sol–gel synthesis of palladium–alumina dried gel at calcinations temperature of 700 °C, lead to the formation of membrane pore size of less than 10 nm with uniform pore size distribution for both membrane sample containing Pd concentration of 0.5 g Pd/100 ml H<sub>2</sub>O and 2 g Pd/100 ml H<sub>2</sub>O. The result observed from Autosorb, FTIR and XRD analysis indicated that, 700 °C was a good processing temperature for palladium–alumina membrane in producing a stable membrane structures. The residual organics completely removed after calcined at 700 °C and without traces of carbon was detected.

Carbon existences lead to low surface area of the membrane. The palladiums also were highly dispersed in the alumina membrane at calcinations temperature of 700 °C. The membrane pore size increased with increased palladium amounts and this brings to the decreasing of membrane surface area. The rough surface of the membrane was reduced after the support was treated or coated by PVA before coating. Pinholes, cracks and bumps developed during first coating were covered by repeating the dipping–drying–calcinations procedure by twice and the coating layer with good adhesion was observed. The final membrane thickness with 9 μm was obtained. Based on this study, the structure and stability of alumina membrane with addition of palladium as additive were improved. It can be applied in H<sub>2</sub> separation process in order to increase the H<sub>2</sub> permeability.

#### Acknowledgement

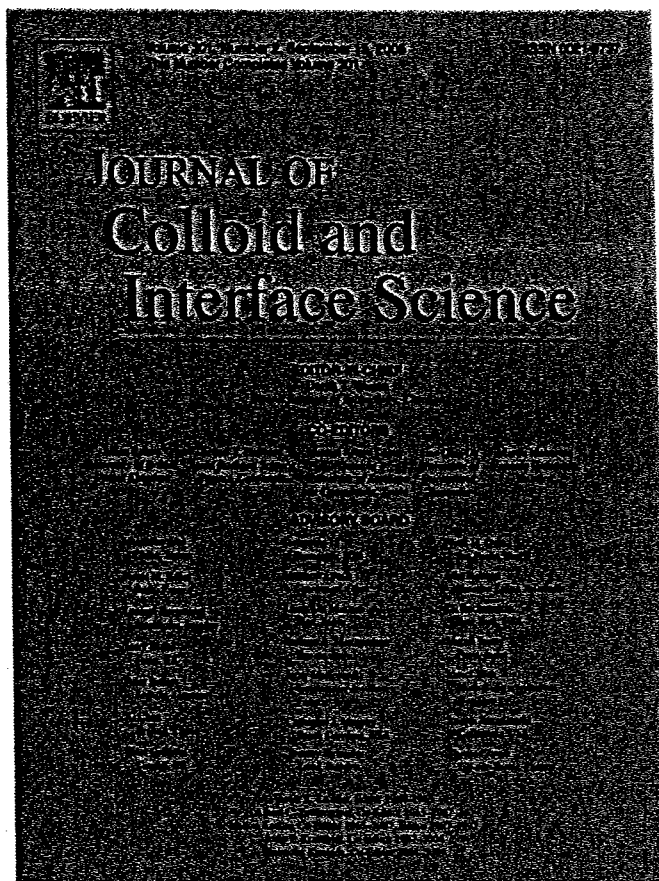
The authors acknowledge the short term grant from USM/MOSTE which enables the production of this article.

#### References

- [1] Bokhimi X, Morales A, Novaro O, López T, Chimal O, Asomoza M. et al. Effect of copper precursor on the stabilization of titania phases, and the optical properties of Cu/TiO<sub>2</sub> prepared with the sol–gel technique. *Chem Mater* 1997;9(11):2616–20.
- [2] Dawson A, Kamat PV. Semiconductor–metal nanocomposites. Photoinduced fusion and photocatalysis of gold-capped TiO<sub>2</sub> (TiO<sub>2</sub>/gold) nanoparticles. *J Phys Chem B* 2001;105(5):960–6.
- [3] Wu Y, Zhang Y, Zhang L. Effects of finely metallic palladium on microstructure and properties of nanocomposites produced by sol–gel technique. *China Particuol* 2004;2(1):19–24.
- [4] Wang JA, Aguilar-Rios G, Wang R. Inhibition of carbon monoxide on methanol oxidation over γ-alumina supported Ag, Pd and Ag–Pd catalysts. *Appl Surf Sci* 1999;147(1):44–51.
- [5] Colomban P. Sol–gel control of the micro/nanostructure of functional ceramic–ceramic and metal–ceramic composites. *J Mater Res* 1998;13(4):803–11.
- [6] Chen H, Shiau JD, Chu CY, Huang TC. Synthesis and characterization of palladium clusters dispersed alumina membranes. *Sep Purif Technol* 2003;32(1–3):247–54.
- [7] Mulder M. Basic principles of membrane technology. Dordrecht, The Netherlands: Kluwer Academic Publishers; 1996.
- [8] Paglieri SN, Roa F, Way JD, McCormick RL. Available from world wide web: (<http://www.netl.doe.gov/publications/proceedings/00/ucr005/wayucr.pdf>), 2000.
- [9] RSC's Chemical Science Network (Chemsoc). Available from world wide web: (<http://www.chemsoc.org/viselements/pages/palladium.html>), 2005.
- [10] Hsieh HP. Inorganic membranes for separation and reaction, membrane science and technology series 3 Amsterdam: Elsevier; 1996.
- [11] Chuah GK, Jaenicke S, Xu TH. The effect of digestion on the surface area and porosity of alumina. *Microporous Mesoporous Mater* 2000;37(3):345–53.
- [12] Schaep J, Vandecasteele C, Peeters B, Luyten J, Dotremont C, Roels D. Characteristics and retention properties of a mesoporous γ-Al<sub>2</sub>O<sub>3</sub> membrane for nanofiltration. *J Membr Sci* 1999;163(2):229–37.
- [13] Díaz E, Ordóñez S, Vega A, Coca J. Adsorption properties of a Pd/γ-Al<sub>2</sub>O<sub>3</sub> catalyst using inverse gas chromatography. *Microporous Mesoporous Mater* 2004;70(1–3):109–18.
- [14] Lambert CK, Gonzalez RD. Effect of binder addition on the properties of unsupported γ-Al<sub>2</sub>O<sub>3</sub> membranes. *Mater Lett* 1999;38(2):145–9.

- [15] Cheong H, Cho WS, Ha JS, Kim CS, Choi DK, Cheong DS. Structural evolution of alumina membrane prepared on an alumina support using a sol-gel method. *J Alloys Compds* 1999;290(1–2):304–9.
- [16] Yang W, Xiong G. Novel porous metal/ceramic membrane materials. *Curr Opin Solid State Mater Sci* 1999;4(1):103–7.
- [17] Lambert CK, Gonzalez RD. Sol-gel preparation and thermal stability of Pd/ $\gamma$ -Al<sub>2</sub>O<sub>3</sub> catalysts. *J Mater Sci* 1999;34(13):3109–16.
- [18] Ahmad AL, Othman MR, Mukhtar H. H<sub>2</sub> separation from binary gas mixture using coated alumina-titania membrane by sol-gel technique at high-temperature region. *Int J Hydrogen Energy* 2004;29:817–28.
- [19] Guimarães AP, Viana APP, Lago RM, Mohallem NDS. The effect of thermal treatment on the properties of sol-gel palladium-silica catalysts. *J Non-Crystalline Solids* 2002;304(1–3):70–5.
- [20] Wu HC, Liu LC, Yang SM. Effects of additives on supported noble metal catalysts for oxidation of hydrocarbons and carbon monoxide. *Appl Catal A* 2001;211(2):159–65.
- [21] Lee BI, Pope EJA. Chemical processing of ceramic. New York: Marcel Dekker; 1994.
- [22] Klein LC. Sol-gel process. New York: Wiley; 1988.
- [23] Khan AU, Luckham PF, Manimaaran S, Rivenet M. The strength of colloidal interactions in the presence of ceramic dispersants and binders. *J Mater Chem* 2002;12(6):1743–7.
- [24] Ahmad AL, Idrus NF, Othman MR. Preparation of perovskite alumina ceramic membrane using sol-gel method. *J Membr Sci* 2005;262(1–2):129–37.
- [25] Haas-Santo K, Fichtner M, Schubert K. Preparation of microstructure compatible porous supports by sol-gel synthesis for catalyst coatings. *Appl Catal A* 2001;220(1–2):79–92.
- [26] Yeung KL, Sebastian JM, Varma A. Mesoporous alumina membranes: synthesis, characterization, thermal stability and nonuniform distribution of catalyst. *J Membr Sci* 1997;131(1–2):9–28.
- [27] Ersoy B, Gunay V. Effects of La<sub>2</sub>O<sub>3</sub> addition on the thermal stability of  $\gamma$ -Al<sub>2</sub>O<sub>3</sub> gels. *Ceram Int* 2004;30(2):163–70.
- [28] Mishra R, Rao KJ. Thermal and morphological studies of binary and ternary composites of poly (vinyl alcohol) with alumina and zirconia. *Ceram Int* 2000;26:371–8.
- [29] Othman MR, Ahmad AL, Mukhtar H. Characteristics of unsupported alumina membrane prepared using sol-gel technique. *ASEAN J Sci Technol Dev* 2001;18:59–70.
- [30] Das N, Maiti HS. Formation of pore structure in tape-cast alumina membranes—effects of binder content and firing temperature. *J Membr Sci* 1998;140(2):205–12.
- [31] Tari G, Olhero SM, Ferreira JMF. Influence of temperature on the colloidal processing of electrostatically stabilised alumina suspensions. *J Mater Process Technol* 2003;137(1–3):102–9.
- [32] Briscoe B, Luckham P. The effects of hydrogen bonding upon the viscosity of aqueous poly (vinyl alcohol) solutions. *Polymer* 2000;41(10):3851–60.
- [33] Fu Q, Cao CB, Zhu HS. Preparation of alumina films from a new sol-gel route. *Thin Solid Films* 1999;348(1):99–102.
- [34] Romero-Pascual E, Larrea A, Monzón A, González RD. Thermal stability of Pt/Al<sub>2</sub>O<sub>3</sub> catalysts prepared by sol-gel. *J Solid State Chem* 2002;168(1):343–53.
- [35] Le Bihan L, Dumeignil F, Payen E, Grimblot J. Chemistry of preparation of alumina aerogels in presence of a complexing agent. *J Sol-Gel Sci Technol* 2002;24(2):113–20.
- [36] Williams DH, Fleming I. Spectroscopic methods in organic chemistry. 5th ed., New York: McGraw-Hill; 1995.
- [37] Bernal JLP, Lopez MAB. Fractal dimension of stone pore surface as weathering descriptor. *Appl Surf Sci* 2000;161(1):47–53.
- [38] Ruckenstein E. In: Stevenson SA, Dumesic JA, Baker RTK, Ruckenstein E, editors. Metal-support interaction in catalysis sintering and redispersion. New York: Van Nostrand Reinhold; 1987.
- [39] Van Gestel T, Vandecasteele C, Buekenhoudt A, Dotremont C, Luyten J, Leysen R. et al. Alumina and titania multilayer membranes for nanofiltration: preparation, characterization and chemical stability. *J Membr Sci* 2002;207(1):73–89.
- [40] Dumeignil F, Sato K, Imamura M, Matsubayashi N, Payen E, Shimada H. Modification of structural and acidic properties of sol-gel prepared alumina powders by changing hydrolysis ratio. *Appl Catal A* 2002;636:1–11.
- [41] Cini P, Blaha SR, Harold MP. Preparation and characterization of modified tubular ceramic membranes for use as catalyst supports. *J Membr Sci* 1991;55(1–2):199–225.
- [42] Changrong X, Feng W, Zhaojing M, Fanqing L, Dingkun P, Guangyao M. Boehmite sol properties and preparation of two-layer alumina membrane by a sol-gel process. *J Membr Sci* 1996;116(1):9–16.

Provided for non-commercial research and educational use only.  
Not for reproduction or distribution or commercial use.



This article was originally published in a journal published by Elsevier, and the attached copy is provided by Elsevier for the author's benefit and for the benefit of the author's institution, for non-commercial research and educational use including without limitation use in instruction at your institution, sending it to specific colleagues that you know, and providing a copy to your institution's administrator.

All other uses, reproduction and distribution, including without limitation commercial reprints, selling or licensing copies or access, or posting on open internet sites, your personal or institution's website or repository, are prohibited. For exceptions, permission may be sought for such use through Elsevier's permissions site at:

<http://www.elsevier.com/locate/permissionusematerial>



## Pore surface fractal analysis of palladium-alumina ceramic membrane using Frenkel–Halsey–Hill (FHH) model

A.L. Ahmad\*, N.N.N. Mustafa

*School of Chemical Engineering, Engineering Campus, Universiti Sains Malaysia, Seri Ampangan, 14300 Nibong Tebal, Penang, Malaysia*

Received 16 January 2006; accepted 16 May 2006

Available online 24 May 2006

### Abstract

The alumina ceramic membrane has been modified by the addition of palladium in order to improve the H<sub>2</sub> permeability and selectivity. Palladium-alumina ceramic membrane was prepared via a sol–gel method and subjected to thermal treatment in the temperature range 500–1100 °C. Fractal analysis from nitrogen adsorption isotherm is used to study the pore surface roughness of palladium-alumina ceramic membrane with different chemical composition (nitric acid, PVA and palladium) and calcinations process in terms of surface fractal dimension, *D*. Frenkel–Halsey–Hill (FHH) model was used to determine the *D* value of palladium-alumina membrane. Following FHH model, the *D* value of palladium-alumina membrane increased as the calcinations temperature increased from 500 to 700 °C but decreased after calcined at 900 and 1100 °C. With increasing palladium concentration from 0.5 g Pd/100 ml H<sub>2</sub>O to 2 g Pd/100 ml H<sub>2</sub>O, *D* value of membrane decreased, indicating to the smoother surface. Addition of higher amount of PVA and palladium reduced the surface fractal of the membrane due to the heterogeneous distribution of pores. However, the *D* value increased when nitric acid concentration was increased from 1 to 15 M. The effect of calcinations temperature, PVA ratio, palladium and acid concentration on membrane surface area, pore size and pore distribution also studied.  
© 2006 Elsevier Inc. All rights reserved.

**Keywords:** Palladium-alumina membrane; Surface fractal dimension; Surface roughness; Nitrogen adsorption isotherms; Sol–gel

### 1. Introduction

Novel porous palladium-alumina ceramic membrane has recently attracted considerable research interest owing to its higher permselectivity to hydrogen due to surface diffusion or hydrogen spillover on palladium and higher permeability of hydrogen due to alumina porous properties [1,2]. The characterization of pore structure (porosity, pore size distribution, surface area, etc.) of this membrane is of great importance. It is well known that the performance of membrane depends on their structure and morphology. However, the surface area and pore size distribution alone do not meet all requirements to describe the characteristics of the pore structure of the membrane. Another parameter to characterize the pore structure is surface fractal analysis that is characterized by the fractal dimension, *D*. Surface fractal analysis provides a parameter char-

acterizing irregularities on the membrane surface or parameter reflecting the roughness of pore structure [3]. The *D* value should lie between 2 and 3 and to be used to describe the irregularities and roughness of pore surface [4]. Surface fractal dimension ranging from *D* = 2, for perfectly smooth surfaces, to *D* = 3, for sponge-like surfaces whereas the degree of surface irregularity increases [3,5]. It is known that the irregularities and roughness of the surface are attributed to the existence of distributed pore size that contributes to the *D* value. Therefore, the surface fractal dimension becomes increasingly important in describing the surface irregularities in many of previous works.

The fractal nature of ceramic has been studied by many means such as SAXS (small angle X-ray scattering) [6,7], SANS (small angle neutron scattering) [8] and adsorption methods [3,9–11]. Chaput et al. [8] had investigated the aluminosilica aerogels and found that their fractal dimensions were all near 2.1 and had no significant temperature dependence up to 800 °C, but the size of fractal domain decreased with the increase of temperature. Lee and Tsay [11] found that the

\* Corresponding author. Fax: +60 4 5941013.  
E-mail address: [chlaticf@eng.usm.my](mailto:chlaticf@eng.usm.my) (A.L. Ahmad).

surface fractal dimension values of alumina and aluminum borate were almost constant (2.5–2.6) after calcinations from 500 to 1100 °C. Meng et al. [12] investigated the surface fractal dimensions of mesoporous aerogels from nitrogen adsorption isotherms by means of the FHH method and the thermodynamics method. They concluded that the fractal surfaces of particulate aerogels were slightly more irregular than those of polymeric aerogels. Blacher et al. [13] applied fractal analysis to characterize the structure of Pd-Ag/SiO<sub>2</sub> catalysts with different concentration of Pd-Ag. Nitrogen adsorption–desorption, mercury porosimetry and small-angle X-ray scattering measurement were used. The analysis showed Pd-Ag/SiO<sub>2</sub> xerogels exhibited open self-similar pore structure. From nitrogen adsorption–desorption measurement, FHH method was selected and the results showed that when the catalyst was added with silver of 0–3.7% concentration, *D* increased from 2.31 to 2.37, indicating the increase in micro surface roughness. Wei and Wang [3] investigated pore surface roughness change in composite Al<sub>2</sub>O<sub>3</sub>-SiO<sub>2</sub> membranes by the analysis of surface fractal dimension. Fractal features were analyzed from N<sub>2</sub> adsorption–desorption measurements. It was found that surface fractal dimension increased with increase of SiO<sub>2</sub> content in composite membrane with different molar ratio of alumina to silica sintered at 600 °C. The surface fractal dimension of membrane with 40 mol% silica content increased slightly at sintering temperature of 200–600 °C but decreased at the temperature of 800 °C.

Fractal analysis of adsorption isotherms was first introduced by Avnir and Pfeifer in the year of 1983. The simplest and most popular method is to fit the adsorption data with a fractal isotherm equation, where the surface fractal dimension *D* appears as a parameter [3]. In this work, the surface fractal dimension of palladium-alumina membrane is calculated using Frenkel–Halsey–Hill (FHH) model. FHH methods are the easiest way to calculate *D* value using Nitrogen adsorption data without having calculated the pore surface area. The FHH model for multilayer adsorption is a method proposed by Avnir and Jaroniec in the year of 1989, which determines surface fractal dimensions from a single adsorption isotherm. FHH equation provides a relationship between the surface fractal dimension and nitrogen adsorption, that is to say, the pore surface roughness can be probed by nitrogen molecules [3]. The surface fractal dimension by FHH model yields the following equation:

$$\frac{N}{N_m} = k \left[ \ln \left( \frac{P_0}{P} \right) \right]^{(D-3)} \quad (1)$$

The surface fractal dimension, *D*, can be calculated from the slope of a plot of  $\ln(N/N_m)$  versus  $\ln[\ln(P_0/P)]$ ,

$$\ln \left( \frac{N}{N_m} \right) = (D - 3) \ln \left[ \ln \left( \frac{P_0}{P} \right) \right], \quad (2)$$

where *N* is the number of adsorbed moles of nitrogen at the given relative pressure (*P/P*<sub>0</sub>) and *N*<sub>m</sub> is the number of adsorbed moles in monolayer. The values of *N*<sub>m</sub> and *N* can be obtained from the Brunauer–Emmet–Teller (BET) model equation. This part aims to study the effect of calcinations tempera-

ture, palladium and platinum amount, and PVA amount on the surface fractal dimension of the membrane.

In order to increase the performance of membrane in H<sub>2</sub> permeability and selectivity, the alumina ceramic membrane has been improved by the addition of palladium as an additive. The present work makes an effort to investigate the influence of palladium and PVA amount, calcinations temperature and acid concentrations on the structures (pore size distribution), and surface fractal dimensions of palladium-alumina membrane prepared by sol–gel synthesis. Surface fractal dimension is used to characterize pore structure of the membrane. In addition, differences between the surface fractal dimension of unaltered and altered alumina membrane with palladium metal on pore structure have to be determined because a good flux performance needs membrane with high porosity (rough pore surface), and good separation selectivity requires homogeneous distribution of pores or a narrow pore size distribution (uniform pore size).

## 2. Experimental

The palladium-alumina membrane was prepared by the sol–gel method. All chemicals in this work were supplied by Acros Organics, USA, except aluminum secondary butoxide and nitric acid which supplied by Merck, Germany. For preparation of palladium-alumina sol, aluminum secondary butoxide (Al(OC<sub>4</sub>H<sub>9</sub>)<sub>3</sub>) was used as alumina precursor, nitric acid (HNO<sub>3</sub>) as peptizing agent and deionized water and butanol (C<sub>4</sub>H<sub>9</sub>OH) as solvent. Based on the reported finding from Refs. [14,15], the molar ratio of aluminum:water:butanol:acid of 1:100:5.5:0.07 was selected. Butanol was added in sol–gel processing as they allow to control the reaction of alkoxide precursors with water, and hence to direct with more flexibility of the structure of sol–gel products [16]. The addition of butanol also was used to slow the hydrolysis rates and thus to stabilize the alkoxides to the formation of clear gel. If the hydrolysis was faster, it will lead to the precipitation of the sol [17].

Based on the given ratio, 12.8 ml aluminum secondary butoxide was dissolved in 25 ml butanol. Then, 90.4 ml deionized water was heated on a hot plate to temperature of 90 °C and was added to the mixture of butanol and aluminum while maintaining the temperature at 90 °C under vigorous stirring of the mixture. After 15 min, PVA and palladium solution (PdCl<sub>2</sub> which was dissolved in hot deionized water (70–80 °C)) were added to alumina sol and were stirred vigorously for 30 min to ensure the sol mixture was well mixed. The palladium concentration used in this work was 0.5 and 2 g palladium in 100 ml deionized water. Later, about 0.16 ml nitric acid (HNO<sub>3</sub>) was added to sol to peptize or stabilize the sol particles and the solution was kept stirring at temperature of 90 °C for 30 min before reflux process. The solution was peptized for about 24 h at range temperature of 85–95 °C under reflux conditions. The sol prepared was stabilized to avoid the particles flocculated and the solution was prepared in a closed beaker to enhance the rate of peptization. About 10 ml of sol was poured into a Petri dish after the sol was cooled to room temperature. Then it was dried at an ambient temperature in a fume cupboard for 48 h to evaporate.

orate water and butanol, until a dried gel layer was obtained. After drying, the samples were calcined to form unsupported palladium-alumina membrane for 24 h. The experimental parameters and the variables are shown in Table 1.

The nitrogen adsorption analysis was performed using surface area analyzer Autosorb I supplied by Quantachrome Corporation, USA. The membrane samples (powder) were first degassed under vacuum at temperature 200 °C for 3 h to remove the moisture and other impurities in the samples. The adsorbed amount of nitrogen was measured by volume at standard temperature and pressure. The data calculations were performed automatically by the software (Micropore version 2.46) available with the Autosorb I instrument.

Table 1  
Experimental parameters and the variables

Experimental parameters	Variables
Effect of calcinations temperature	500, 700, 900, 1100 °C
Effect of palladium	0.5 g Pd/100 ml H <sub>2</sub> O and 2 g Pd/100 ml H <sub>2</sub> O (2:100, 4:100, 6:100, 8:100 volume ratio of palladium to alumina sol)
Effect of PVA	4 g PVA/100 ml H <sub>2</sub> O (2:100, 4:100, 6:100, 8:100 volume ratio of PVA to alumina sol)
Effect of acid	1, 5, 10, 15 M

### 3. Results and discussion

#### 3.1. Effect of calcination temperature

The palladium concentration of 2 g palladium/100 ml H<sub>2</sub>O with 6:100 volume ratio of palladium to sol, 4:100 volume ratio of PVA (4 g PVA/100 ml deionized water) to sol and 5 M acids were used in this experiment. Figs. 1 and 2 show the adsorption–desorption isotherms of pure alumina and palladium-alumina membranes at calcinations temperature of 500–1100 °C. As shown in Fig. 1, it shows a typical adsorption isotherm for the alumina [18]. The alumina membrane at calcinations temperature of 500–900 °C exhibited type IV isotherm (mesoporous material characteristic) based upon Brunauer, Deming, Deming and Teller (BDDT) classification. The isotherm curves also show a hysteresis that associated with capillary condensation in the mesopore range (20–1000 Å) [18]. However, the adsorption isotherm for alumina membrane at calcinations temperature of 1100 °C is characterized as type II isotherm. Type II isotherm is encountered when adsorption occurs on low porosity material or on material with pore diameters mostly mesoporous. It also showed hysteresis on desorption isotherm curve with a smaller desorption step [19,20].

The palladium-alumina membrane at calcinations temperatures of 500 and 700 °C also exhibited isotherm type IV, which

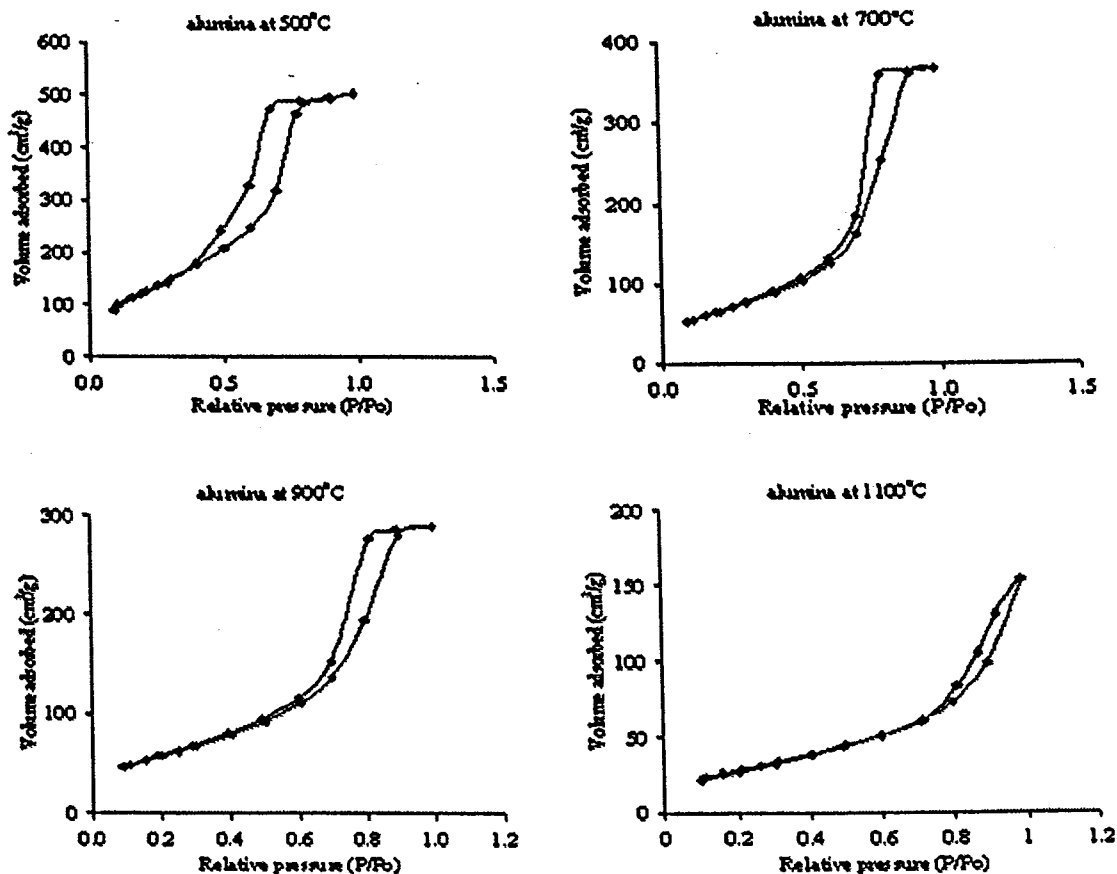


Fig. 1. Adsorption–desorption isotherms of alumina membrane at different calcination temperatures.

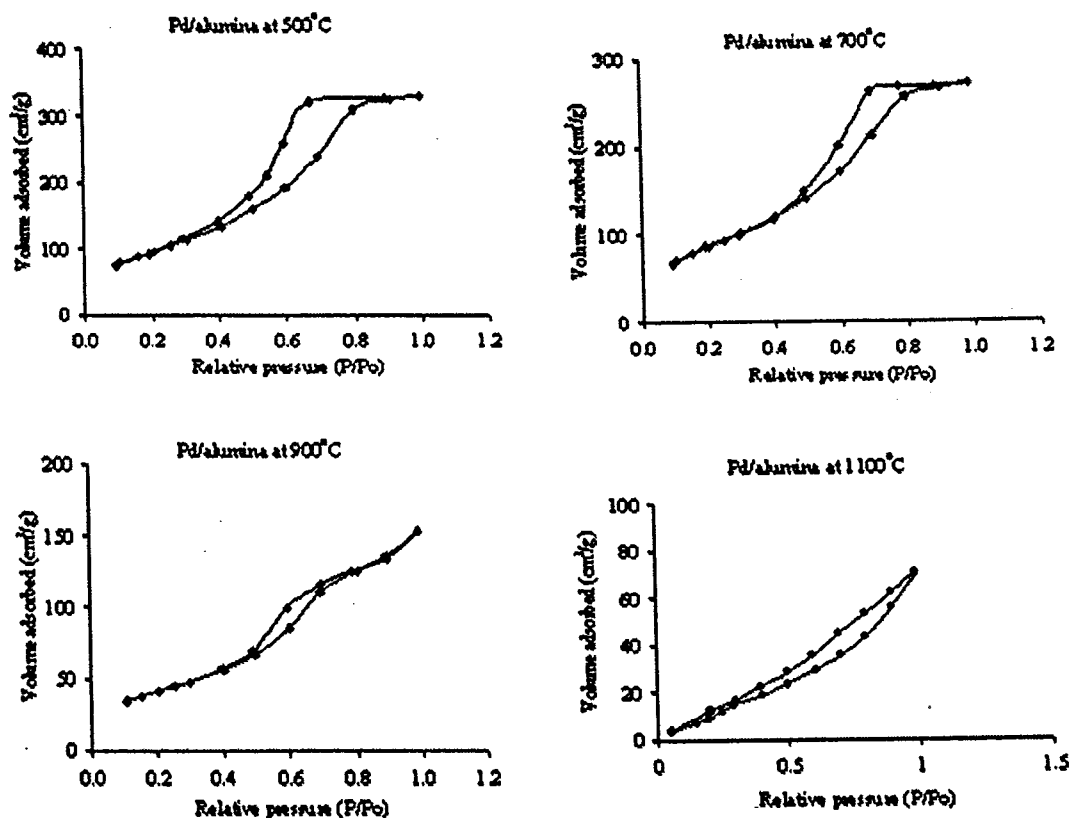


Fig. 2. Adsorption-desorption isotherms of palladium-alumina membrane at different calcination temperatures.

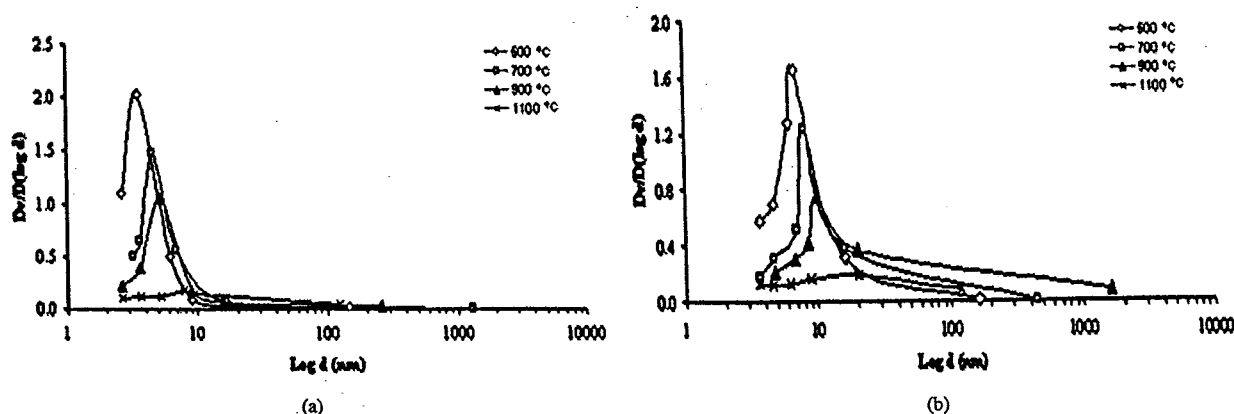


Fig. 3. Pore size distribution of (a) alumina and (b) palladium-alumina membrane at different calcination temperatures.

associated with mesoporous materials characteristic (Fig. 2) as same as alumina sample. The isotherm shape progressively changed with increasing the calcinations temperature. At 900 °C, the shape of isotherm changed to type V isotherm. Type V isotherm was also associated with pores in the same range as those of the type IV isotherms [19]. The isotherm shape of palladium-alumina membrane at calcinations temperature of 1100 °C is characterized as type II, indicating the presence of larger pore [20].

Figs. 3a and 3b show the pore size distribution profile of pure alumina and palladium-alumina membrane at calcinations

temperature of 500–1100 °C. Pore size distributions were obtained from the computational method of Barrett, Joyner, and Halenda (BJH). As can be seen in Fig. 3, the pore size distribution profile for both membrane sample shows the mesopore volume sharply decreased and the average pore diameter gradually increased as the calcinations temperature was increased from 500 to 1100 °C. The trend is consistent with the work of Leenars et al. [21]. The decrease in pore volume may be caused by volume shrinkage at high temperature, which eliminates some pores. The pore size distribution profiles for palladium-alumina and alumina membrane at calcinations temperature of

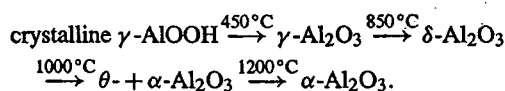


Table 2  
Surface fractal dimension of membranes at different calcination temperatures by FHH model

Samples	Temperature (°C)	Surface fractal dimension, <i>D</i>
Alumina	500	2.3712
	700	2.4626
	900	2.4855
	1100	2.3148
Palladium-alumina (6:100 volume ratio of palladium to sol with concentration 2 g Pd/100 ml H <sub>2</sub> O)	500	2.3612
	700	2.4335
	900	2.4005
	1100	2.3045

500–700 °C show narrow pore size distribution. This indicates that, the membrane samples at these temperatures had relatively uniform pore size [22]. However, when calcinations temperature was increased to 900 and 1100 °C, the pore size distribution profile for both membrane samples become wider and isotherm shape also attributed to the larger pore. This result indicates that, the uniform pore size of membrane is attributable to the crystalline formation of the alumina phase.

At higher temperatures (1100 °C), the formation of larger pores due to the collapse of the pores with shrinkage (densification process) of the material structure resulted in a strong increase in crystallite size and decrease of surface area and pore volume [23,24]. It means that, the rapidly collapse of the fine mesoporous structure started as conversion to the stable  $\alpha$ -Al<sub>2</sub>O<sub>3</sub> phase took place which is at temperature of 1100 °C. The transformation of  $\alpha$ -Al<sub>2</sub>O<sub>3</sub> occurred at calcinations temperature of higher than 1000 °C [25]. As stated by Gestel et al., after  $\alpha$ -Al<sub>2</sub>O<sub>3</sub> transformation, pore size grew up which was accompanied by strong surface area reduction. In 1964, Lippens and de Boer using XRD analysis found that alumina went through several transition stages depending upon the temperature [20]:



It was noted that poorly crystalline AlOOH could convert to  $\gamma$ -Al<sub>2</sub>O<sub>3</sub> at temperatures as low as 450 °C [25].

The surface fractal dimensions, *D* of the palladium-alumina and alumina membrane are listed in Table 2. The experimental data fitted the model will with an *r*-squared of more than 0.99 for each fit, and *D* of the membrane have been recovered from the slopes of the plots according to the FHH equation (Eq. (2)). It shows that, the *D* value displays an almost similar trend of result for both membrane samples. It can be seen that, the *D* value increased at lower calcinations temperature but starting to decrease when the calcinations temperature increased to higher temperature. For the alumina membrane, increasing the calcinations temperature from 500 to 900 °C resulted an increasing in the surface fractal dimension from 2.37 to 2.48. This is due to the pore formation mechanism of the membrane which caused higher surface roughness and more irregular surfaces [3]. This indicates that, the surface roughness increased as the calcinations temperature increased from 500 to 900 °C for alumina

membrane. Wei and Wang [3] stated that, calcinations process induces a restructuring phenomenon and results in the increase of the mass fractal dimension of alumina clusters; hence there will be slight increase of surface fractal dimension in the membrane. The increasing in pore surface fractal dimension also can be associated with the appearance of new pores due to solubilization of membrane constituents and to the crystallization of alumina substances inside the pores, making them narrower and with more irregular surface [26].

However, at 1100 °C the surface fractal dimension of alumina membrane decreased to 2.31 as shown in Table 2. As stated by Huang et al. [27], the deformation mechanism of the pore size will occur at higher calcinations temperature. At higher calcinations temperature, the formation of larger pores occurred due to the collapse of the pores and this leads to decrease in porosity [24]. The broadening of pores contributed to the decrease of surface fractal dimension [27]. Wei and Wang [3] also stated that, pores located between alumina clusters will collapse as calcinations temperature increases because alumina clusters are swallowed by larger ones.

Similar trend was observed for palladium-alumina membrane (shown in Table 2). However this membrane shows the decreasing surface fractal dimension at 900 °C (compared to 1100 °C for alumina). The value of surface fractal of palladium-alumina membrane increased from 2.36 to 2.43 as temperature increased from 500–700 °C and decreased to 2.40 and 2.30 after calcined at 900 and 1100 °C, respectively. This result was consistent with the deduction from adsorption isotherms and pore size distribution analysis. At temperature of 1100 °C, membrane exhibit a wider pore size distribution (Fig. 3), thereby indicated that the membrane are not porous and this contributed to the smoother surface of membrane. Similar trend was reported by Wei and Wang [3] and Huang et al. [27].

It also can be seen from Table 2, the palladium-alumina membrane have smoother pore surface compared to alumina membrane as their fractal dimension was lower than alumina. These are due to the pore formation in composite membrane becomes rather more complex than alumina membrane because the porous network in the composite membrane is controlled by both the metal particles and the alumina clusters aggregation mechanism [27]. The decreasing of surface fractal was due to the pore blocking effect which is a metal particle in alumina membrane clogged some membrane pores and made the pore surface of the membrane smoother and this also related to the decreasing of porous texture of membrane surface [28]. This occurrence will be discussed more in effect of palladium on membrane microstructure.

### 3.2. Effect of palladium

The palladium solution with concentration of 0.5 and 2 g palladium in 100 ml of deionized water were used in this study. The volume ratio of palladium to alumina sol employed in this work was varied from 2:100 to 8:100. Acid concentration of 5 M and 4:100 volume ratio of PVA (4 g PVA/100 ml deionized water) to sol were added in sol.

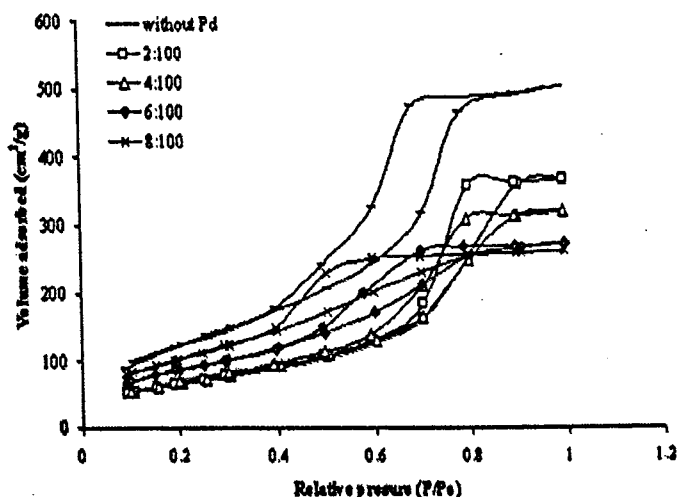


Fig. 4. Adsorption-desorption isotherms of palladium-alumina membrane with different amount of palladium.

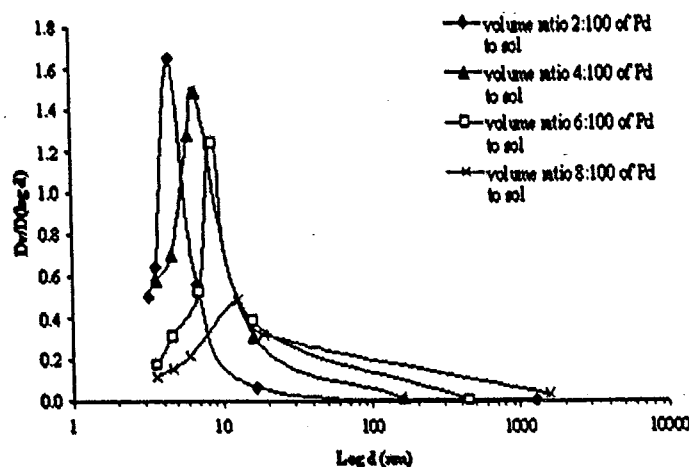


Fig. 5. Pore size distribution of palladium-alumina membrane with different amount of palladium.

The nitrogen adsorption/desorption isotherms on palladium-alumina membranes (2 g Pd/100 ml H<sub>2</sub>O with different volume ratio of palladium to sol) calcined at 700 °C for 24 h are shown in Fig. 4, in which isotherm of pure alumina membrane is also presented as comparison. The isotherms of entire membrane samples at calcinations temperature of 700 °C exhibited type IV isotherm. This means that all samples were porous that contained mostly mesopores area.

Fig. 5 shows the pore size distribution of palladium-alumina membrane with different amount of palladium using concentration of 2 g Pd/100 ml H<sub>2</sub>O. It clearly shows that the pore size distribution profiles become wider, average pore size gradually increased and pore volume slightly decreased as the palladium amount increase. The result shows that, with increasing palladium amount, it will decrease homogeneity distribution of pore due to the surface screening effects (pore blocking by palladium metal). This effect also leads to smoothing membrane pore surface. Based on the result, the optimum palladium concentration that was chosen is 2 g Pd/100 ml H<sub>2</sub>O with volume ratio 6:100

Table 3

Surface fractal dimension of palladium-alumina membranes with different volume ratios of palladium to sol after calcined at 700 °C by FHH model

Volume ratio of palladium to sol	Surface fractal dimension, <i>D</i>	
	0.5 g Pd/100 ml H <sub>2</sub> O	2 g Pd/100 ml H <sub>2</sub> O
2:100	2.4922	2.4594
4:100	2.4894	2.4489
6:100	2.4690	2.4335
8:100	2.4529	2.4058

of palladium to sol. This deduction further examined by fractal analysis to determine more on the changes in surface roughness.

The surface fractal dimensions, *D* of membrane synthesized using palladium concentration of 0.5 g Pd/100 ml H<sub>2</sub>O and 2 g Pd/100 ml H<sub>2</sub>O with different volume ratio of palladium to sol were measured from FHH model and the data was fit with the correlation. *D* values calculated from the slope of the linear portion of the log-log plots are listed in Table 3. It can be seen that,

the surface fractal dimensions decreased significantly with increasing amount of palladium to sol. It clearly shows that, the  $D$  value for membrane using higher palladium concentration (2 g Pd/100 ml H<sub>2</sub>O) was lower than  $D$  value for membrane using lower palladium concentration (0.5 g Pd/100 ml H<sub>2</sub>O). This indicates that the pore surface of alumina became smoother and less irregular as it contains more palladium particles. The smoothing of pore surface roughness was due to the blocking of alumina pore by palladium particles [28]. The agglomerated would enlarge metal particle size when the metal amount increased [29,30]. A larger palladium particle may screen some membrane surface irregularity regions, and this effect make it a smoother surface [3]. As stated by Lee et al. [28], larger metal particles will enlarge the mean pore size. This large metal particle would close some smaller pores and which becomes in accessible for the nitrogen molecule during membrane analysis and then lead to the decreasing in the BET surface area and pore volume [28,30].

This analysis shows that, homogeneity of palladium-alumina pore surface depends on the palladium content. As reported by Blacher et al. [13], fractal behavior does not reflect the structure of the basic object (such as pores structure or clusters) but their distributions. El-Shafei et al. [10] also stated that, rough surfaces may be divided into two general categories; roughness due to the presence of uniform pores and roughness due to the presence of a distribution of pore sizes.

Figs. 6a, 6b, and 6c show TEM image of palladium-alumina membrane containing palladium concentration of 2 g Pd/100 ml H<sub>2</sub>O with a 6:100, 8:100, and 10:100 volume ratio of palladium to sol respectively. The effect of palladium amount on the shape and size of the palladium particle was observed and was in agreement with finding that was reported by Chen et al. [29]. The crystallite spherical shape of palladium particles with size range of 5–15 nm were observed for the membrane sample containing 6:100 volume ratio of palladium to sol (Fig. 6a). TEM observations of palladium-alumina membrane as can be seen in Fig. 6a reveal that palladium particles are well dispersed within the alumina matrix. When volume ratio of palladium to sol increased up to 8:100 and 10:100, the palladium size increased to 10–30 and 15–50 nm, respectively, that was evaluated from TEM micrograph. The palladium particle in sample containing 8:100 and 10:100 volume ratio of palladiums to sol were less well dispersed in alumina matrix as can be seen in Figs. 6b and 6c compared to sample containing 6:100 volume ratios of palladium to sol (Fig. 6a).

These results show that, with increasing the palladium amount, the size of palladium particle increased. The dispersing of palladium particle also would be less dispersed which they tend to convergent or concentrated at some part of the membrane. This is due by palladium particles that agglomerated in the alumina matrix which is lead to the growing of the palladium particle to larger sizes as the palladium amounts increased [30]. From this result, it can be concluded that, the decreasing of surface area and increasing in pore size as Pd amount was increased were due to the pore blocking effect caused by the metal particles that agglomerated and located along the pore channel.

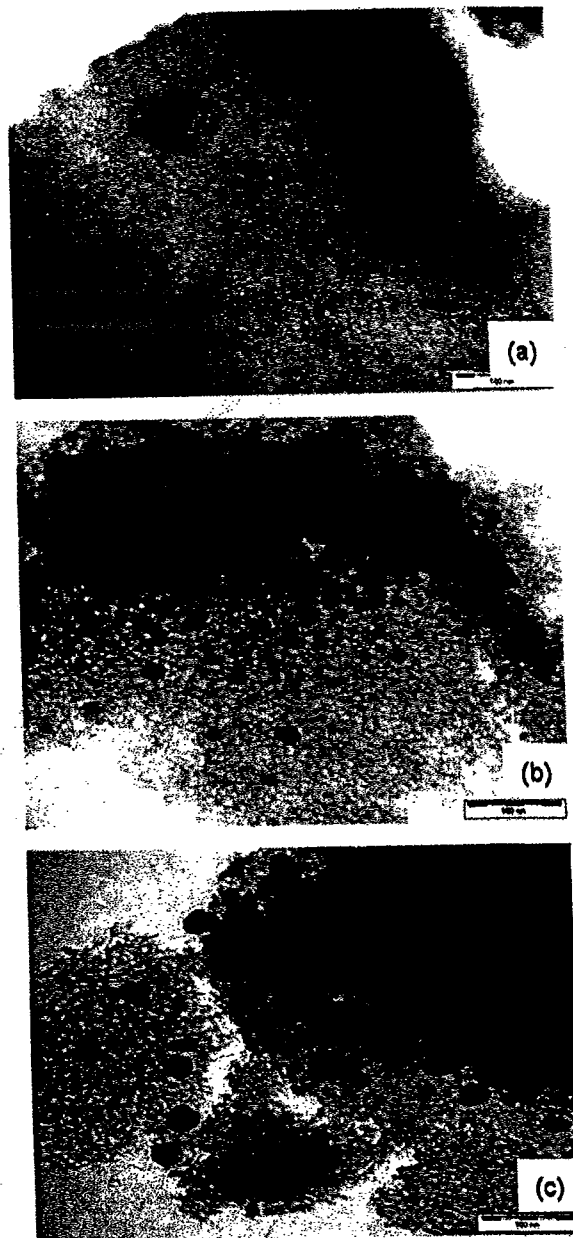


Fig. 6. TEM images of palladium-alumina membrane at calcination temperature of 700 °C containing Pd concentration of 2 g Pd/100 ml H<sub>2</sub>O with (a) 6:100 volume ratio of Pd to sol, (b) 8:100 volume ratio of Pd to sol, and (c) 10:100 volume ratio of Pd to sol.

### 3.3. Effect of PVA

Polyvinyl alcohol (PVA) was used as a binder to prevent the formation of cracks and increase the strength of materials and also adjust the viscosity of membrane sol. It has been used for a long time in many ceramic applications. The high binding strength, water solubility, anti heat stress agent and cost effectiveness have made it a reliable performer [31].

Based on the preliminary study, the optimum PVA concentration in this study is 4 g PVA/100 ml H<sub>2</sub>O with volume ratio

4:100 of PVA to sol was chosen. The volume ratio of PVA to sol was varied from 2:100 to 8:100. 6:100 volume ratio of palladium (2 g Pd in 100 ml deionized water) to alumina sol and 5 M of acid concentration were used in this work. Calcinations process was done at 700 °C. The effect of PVA on the surface fractal dimension of membrane,  $D$  which obtained from the slope of the plots is listed in Table 4. It shows that, the surface fractal dimension decreased with increased of volume ratio of PVA to sol. The surface fractal dimension of membrane with binder was lower than that without binder. These indicate that the addition of binder reduces the irregularity of the membrane surface. The decrease in  $D$  value may be attributed to the dispersion of binder into the narrow pores of alumina and smoothing out of the surface, as reported by Tsay et al. [32] in their work. The increasing amount of PVA increases the pore size of the membrane. Higher PVA amount promotes agglomeration of the ceramic particles, which on calcinations leads to wider pore size [33]. The agglomeration causes inhomogeneous grain growth. When the PVA concentration in the sol was fairly low, the sol became highly dispersed. Well-dispersed sol tends to produce homogeneous product [34].

Table 4  
Surface fractal dimension of palladium-alumina membranes with different volume ratios PVA to sol after calcined at 700 °C by FHH model

Volume ratio of PVA to sol	Surface fractal dimension, $D$
Without PVA	2.5600
2:100	2.4705
4:100	2.4335
6:100	2.3799
8:100	2.3446

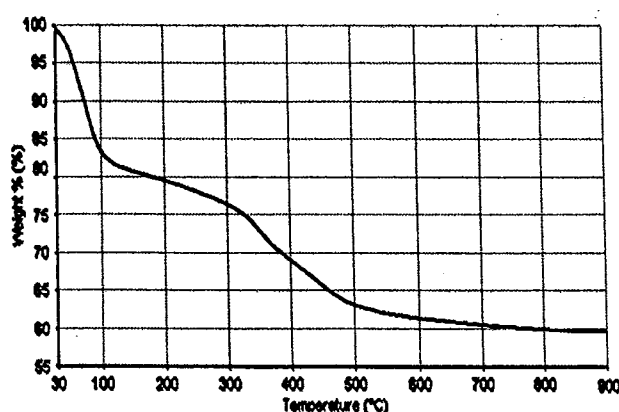


Fig. 7. TGA curve of palladium-alumina dried membrane dried at ambient temperature for 48 h under  $N_2$  flow at  $20^\circ C \text{ min}^{-1}$ .

Thermogravimetric analysis (TGA) was performed to determine the membrane's weight loss during calcinations and to investigate the temperature for complete decomposition of the hydroxyl and organics compound such as PVA. The analysis was performed on the dried membrane gel that was dried in ambient temperature for 48 h. TGA curve for the composite membrane is shown in Fig. 7. Three stages of weight loss occurred as can be seen in Fig. 7. In the first stage (30–130 °C), a drastic weight loss of 20% was observed. This is due by evaporation of residual alcohol and water and also the pyrolysis of the surfactant and residual organics (copolymer). In the second stage at 130–700 °C, weight loss of 20% was observed. The weight loss at this stage was due to the thermal decomposition of surface organic (hydroxyl and alkoxy) groups and removal of water during the phase transformation of  $\gamma\text{-Al}_2\text{O}_3$  ( $2[\text{Al}(\text{OH})_3] \rightarrow \gamma\text{-Al}_2\text{O}_3 + \text{H}_2\text{O}$ ). In the third stage at 700–900 °C, a small weight loss of 1% occurred due to the crystallized phase transformation of alumina ( $\gamma$ - to  $\delta$ - and  $\theta$ - $\text{Al}_2\text{O}_3$ ). The results suggest that during the calcination process the organic groups or substantial portion of the copolymer was pyrolyzed at 130 °C but not completely removed until 700 °C. Based on the observed result, the minimum calcination temperature for palladium-alumina membrane was 700 °C. At these observed temperature, copolymer or organic compounds were completely removed [22].

#### 3.4. Effect of acid concentration

Membrane containing volume ratio 6:100 of palladium to sol with concentration of 2 g Pd/100 ml  $\text{H}_2\text{O}$  with different acid concentration (1, 5, 10, and 15 M) were compared to study the effects of the acid concentration on pore structure and pore surface fractal dimension of membrane. Mol ratio acid to aluminum was 0.07:1 for all acid concentration that was used. 4:100 volume ratio of PVA (4 g PVA/100 ml deionized water) to sol were added in sol and the gels were dried and calcined at 700 °C. Table 5 shows the palladium-alumina sol characteristics and membrane properties data at calcinations temperatures of 700 °C with different acid concentrations during synthesis. It can be seen that, the pH value of sol gradually decreased when acid concentration increased. It is noticeable from Table 5 that, the membrane pore size, pore volume and BET surface area decreased gradually with increasing acid concentration at calcinations temperature of 700 °C. Similar trend of finding were also reported in the previous literatures. The pore volume and the surface area diminished with increasing acid concentration and with lower pH value. As reported by Haas-Santo et al., higher pH promotes polycondensation reactions [14,25]. At lower acid concentration, the stability of alumina particles decreases and hence causes higher agglomeration of the alu-

Table 5  
The effect of different acid concentrations on sol and membrane characteristic properties

Acid (M)	pH	Sol appearance	BET surface area ( $\text{m}^2/\text{g}$ )	Pore size (nm)	Pore volume ( $\text{cc}/\text{g}$ )
1	6.84	Sedimentation appear	199.5	10.67	0.4031
5	5.40	Well dissolve sol	189.5	7.45	0.3948
10	4.98	Well dissolve sol	175.2	7.05	0.3759
15	3.18	Well dissolve sol	142.4	6.59	0.3735

Table 6  
Surface fractal dimension of palladium-alumina membrane with different acid concentrations calcined at 700 °C

Acid concentration (M)	Surface fractal dimension, <i>D</i>
1	2.4328
5	2.4335
10	2.4814
15	2.4822

mina particles, which results in the increase of pore size [9]. This suggests that, sol containing 1 M acid concentration cannot stabilize the sol which is tend to agglomerated and produce larger pore size.

It was found that, palladium-alumina sol with 1 M acid concentration shows sedimentation appeared. As stated by Huang et al., stable sols can not be obtained when the concentration of peptization acid is too low [15]. This suggests that, sol containing 1 M acid concentration cannot stabilize the sol which is tend to agglomerated and produce larger pore size. With increasing acid concentration to 5 M and above a well dispersed and well dissolved sol was obtained. The state of sol also has an important influence on the structure of membrane after calcined. Well dissolved sol tends to produce homogeneous membrane. While membrane formed from sol that was not fully dissolved or agglomerated sol tends to have larger pore after calcined [34]. As reported by Haas-Santo et al., higher pH promotes polycondensation reactions. If the gel network is not very strong and does not have any high degree of condensation, e.g., at a lower pH value, it collapses during heat treatment, leading to a dense structure with a low specific surface area. Based on the result, acid concentration of 5 M is chosen in membrane synthesis [25].

The fractal dimension, *D* which obtained from the slope of the FHH plots is listed in Table 6. It shows that, the membrane samples prepared with higher acid concentration gave the higher surface fractal dimension compared to the membrane samples prepared with lower acid concentration. The *D* value increased from 2.43 to 2.48 as acid concentration increased from 1 to 15 M. This indicated that, with increasing acid concentration the pore surface roughness of the membrane surface increased due to formation of smaller pore with homogeneous and this was in agreement with the result observed for palladium-alumina microstructure properties.

#### 4. Conclusions

The fractal analysis allows us to study and to understand a wide range of phenomena associated with the complex structure of porous material by quantifying the degree of geometry irregularities through a single number; the surface fractal dimension, *D*. The surface fractal dimension, *D*, of the palladium-alumina ceramic membranes have been evaluated from their nitrogen adsorption isotherms by FHH method. Calcinations temperature induces a change of pore surface roughness of porous materials. The surface fractal dimension of palladium alumina membrane increases slightly when the calcinations temperature rises from 500 to 700 °C and then decreases at 900 and 1100 °C.

This phenomenon can be explained by deformation mechanism of the pore size. Alumina undergoes several structural reforming phases with increasing temperature which attribute to the changes of pore size. When the calcinations temperature increases, the average pore size increase and the pore volume decrease caused by volume shrinkage, which eliminates some smaller pores. With the increasing of palladium amount, the average pore size of the membrane increase and the surface fractal value of palladium-alumina membrane decrease, indicating to the smoothening of surface structure. The decreasing in surface fractal was due to the pore blocking effect caused by metal particles that agglomerated and close some membrane smaller pores. Meanwhile, PVA will reduce the surface irregularities of membrane and thus lower the value of fractal dimension, *D*. Smaller pore size was obtained when the nitric acid concentration added increase. The fractal dimension, *D* tends to increase with the increase of acid concentration in palladium-alumina ceramic membrane. Based on the observed result, it shows that the pore distribution of the membrane contributes to the irregularities and roughness of the membrane surface which is attributed to the *D* value. Surface fractal analyses also provide parameter that gives more information on pore growth of the membrane or describe the porous solid structure more effectively.

#### Acknowledgments

The authors acknowledge the research grants from USM and MOSTE which enables the production of this article.

#### References

- [1] H.B. Zhao, K. Pflanz, J.H. Gu, A.W. Li, N. Stroh, H. Brunner, G.X. Xiong, *J. Membr. Sci.* 142 (1998) 147–157.
- [2] B.S. Liu, H.X. Li, Y. Cao, J.F. Deng, C. Sheng, S.Y. Zhou, *J. Membr. Sci.* 135 (1997) 33–39.
- [3] Q. Wei, D. Wang, *Mater. Lett.* 57 (2003) 2015–2020.
- [4] W. Xu, T.W. Zerda, H. Yang, M. Gerspacher, *Carbon* 34 (1996) 165–171.
- [5] Z.H. Huang, F. Kang, W.L. Huang, J.B. Yang, K.M. Liang, M.L. Cui, Z. Cheng, *J. Colloid Interface Sci.* 249 (2002) 453–457.
- [6] T. Lours, J. Zarzycki, A. Craievich, D.I. dos Santos, M. Aegerter, *J. Non-Cryst. Solids* 95–96 (1987) 1151–1158.
- [7] D.W. Schaefer, K.D. Keefer, *Phys. Rev. Lett.* 56 (1986) 2199–2202.
- [8] F. Chaput, J.P. Boilot, A. Dauge, F. Devreux, A. de Geyer, *J. Non-Cryst. Solids* 116 (1990) 133–139.
- [9] G.J. Lee, S.I. Pyun, *Carbon* 43 (2005) 1778–1814.
- [10] G.M.S. El-Shafei, C.A. Philip, N.A. Moussa, *J. Colloid Interface Sci.* 277 (2004) 410–416.
- [11] C.K. Lee, C.S. Tsay, *J. Phys. Chem. B* 102 (1998) 4123–4130.
- [12] F. Meng, J.R. Schlup, L.T. Fan, *J. Colloid Interface Sci.* 197 (1998) 88–93.
- [13] S. Blacher, B. Heinrichs, B. Sahouli, J.P. Pirard, *J. Colloid Interface Sci.* 226 (2000) 123–130.
- [14] B.E. Yoldas, *Ceram. Bull.* 54 (33) (1975) 289–290.
- [15] X.R. Huang, G.L. Meng, Z.T. Huang, J.M. Geng, *J. Membr. Sci.* 133 (1997) 145–150.
- [16] M. Mulder, *Basic Principles of Membrane Technology*, Kluwer, Dordrecht, 1996.
- [17] B.I. Lee, E.J.A. Pope, *Chemical Processing of Ceramic*, Dekker, New York, 1994.
- [18] D. Quattrini, D. Serrano, S.P. Catan, *Granul. Matter* 3 (2001) 125–130.
- [19] S. Lowell, J.E. Shields, *Powder Surface Area and Porosity*, Chapman & Hall, New York, 1991.

- [20] T. Van Gestel, C. Vandecasteele, A. Buckenhoudt, C. Dotremont, J. Luyten, R. Leysen, B.V. der Bruggen, G. Maes, *J. Membr. Sci.* 207 (2002) 73–89.
- [21] A.F.M. Leenars, K. Keizer, A.J. Burgraff, *J. Mater. Sci.* 19 (1984) 1077–1088.
- [22] F. Dumeignil, K. Sato, M. Imamura, N. Matsubayashi, E. Payen, H. Shimada, *Appl. Catal. A Gen.* 6361 (2002) 1–11.
- [23] A.P. Guimaraes, A.P.P. Viana, R.M. Lago, N.D.S. Mohallen, *J. Non-Cryst. Solids* 304 (2002) 70–75.
- [24] C. Falamaki, M.S. Afarani, A. Aghaie, *J. European Ceram. Soc.* 24 (2004) 2285–2292.
- [25] K. Haas-Santo, M. Fichtner, K. Schubert, *Appl. Catal. A Gen.* 220 (2001) 79–92.
- [26] J.L.P. Bernal, M.A.B. Lopez, *Appl. Surf. Sci.* 161 (2000) 47–53.
- [27] W.L. Huang, S.H. Cui, K.M. Liang, S.R. Gu, *J. Phys. Chem. Solids* 62 (2001) 1205–1211.
- [28] J.F. Lee, C.K. Lee, L.C. Juang, *J. Colloid Interface Sci.* 217 (1999) 172–176.
- [29] H.I. Chen, J.D. Shiau, C.Y. Chu, T.C. Huang, *Separat. Purif. Technol.* 32 (2003) 247–254.
- [30] Y. Wu, Y. Zhang, L. Zhang, *China Particology* 2 (1) (2004) 19–24.
- [31] C.K. Lambert, R.D. Gonzalez, *Mater. Lett.* 38 (1999) 145–150.
- [32] C.S. Tsay, C.K. Lee, A.S.T. Chiang, *Chem. Phys. Lett.* 278 (1997) 83–90.
- [33] N. Das, H.S. Maiti, *J. Membr. Sci.* 140 (1998) 205–212.
- [34] G. Tari, S.M. Olhero, J.M.F. Ferreira, *J. Mater. Process. Tech.* 137 (2003) 102–109.



# Effect of thermal treatment on the microstructure of sol–gel derived porous alumina modified platinum

M.R. Othman \*, N.N.N. Mustafa, A.L. Ahmad

*School of Chemical Engineering, Engineering Campus, Universiti Sains Malaysia, Seri Ampangan, 14300 Nibong Tebal, Pulau Pinang, Malaysia*

Received 11 July 2005; received in revised form 5 December 2005; accepted 8 December 2005

Available online 25 January 2006

## Abstract

Thin films of sol–gel derived Pt/alumina were prepared from a boehmite solution containing alumina-*sec*-butoxide and chloroplatinic acid. At 1100 °C,  $\gamma$ -Al<sub>2</sub>O<sub>3</sub> phase was not present in the alumina sample but it remained in the Pt/alumina sample, suggesting that improved thermal stability of the  $\gamma$ -Al<sub>2</sub>O<sub>3</sub> or the transition aluminas ( $\gamma$ -,  $\delta$ - and  $\theta$ -) was achieved. Except for samples thermally treated at 1000 °C, pore size distribution profiles of both, alumina and Pt/alumina composite thermally treated at 500–900 °C demonstrated a narrow pore size distribution. Alumina and Pt/alumina treated at 500 °C, 700 °C, 900 °C and 1100 °C, exhibited a type IV isotherm according to the BDDT classification, characteristic of mesoporous materials. Increasing the calcination temperature of the alumina sample from 500 °C to 700 °C increased the fractal dimension from 2.37 to 2.46. However, further increase from 900 °C to 1100 °C caused the surface fractal to decrease from 2.43 to 2.39, respectively.

© 2005 Elsevier Inc. All rights reserved.

**Keywords:** Pt/alumina; Thermal treatment; Surface morphology; Pore structure; Fractal

## 1. Introduction

### 1.1. Inorganic membrane

Inorganic membranes have the potential of being used in gas separation, enrichment, adsorption and/or in filtration process in conditions where organic polymer membranes cannot be used. Some inorganic membranes also offer considerable promise in catalytic membrane reactor application due to their high thermal, chemical and mechanical stability at elevated temperature and chemically reactive environments [1].

Alumina is a ceramic material having a compact crystal structure, strong chemical bonding and stability. Palladium, platinum, nickel and the metals in groups 3–5 in the periodic table are all permeable and have affinity

towards hydrogen to a certain extent. Hydrogen permeable metal membranes made of platinum, palladium and its alloys are widely studied due to their high hydrogen permeability and selectivity and chemical compatibility with many hydrocarbon containing gas stream, and the fact that they exhibit infinitely high selectivity for hydrogen. Previous articles [2–7] reported about nanoparticles of palladium and platinum deposited in alumina or the other ceramic materials by sol–gel processes whether as a catalyst or membrane. In this work, the study of the effect of thermal treatment on the microstructure of sol–gel derived alumina modified platinum was carried out and results are reported. The sol–gel method was chosen in this study because it allows for the control of pore size, surface area and uniformity of particle dispersion in a solution [1,8–12].

In the study of microporosity, hysteresis loops obtained from adsorption/desorption analysis can be used to correlate pore shape or structure. Five different types of hysteresis loops are commonly encountered. Type A hysteresis is principally due to cylindrical pores open at both ends. Type B hysteresis is principally due to slit-shaped pores

\* Corresponding author. Tel.: +604 5996426; fax: +604 5941013.

E-mail addresses: [chroslee@eng.usm.my](mailto:chroslee@eng.usm.my), [mohd\\_roslee@yahoo.com](mailto:mohd_roslee@yahoo.com) (M.R. Othman).

or the space between parallel plates. Type C hysteresis is principally due to a mixture of tapered or wedge-shaped pores with open ends. Type D hysteresis is principally due to tapered or wedge-shaped pores but with narrow necks at one or both open ends. Type E hysteresis is principally due to McBain's 'bottle neck' pores, the so-called 'bottle neck' shape [13].

The characterization of the micropore structure is of great importance. It is well known that the performance of membranes depends on their structure and morphology. The magnitude of the surface fractal dimension of membranes has great influence on physico-chemical processes

such as adsorption, surface diffusion and catalysis. Fractal analysis provides a parameter characterizing irregularities on a surface and was used to investigate the surface morphology. The surface fractal is an important parameter that reflects the roughness of pore surface. The surface area and pore size distribution alone may not describe the characteristics of the pore structure of membrane. Surface fractal dimension,  $D$ , ranging from  $D = 2$ , for perfectly smooth surfaces, to  $D = 3$ , for sponge-like surfaces, can be used to describe the irregularities and roughness of pore surfaces. The following Frenkel–Halsey–Hill (FHH) model can be used to determine  $D$ :

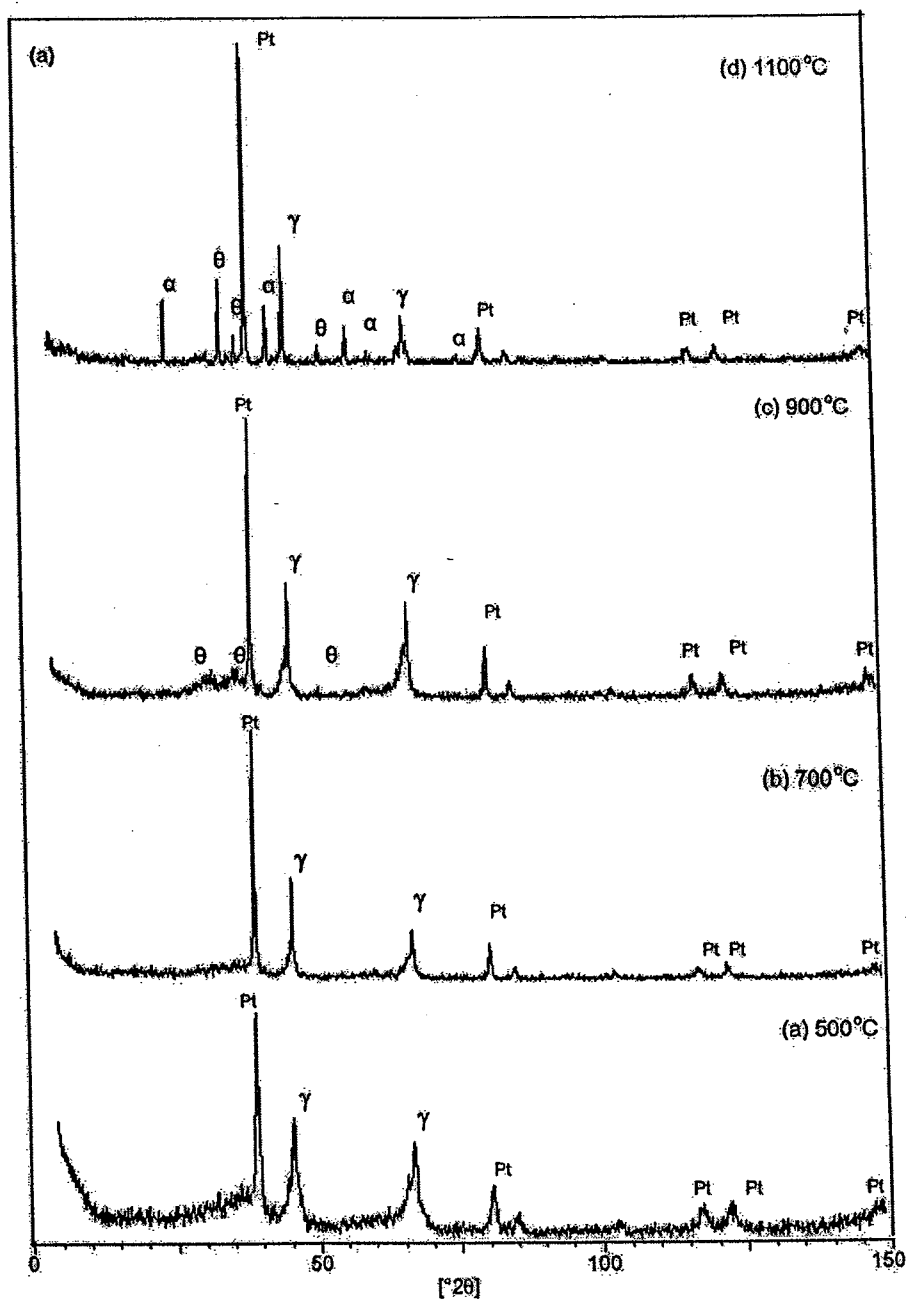


Fig. 1. X-ray diffraction patterns of the (a) Pt/alumina after being calcined at different temperatures and (b) alumina and Pt/alumina after being calcined at 1100 °C showing transition alumina phases ( $\gamma$ -,  $\delta$ - and  $\theta$ -) and metal Pt.



$$\frac{N}{N_m} = \left[ \ln \left( \frac{P_0}{P} \right) \right]^{(D-3)} \quad (1)$$

In Eq. (1),  $N$  is the number of adsorbed moles of nitrogen at the given relative pressure,  $P/P_0$ ;  $N_m$  is the number of adsorbed moles in monolayer;  $P/P_0$  is the relative pressure of nitrogen adsorbed. The value of  $N_m$  and  $N$  can be obtained from the BET model given by Eq. (2), and the surface fractal dimension,  $D$  can be calculated from the slope of a plot of  $\ln(N/N_m)$  vs.  $\ln[\ln(P_0/P)]$ :

$$\ln = \left( \frac{N}{N_m} \right) = (D - 3) \ln \left[ \ln \left( \frac{P_0}{P} \right) \right] \quad (2)$$

## 2. Experiment

### 2.1. Preparation of Pt–alumina membranes

The Pt/ $\gamma$ - $\text{Al}_2\text{O}_3$  gels were formed using a sol–gel procedure based on the work of Yoldas [14]. In a typical synthesis, aluminum *sec*-butoxide was mixed with deionized water and butanol for 15 min at temperatures of  $\sim 90^\circ\text{C}$ . The molar ratio used was  $\text{Al}(\text{OC}_4\text{H}_9)_3:\text{H}_2\text{O}:\text{HNO}_3 = 1:100:0.07$  with the addition of 25 ml butanol. After 15 min, 6 vol% of 0.2 g  $\text{H}_2\text{PtCl}_6$  dissolved in 100 ml deionized water was added directly to the sol. The mixture was stirred vigorously in a closed beaker for 30 min. Then the sol was peptized for 24 h at temperature of  $\sim 90^\circ\text{C}$  by adding  $\text{HNO}_3$ . Then the sol was allowed to cool slowly and steadily at ambient temperature to form a dried gel. The dried samples were then thermally treated at 500–1100  $^\circ\text{C}$  for 24 h to form Pt–alumina composites.

### 2.2. Characterization of the membranes

The morphology of the films was examined using a scanning electron microscope (SEM), Leo. Supra 50 VP from Germany. Porosities, surface area, pore volume and pore sizes of the samples were analyzed using Autosorb I (Quantachrome, Nova 1200). XRD analysis was carried out to determine phase composition and the crystal structure of the sample using a Philips PW 1729 X-ray generator, Philips PW 1820 diffractometer ( $\text{CuK}\alpha$  radiation and graphite monochromator) and Philips PW 1710 diffraction controller.

## 3. Results and discussion

Fig. 1(a) shows the XRD pattern for the Pt– $\text{Al}_2\text{O}_3$  composite after thermal treatment at a temperature of 500, 700, 900 and 1100  $^\circ\text{C}$ , respectively. Peaks of  $\gamma$ - $\text{Al}_2\text{O}_3$  and metallic platinum were clearly visible at all temperatures, indicating a well-crystallized phase was achieved. The intensity of  $\gamma$ - $\text{Al}_2\text{O}_3$  and metallic Pt peaks increased as the temperature increases, indicating that the degree of crystallinity of alumina and platinum particle increased. At 900  $^\circ\text{C}$ , the crystalline phase of  $\theta$ - $\text{Al}_2\text{O}_3$  started to form. When the temperature was increased to 1100  $^\circ\text{C}$ , more intense peaks and the appearance of  $\alpha$ - $\text{Al}_2\text{O}_3$  phase were observed in the XRD spectra [4].  $\gamma$ - $\text{Al}_2\text{O}_3$  phase remained at all temperature conditions. This is different from alumina sample treated at 1100  $^\circ\text{C}$  (Fig. 1(b)) where the  $\gamma$ - $\text{Al}_2\text{O}_3$  phase was no longer in existence. This shows that the thermal stability of  $\gamma$ - $\text{Al}_2\text{O}_3$  or the transition aluminas ( $\gamma$ -,  $\delta$ - and  $\theta$ -) modified platinum was improved remarkably.

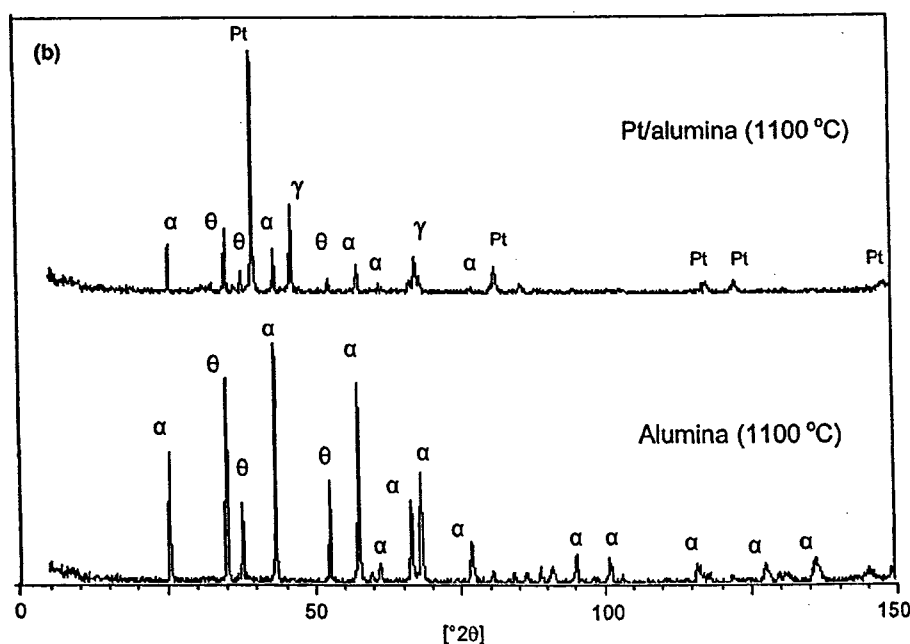


Fig. 1 (continued)

Fig. 2 shows the effect of the thermal treatment on the surface area, pore diameter, and pore volumes of alumina and Pt/alumina. This data were obtained from nitrogen adsorption/desorption analysis. The texture of the alumina and Pt/alumina also changed with the thermal treatment. The surface area decreased as the temperature increased for both sample due to particle agglomeration. The total pore volume also decreased with increasing thermal treatment but the pore sizes increased as shown in Fig. 2(a).

Fig. 3(a) and (b) shows broadened pore size distribution as the temperature was increased. This was due to the collapse of the pores with the shrinkage of the material structure as the temperature increased. Except for samples thermally treated at 1000 °C, pore size distribution profiles of both, alumina and Pt/alumina composite thermally treated at 500–900 °C demonstrated narrow pore size distribution.

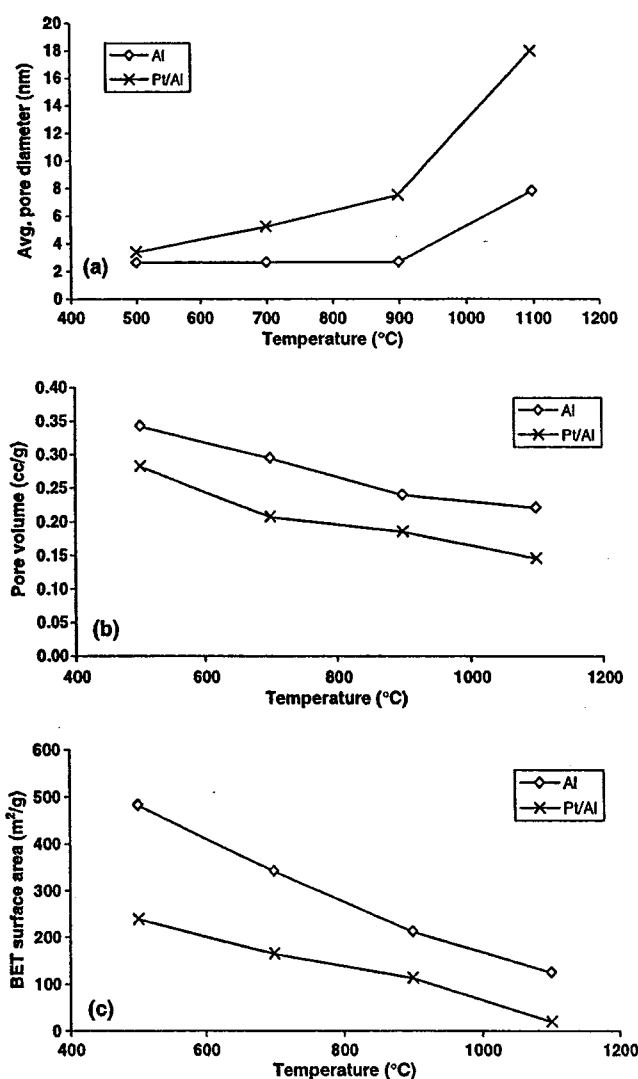


Fig. 2. (a) Average pore diameter, (b) pore volume, and (c) BET surface area of alumina and Pt/alumina membranes as a function of heat treatment temperature.

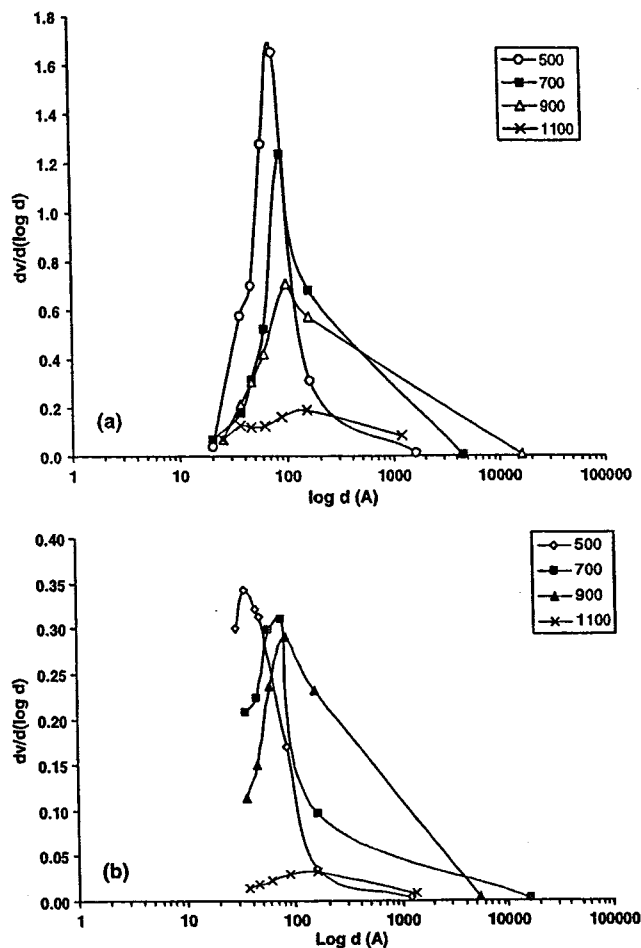


Fig. 3. Pore size distribution of (a) alumina samples and (b) Pt/alumina samples from the adsorption branch of the isotherm.

A typical isotherm for the alumina and Pt/alumina treated at 500 °C, 700 °C, 900 °C and 1100 °C, are shown in Figs. 4 and 5 respectively. All of them exhibited a type IV isotherm based upon the BDDT classification, that the characteristics of the sample were typical of mesoporous materials, associated with high BET values as well as a marked hysteresis associated with capillary condensation in the mesopore range (20–1000 Å) [13,15]. The hysteresis loop for the alumina and Pt/alumina sample moves toward higher relative pressure values as the temperature of treatment increased, indicating that pore sizes increased as well.

For the alumina calcined at temperature of 500 °C and 700 °C, the observed isotherm curves were those characteristic of ink bottle type pores (type E). Pt/alumina samples heated at temperature of 500 °C, 700 °C and 900 °C also exhibited ink bottle shape pore characteristics. The isotherm shape progressively changed with increasing temperature. Alumina samples heated at 900 °C exhibited cylindrical type pore (type A) and both of alumina and Pt/alumina samples thermally treated at 1100 °C exhibited type C feature, corresponding to tapered or wedge-shaped pores with open ends (V shape).

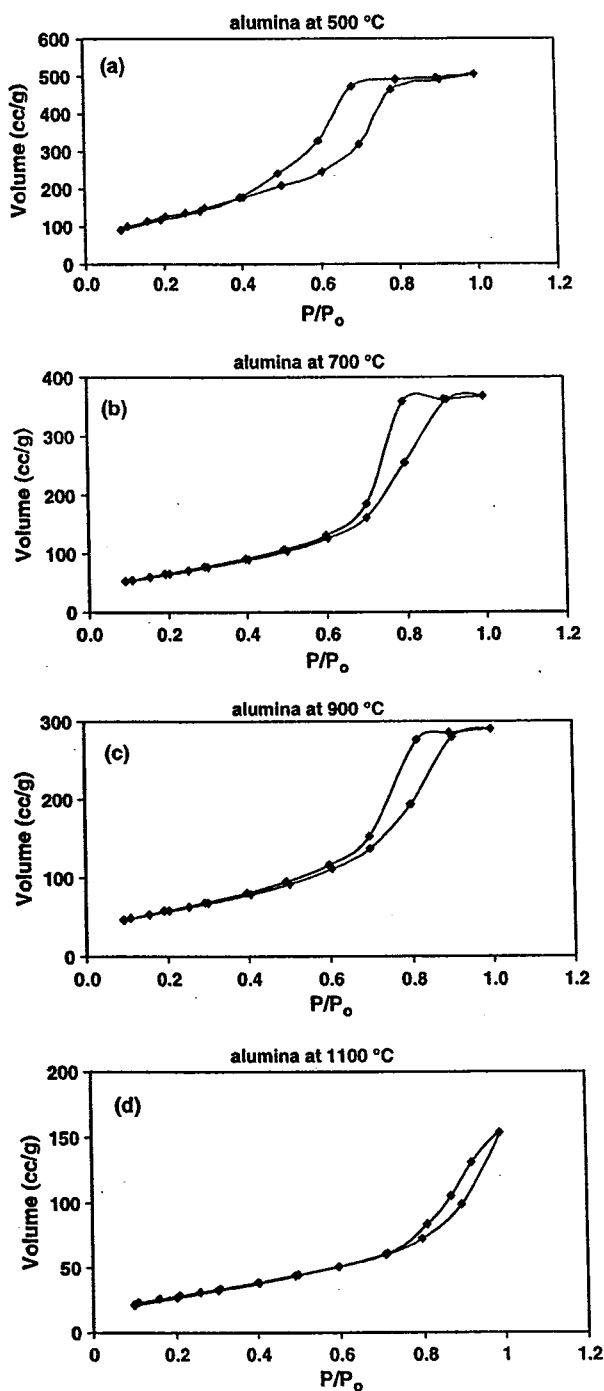


Fig. 4. Adsorption/desorption isotherms of alumina calcined at (a) 500 °C, (b) 700 °C, (c) 900 °C and (d) 1100 °C.

The surface fractal dimensions were determined from their nitrogen adsorption isotherms by means of the Frenkel–Halsey–Hill (FHH) method. Fig. 6(a) and (b) shows FHH plots of alumina and Pt/alumina membrane respectively at different calcinations temperature and the surface fractal dimensions are listed in Table 1.  $D$  values calculated from the slope of the linear portion of these log-log plots

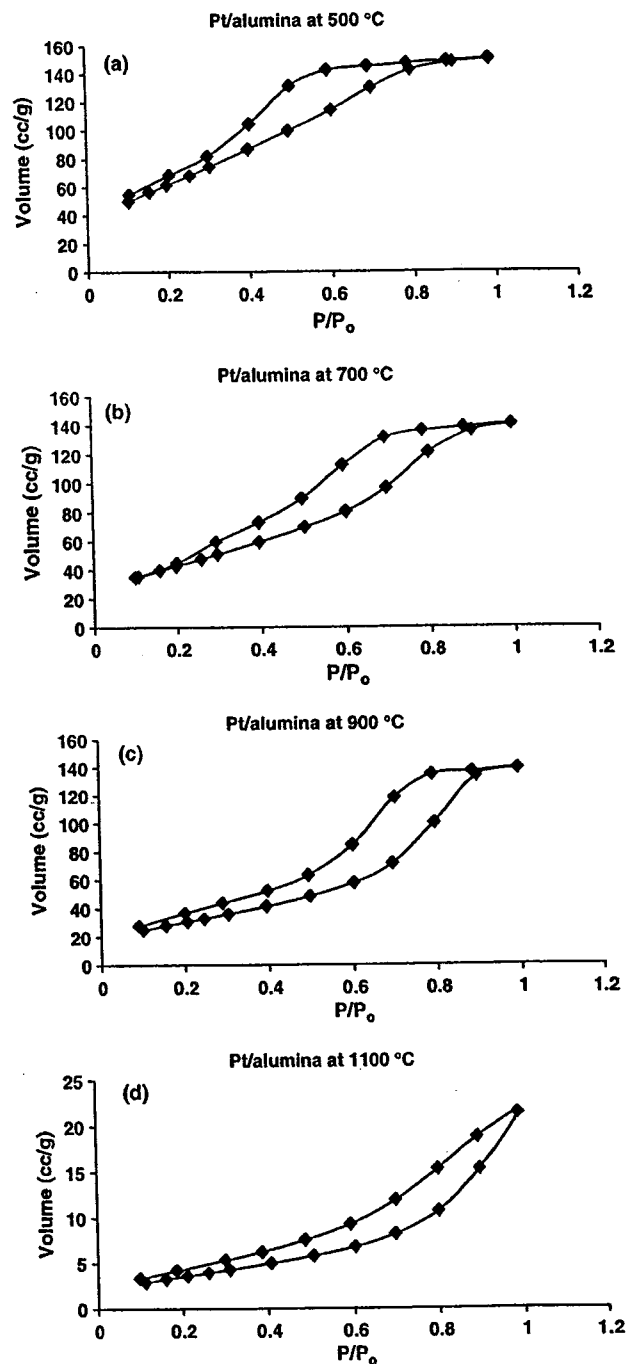


Fig. 5. Adsorption/desorption isotherms of Pt/alumina samples calcined at (a) 500 °C, (b) 700 °C, (c) 900 °C and (d) 1100 °C.

based on Eq. (2). Increasing the calcination temperature of the alumina samples from 500 °C to 700 °C increased the fractal dimension from 2.37 to 2.46. However, further increase from 900 °C to 1100 °C caused the surface fractal to decrease from 2.43 to 2.39, respectively. This is probably due to smoothing of the surface as particles melted and agglomerated as reported in [16]. Pores located between

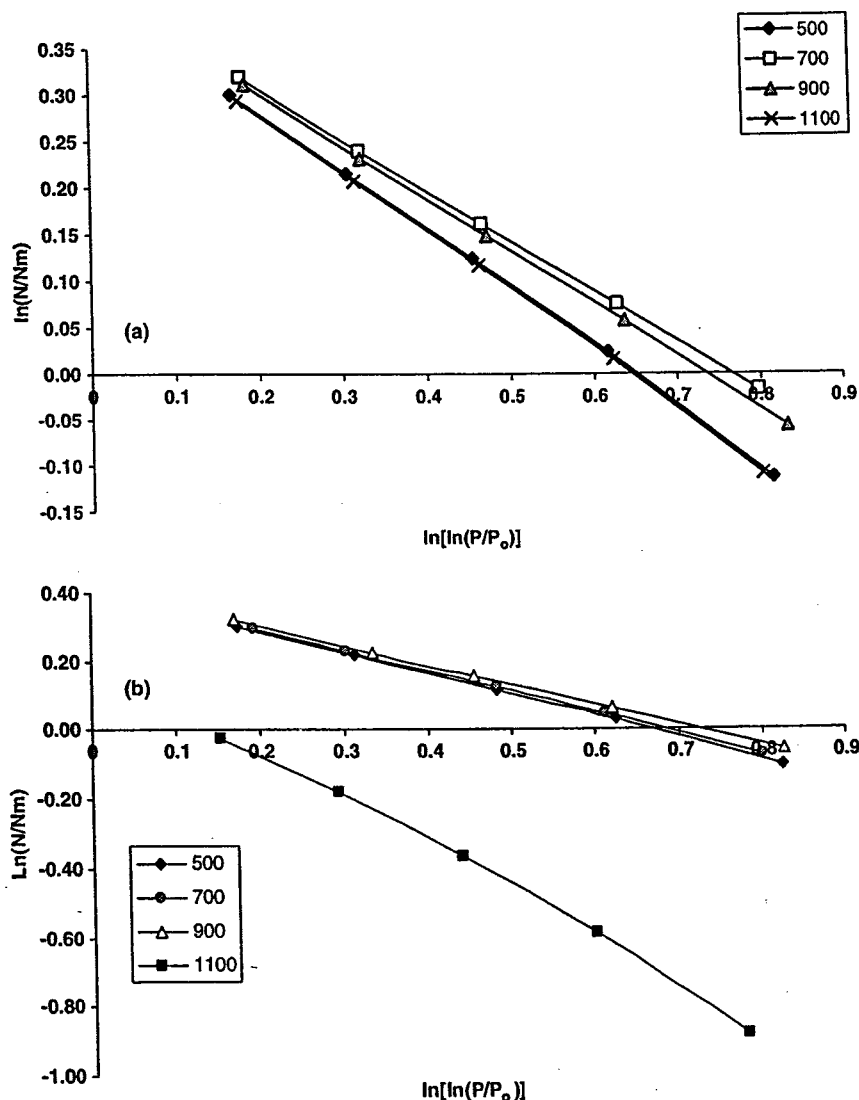


Fig. 6. FHH plots for the (a) alumina membranes and (b) Pt/alumina membranes at calcination temperatures of 500 °C, 700 °C, 900 °C and 1100 °C.

Table 1  
Surface fractal dimensions of alumina and Pt/alumina membranes (6 vol% of 0.02 g/ml Pt) calcined at different temperatures

Temperature (°C)	Surface fractal, $D$	
	Alumina	Pt/alumina membranes (6 vol% of 0.02 g/ml Pt)
500	2.3712	2.3682
700	2.4555	2.3989
900	2.4326	2.4293
1100	2.3048	1.6294

alumina clusters collapsed because clusters were swallowed by larger ones. A similar trend was observed for Pt/alumina samples. The value of the surface fractal of Pt/alumina initially increased when temperature was increased from 500 to 900 °C, but then decreased when temperature was raised further to 1100 °C. Comparing to the fractal dimen-

sion values of alumina to that of Pt/alumina, it can be implied that the pore blocking effect had taken place and that the pore formation in alumina was rather more complex than in Pt/alumina because the porous network was governed by three different types of pore structure (ink bottle, cylinder and V) whereas, Pt/alumina by only two types of pore structures (ink bottle and V) during the course of thermal treatment. The surface fractal dimension of the pores depends on the amount, size and the mass fractal dimension of clusters, as well as the extent to which clusters interpenetrate [16].

Fig. 7(a) and (b) shows SEM images of Pt/ $\gamma$ -Al<sub>2</sub>O<sub>3</sub> membrane surface and cross-sectional image of the membrane layer on the  $\alpha$ -alumina support respectively, thermally treated at temperature of 700 °C. It can be observed that the film (about 9  $\mu$ m thick) deposited on the porous alumina support was even, smooth and compact. There was an absence of cracks, pinholes or bumps.

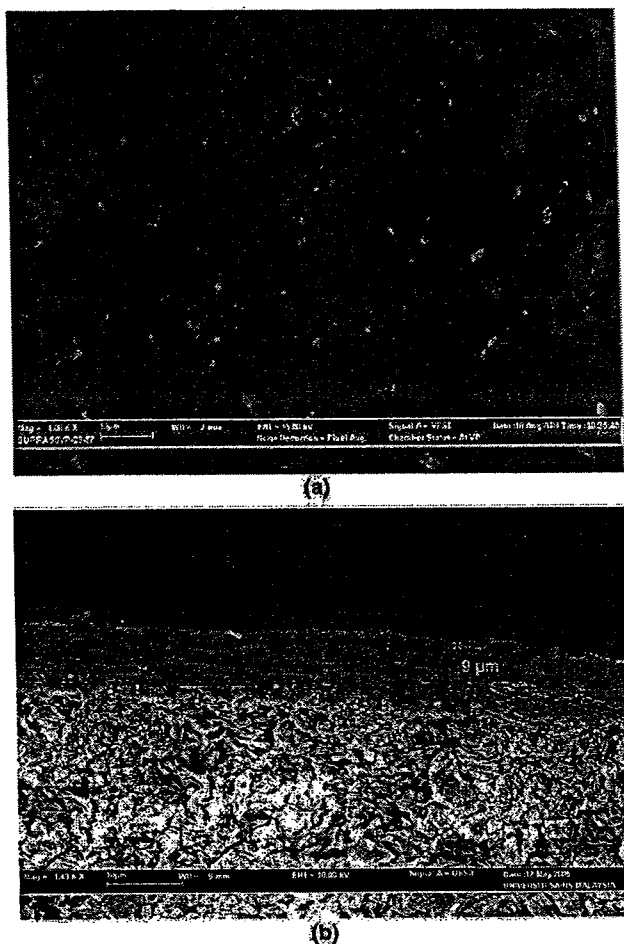


Fig. 7. SEM images of supported membrane calcined at 700 °C: (a) membrane surface and (b) cross-sectional image of the supported membrane with thickness about 9  $\mu\text{m}$ .

Fig. 8 shows the transmission electron micrograph (TEM) of Pt/alumina membranes. In the synthesis of Pt/ $\gamma\text{-Al}_2\text{O}_3$  membrane, thermal treatment was carried out to decompose the Pt precursor to metallic Pt. This process promoted the possibility of collisions of Pt clusters and the growth of bigger Pt clusters was anticipated. TEM observations of the composite membrane reveal that the platinum particles were well dispersed within the alumina matrix for membrane calcined at 700 °C. The size of platinum particles was evaluated from measurements on the TEM micrograph. The metal particles were in a size range between 5 and 20 nm. The size of the platinum particles increased with increase in calcination temperature to a size range between 10 and 45 nm. Heating the Pt/alumina samples at higher temperature caused the platinum to grow to larger sizes as they agglomerated in the encapsulating matrix. When the metal content and the calcination temperature increased, interface interactions between the metal particles and the matrix occurred in the nanocomposites and became evident with a variation in the size of the particles [4].

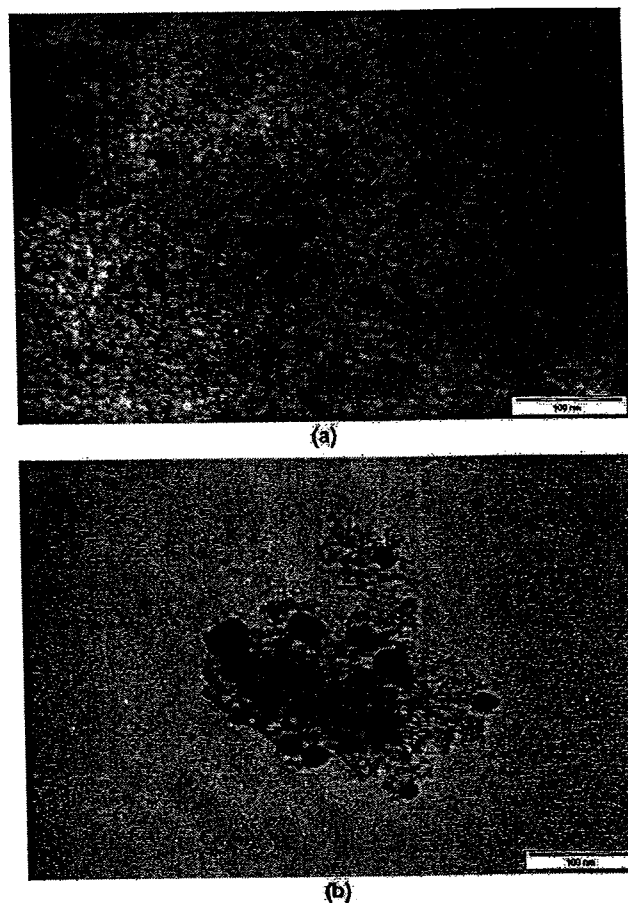


Fig. 8. TEM image of Pt/ $\gamma\text{-Al}_2\text{O}_3$  composite membrane (a) at calcination temperature of 700 °C and (b) at calcination temperature of 900 °C.

#### 4. Conclusion

The isotherms of alumina and Pt/alumina composites exhibited type IV pore structure according to BDDT and the presence of the hysteresis loops confirmed that porosity existed in the samples heated at 500–900 °C. The pore surface irregularities increased with increase in temperature from 500 °C to 900 °C but decreased at 1100 °C. Pt/alumina membrane that was free from cracks and pinholes with sufficient adhesion to the porous support was obtained. The membrane pore size was less than 10 nm (<900 °C) with uniform pore size and the metals were highly dispersed in the alumina matrix.

#### Acknowledgments

The authors acknowledge the short term Grant from USM/MOSTI which enables the production of this article.

#### References

- [1] H.P. Hsieh 3, *Membrane Science and Technology Series*, Elsevier, Amsterdam, 1996, pp. 1–150.

- [2] J. Deng, Z. Chao, B. Zhou, *Applied Catalysis A: General* 132 (1995) 9–20.
- [3] M. Kajiwara, S. Uemiya, T. Kojima, E. Kikuchi, *Catalysis Today* 56 (2000) 65–73.
- [4] Y. Wu, Y. Zhang, L. Zhang, *China Particuology* 2 (1) (2004) 19–24.
- [5] C.K. Lambert, R.D. Gonzalez, *Applied Catalysis A: General* 172 (1998) 233–239.
- [6] E.R. Pascual, A. Larrea, A. Monzon, R.D. Gonzalez, *Journal of Solid State Chemistry* 168 (2002) 343–353.
- [7] Z. Hongbin, X. Guoxing, G. Jinghua, S. Shishan, H. Bauser, N. Stroh, K. Pflanz, *Catalysis Today* 25 (1995) 237–240.
- [8] A.F.M. Leenars, A.J. Burggraaf, *Journal of Colloid and Interface Science* 105 (1985) 27–40.
- [9] H.A. Rangwala, J.E. Taylor, High temperature separation of hydrogen using novel ceramic membranes, Final Report, Alberta Research Council, Devon, Alberta, 1993.
- [10] X.R. Huang, G.L. Meng, Z.T. Huang, J.M. Geng, *Journal of Membranes Science* 133 (1997) 145–150.
- [11] Q. Fu, C.B. Cao, H.S. Zhu, *Thin Solid Film* 348 (1999) 99–102.
- [12] C.K. Lambert, R.D. Gonzalez, *Journal of Material Science* 34 (1999) 3109–3116.
- [13] S. Lowell, J.E. Siels, *Powder Surface Area and Porosity*, Chapman and Hall Ltd., New York, 1991, pp. 10–45.
- [14] B.E. Yoldas, *Ceramic Bulletin* 54 (33) (1975) 289–290.
- [15] D. Quattrini, D. Serrano, S.P. Catan, *Granular Matter* 3 (2001) 125–130.
- [16] Q. Wei, D. Wang, *Materials Letters* 57 (2003) 2015–2020.



# On the characteristics and hydrogen adsorption properties of a Pd/ $\gamma$ -Al<sub>2</sub>O<sub>3</sub> prepared by sol–gel method

M.R. Othman \*, I.S. Sahadan

*School of Chemical Engineering, Engineering Campus, Universiti Sains Malaysia, Seri Ampangan, Nibong Tebal, Seberang Perai Selatan, Penang 14300, Malaysia*

Received 20 July 2005; received in revised form 11 November 2005; accepted 16 November 2005  
Available online 9 January 2006

## Abstract

Alumina modified palladium prepared by the sol–gel method was characterized by nitrogen adsorption, transmission electron (TEM), thermal gravimetric (TGA) and X-ray diffraction (XRD). Gamma alumina ( $\gamma$ -Al<sub>2</sub>O<sub>3</sub>) modified palladium exhibited ink bottle shape mesopore characteristics with pore diameter of 15 nm. Pd particles with diameter ranging from 5 to 15 nm were well dispersed in the porous alumina matrix. The particles were well crystallized at temperature of 700 °C. TGA results show that Pd precursors decomposed at temperature between 300 and 400 °C, while copolymer was not completely removed until 500 °C. Adsorption of H<sub>2</sub> on coated Pd/ $\gamma$ -Al<sub>2</sub>O<sub>3</sub> zeolite beads was improved substantially with time at temperature of 300 °C.  
© 2005 Elsevier Inc. All rights reserved.

**Keywords:** Zeolite; Gamma-alumina; Palladium; Adsorption; Hydrogen; Carbon dioxide; Characterization

## 1. Introduction

The potential applications of the sol–gel derived  $\gamma$ -Al<sub>2</sub>O<sub>3</sub> as a ceramic membrane or catalyst in separation, filtration and catalytic reactions have favored research on synthesis, characterization and property improvement of these inorganic materials for many years [1,2]. Sol–gel derived  $\gamma$ -Al<sub>2</sub>O<sub>3</sub> adsorbent offers a number of advantages. These include excellent mechanical strength, low attrition rate, high thermal and chemical stability and uniform pore size distribution. In addition, they preserve microbial resistance and durability as well as excellent catalytic properties while offering high permeability and selectivity for hydrogen [3,9,12]. In the present work,  $\gamma$ -Al<sub>2</sub>O<sub>3</sub> modified palladium was synthesized for use as adsorbent/membrane, for hydrogen separation or enrichment.

Alumina was selected due to its compact crystal structure, strong chemical bonding and is stable at elevated tem-

perature. Palladium and its alloys, platinum and the metals in groups 3–5 of the periodic table may be used alongside alumina to facilitate transport of hydrogen since the gas has high affinity toward the metals. Pd/ $\gamma$ -Al<sub>2</sub>O<sub>3</sub> have chemical compatibility with many hydrocarbon containing gas streams and they exhibit relatively large surface area with active sites on the alumina surface for better adsorption property as catalysts (such as Lewis and/or Brønsted acid sites) [4,5]. These features lead to a good activity and selectivity of alumina as supported catalyst.

Molecular sieves are synthetically produced zeolites. It is characterized by pores and crystalline cavities of extremely uniform dimensions. Molecular sieves are available in four different grades. These grades are unique from one another due to their chemical composition and pore size. Type 3A is the potassium form of the zeolite and adsorbs those molecules which have a critical diameter of <3 Å. While Type 4A is the sodium form of the zeolite and adsorb those molecules having a critical diameter of <4 Å. Type 5A is the calcium form of the zeolite. It adsorbs those molecules having a critical diameter of <5 Å. Type 13X is a modified form of the sodium zeolite with a pore diameter of 10 Å [7].

\* Corresponding author. Tel.: +604 5996426; fax: +604 5941013.  
E-mail address: [chroslee@eng.usm.my](mailto:chroslee@eng.usm.my) (M.R. Othman).

In this studies commercially available molecular sieve 5A was selected for use as both adsorbent and support due to its unique adsorption characteristic and ability to trap contaminate molecules [11,6].

In the upstream petroleum production activity, natural gas which consists of mostly methane is often produced. If released to the atmosphere, methane (a strong greenhouse gas) can contribute to global warming. However, methane can be broken down into useful components, namely carbon and hydrogen. Combining methane with oxygen, creating a mixture of carbon monoxide and hydrogen called 'syngas'. Syngas is reacted with steam to form carbon dioxide and more hydrogen. The hydrogen gas, thus isolated, is collected, while the carbon dioxide can be stored to reduce global warming [1].

The objective of this work is to synthesize alumina modified with palladium by sol-gel method, for use as coating on commercially available molecular sieve adsorbent (zeolite beads) to adsorb  $H_2$ . The Pd/ $\gamma$ - $Al_2O_3$  were characterized using TG/DTA, XRD, TEM and nitrogen adsorption/desorption analysis. The performance of coated and uncoated zeolite beads was then compared.

## 2. Materials and methods

### 2.1. Synthesis of palladium/alumina sol for coating

For preparation of Pd/alumina sol, aluminum secondary butoxide ( $Al(OC_4H_9)_3$ ) was used as alumina precursor, nitric acid ( $HNO_3$ ) as peptizing agent and deionized water and butanol ( $C_4H_9OH$ ) as solvent. The alkoxide to water and acid molar ratio was 1:100:0.07. Twenty-five milliliter of butanol was added to enhance adhesion of coating to the support whereas 2 vol% of 0.04 g/ml PVA was added to prevent crack formation on the layer of the coated zeolite beads during drying process. Eight vol% of 0.02 g/ml palladium chloride ( $PdCl_2$ ) was employed as palladium precursor. All these chemicals were mixed, heated at temperature of 90 °C and stirred vigorously for 30 min before undergoing reflux process for 24 h at 90 °C. The resulting sol was cooled to room conditions until gelation and later solid samples was obtained. A part of the sol was used to dip coat onto the zeolite beads before drying, after which the solid samples and coated zeolite beads were calcined at temperature 700 °C to produce Pd/ $\gamma$ - $Al_2O_3$  samples and Pd/ $\gamma$ - $Al_2O_3$  coated zeolite beads having thin layer coating of approximately 5  $\mu m$  thickness. Commercially available zeolite beads adsorbents with pore size of 5 Å (Zeosorb, Molsieb 5A) were used in the experiment.

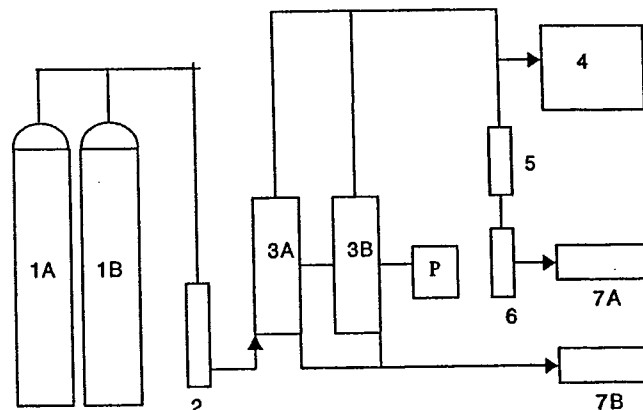
### 2.2. Characterization and adsorption analyses

Pore properties including the BET surface area, pore volume and pore size of the Pd/ $\gamma$ -alumina solid samples were determined by a nitrogen adsorption/desorption measurements using an autosorb I (Quantachrome, Nova 1200). The thermal stability of Pd/ $\gamma$ -alumina was analyzed

by thermal gravimetric and differential thermal analyses (TG/DTA) supplied by Perkin Elmer. TEM image of the Pd/ $\gamma$ -alumina was taken by using CM12 (Philips) with an accelerator voltage of 80 kV. The images were captured with a SIS Image Analysis System version 3.11. XRD analysis was carried out to identify phase transformation and crystal structure of the sample using Philips PW 1729 X-ray generator, Philips PW 1820 diffractometer ( $CuK\alpha$  radiation and graphite monochromator) and Philips PW 1710 diffraction controller.

The gas adsorption studied of Pd/ $\gamma$ - $Al_2O_3$  was performed on adsorption column separation unit. The schematic representation of the experimental system employed is shown in Fig. 1. The unit consists of two alternatively switched, electrically heated column (3A) and (3B). Each column is equipped with a temperature sensor, *P* that measure temperature of the adsorbent. The width and length of the column were 8.5 cm and 39.5 cm, respectively. A rotameter (2) located downstream of the adsorbers was used to measure the flow rate of the feeding gas. The downstream of the columns was connected to a vacuum pump (7). The composition of the product stream gas leaving the adsorbers was measured by means of a Gas Chromatography 5890, HP Series 8 (1) equipped with a TCD detector. The detail specifications are given in Table 1. The column used was porapak Q.

Sixty grams of sample was weighed and fed into the adsorption column. Hydrogen and carbon dioxide gas from tank was fed into the adsorption column at a flow rate of 50 L/h. The experiment was run for the duration of 80 min. The product stream was detected by GC for every 10 min. Similar procedure was repeated for the temperature of 100 °C, 200 °C, and 300 °C. Prior to experiment, the adsorption column was vacuumed to ensure complete removal of contaminants.



1. Gas cylinder
2. Rotameter
3. Adsorber columns
4. Gas chromatograph
5. Reflux cooler
6. Cold trap
7. Vacuum pump

Fig. 1. Schematic diagram of adsorption unit.



Table 1  
Specification of the gas chromatography unit

Oven temperature	50 °C
Detector temperature	250 °C
Polarity	Negative
Rate	20 min <sup>-1</sup>
Detector	TCD
Carrier gas	Helium

### 3. Results and discussion

#### 3.1. Pd/ $\gamma$ -Al<sub>2</sub>O<sub>3</sub> characterization

Table 2 summarizes the characteristics of the Pd/ $\gamma$ -Al<sub>2</sub>O<sub>3</sub> calcined at temperature of 700 °C. Calcination temperature of 700 °C was chosen because it was found to be sufficiently high to affect the metal dispersion ( $T > 500$  °C) while not causing a phase change ( $\gamma$ -Al<sub>2</sub>O<sub>3</sub>) [8]. The pore size distribution of the Pd/ $\gamma$ -Al<sub>2</sub>O<sub>3</sub> was determined by the adsorption branch of the isotherms and is shown in Fig. 2. The result shows a narrow pore size distribution, indicating that the sample exhibits relatively uniform pore sizes. The nitrogen adsorption isotherm of Pd/ $\gamma$ -Al<sub>2</sub>O<sub>3</sub> was shown in Fig. 3. The isotherm of this sample exhibits type's IV isotherm, according to the BDDT theory and ink bottle shape pore based from the de Boer theory

Table 2  
Pd/ $\gamma$ -Al<sub>2</sub>O<sub>3</sub> characteristic obtained from adsorption isotherm

BET surface area (m <sup>2</sup> /g)	189.2
Mesopores area (m <sup>2</sup> /g)	189.2
Average pore diameter (nm)	15
Pore volume (cm <sup>3</sup> /g)	0.29

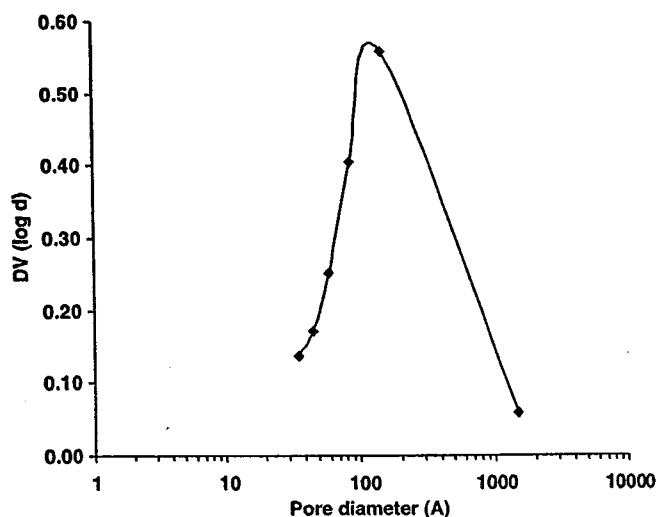


Fig. 2. Pore size distribution of the Pd/alumina.

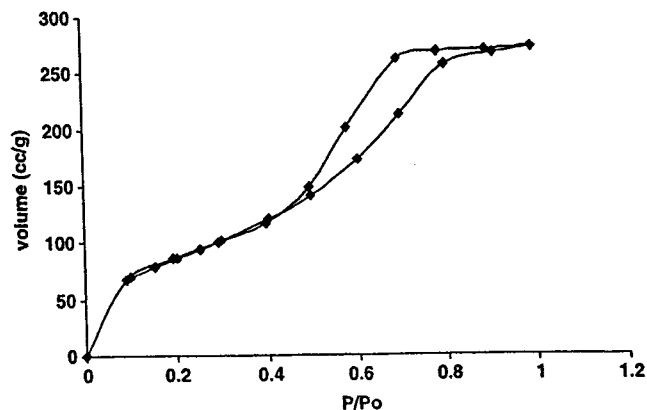


Fig. 3. Adsorption/desorption isotherms of Pd/ $\gamma$ -Al<sub>2</sub>O<sub>3</sub>.

[10]. This type of isotherm associated with porous material containing mostly mesopores.

Fig. 4 shows TG/DTA curve for the dried Pd/alumina gel. Three stages of weight loss occurred at three temperature regions, namely, below 130 °C, from 130 to 500 °C and from 500 to 900 °C. In the first stage, a drastic weight loss of ~20% was observed with the presence of endothermic peak on DTA curve at 80 °C. This loss was due respectively to the departure of water and traces of butanol (boiling point 100 °C) from the remaining alkoxy groups. It may also be due to the pyrolysis of the surfactant and residual organics (copolymer). In the second stage, a weight loss of ~15% was observed. The loss was probably related to the thermal decomposition of surface organic (hydroxyl and alkoxy) groups and removal of water during the formation of the oxide phase. The endothermic peak between 300 and 400 °C at DTA curve probably corresponds to Pd precursor's decomposition. A small exothermic peak at 380 °C may be assigned to the formation of PdO [8]. The endothermic peak between 400 and 500 °C was attributed to the crystallization of aluminum hydroxide (AlOOH) to crystallite  $\gamma$ -Al<sub>2</sub>O<sub>3</sub> and also due to water removal during the phase transformation of  $\gamma$ -Al<sub>2</sub>O<sub>3</sub> ( $2[\text{AlOOH}] \rightarrow \gamma\text{-Al}_2\text{O}_3 + \text{H}_2\text{O}$ ). In the third stage, a small weight loss of about 2% was due to the phase transformation of alumina. The smaller exothermic features observed at temperature above 700 °C corresponds to the formation of better crystallized phases of alumina. A small weight loss of about 0.5% was also observed from 700 °C to 900 °C. This was attributed to the phase transformation from  $\gamma$ -, to  $\delta$ - and  $\theta$ -Al<sub>2</sub>O<sub>3</sub>. A substantial portion of the copolymer pyrolyzed at 130 °C was not completely removed until 500 °C was reached.

XRD pattern for the sample calcined at 700 °C is shown in Fig. 5. The peak at highest intensity corresponds to Pd. The XRD pattern also shows a well crystalline  $\gamma$ -Al<sub>2</sub>O<sub>3</sub> phase at this temperature. Fig. 6 shows that good dispersion of the palladium particles in the porous alumina matrix. The palladium particles with diameter ranging from 5 to 15 nm can be observed from TEM images.

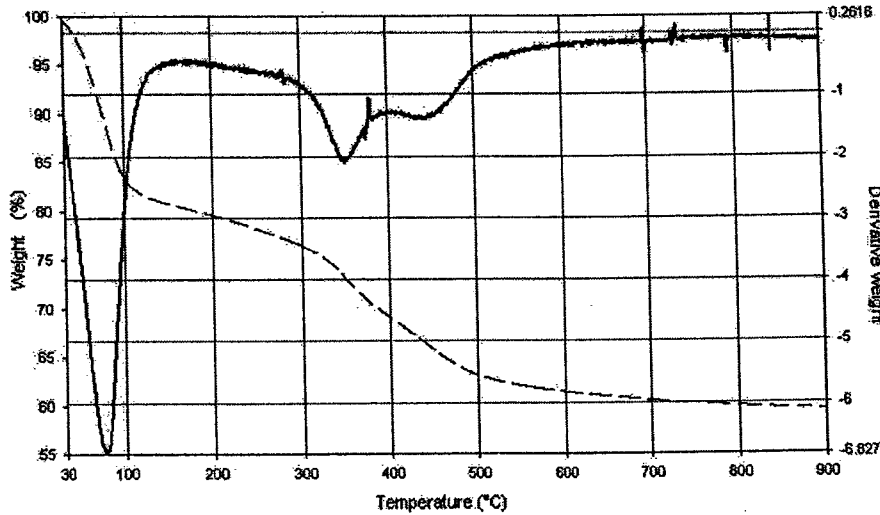


Fig. 4. TG/DTA curve of Pd/alumina gel dried at ambient temperature, under  $N_2$  flow at  $20^\circ C/min$ .

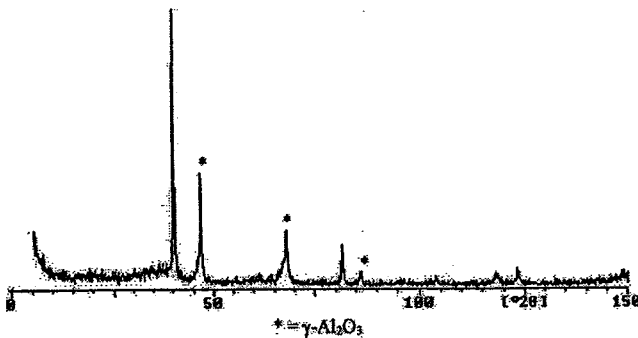


Fig. 5. X-ray diffraction patterns calcined at  $700^\circ C$ .

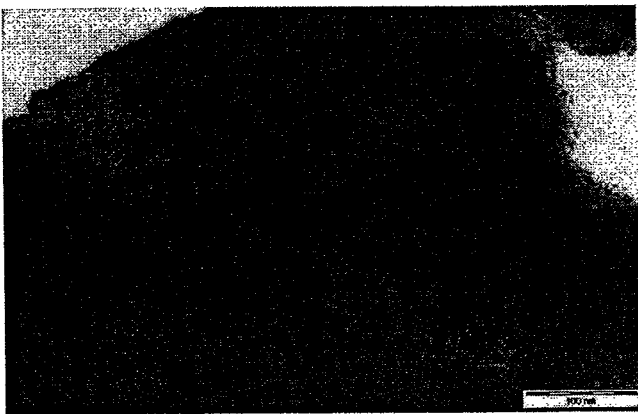


Fig. 6. TEM image of Pd/ $\gamma$ - $Al_2O_3$  calcined at  $700^\circ C$ .

### 3.2. Adsorption studies

#### 3.2.1. Adsorption of single gas (hydrogen)

The tests were carried out on coated and uncoated Pd/ $\gamma$ - $Al_2O_3$  on zeolite 5 Å at temperature of 30, 100, 200, and  $300^\circ C$ , respectively. Fig. 7 showed that  $H_2$  adsorption

on both coated and uncoated zeolite beads was higher at lower temperature. The adsorption study was performed in single/pure  $H_2$  gas system. For the coated zeolite beads, the linear graph shows the adsorbed amount was proportional with time. The highest measured adsorption of  $H_2$  was  $0.045 \text{ mol/g}$  at temperature of  $30^\circ C$ . While the lowest amount of  $H_2$  gas adsorbs was  $0.025 \text{ mol/g}$  at temperature  $300^\circ C$ . The adsorbed amount of  $H_2$  gas was  $0.037 \text{ mol/g}$  and  $0.030 \text{ mol/g}$  at temperature  $100^\circ C$  and  $200^\circ C$ , respectively. This was due to palladium metal that exhibits a remarkable property of adsorbing considerable volumes of hydrogen at ambient temperature [11]. The figure also shows that addition of Pd/ $\gamma$ - $Al_2O_3$  promoted adsorption of  $H_2$  in the zeolite beads at all temperature being investigated. Substantial improvement was observed at the highest operating temperature of  $300^\circ C$  as shown in Fig. 7(d).

#### 3.2.2. Adsorption of $H_2$ in a binary mixture of $H_2/CO_2$

In this experiment, only coated zeolite beads were used. The adsorption of  $H_2$  and  $CO_2$  was performed in a binary mixture of  $H_2/CO_2$  at temperature of 30, 100, and  $200^\circ C$  respectively. 50/50 molar concentration of  $H_2/CO_2$  was used throughout the experiment. Fig. 8 shows that the  $H_2$  adsorption increased almost linearly with increase in time. Whereas,  $CO_2$  adsorption was quite erratic at  $30^\circ C$ , remained constant at  $100^\circ C$  and then increased with increase in time at  $200^\circ C$ . Nevertheless, adsorption of  $H_2$  was higher than  $CO_2$  at all time, indicating that  $H_2$  has higher affinity towards Pd/ $\gamma$ - $Al_2O_3$  coated zeolite beads. Comparing Fig. 8 to that of Fig. 7, it can be observed that Pd/ $\gamma$ - $Al_2O_3$  was capable of maintaining the adsorption performance despite change of system into binary in which competition adsorption usually takes place.

### 4. Conclusion

Pd/ $\gamma$ - $Al_2O_3$  prepared by sol-gel method was characterized by nitrogen adsorption and TEM. The result shows that

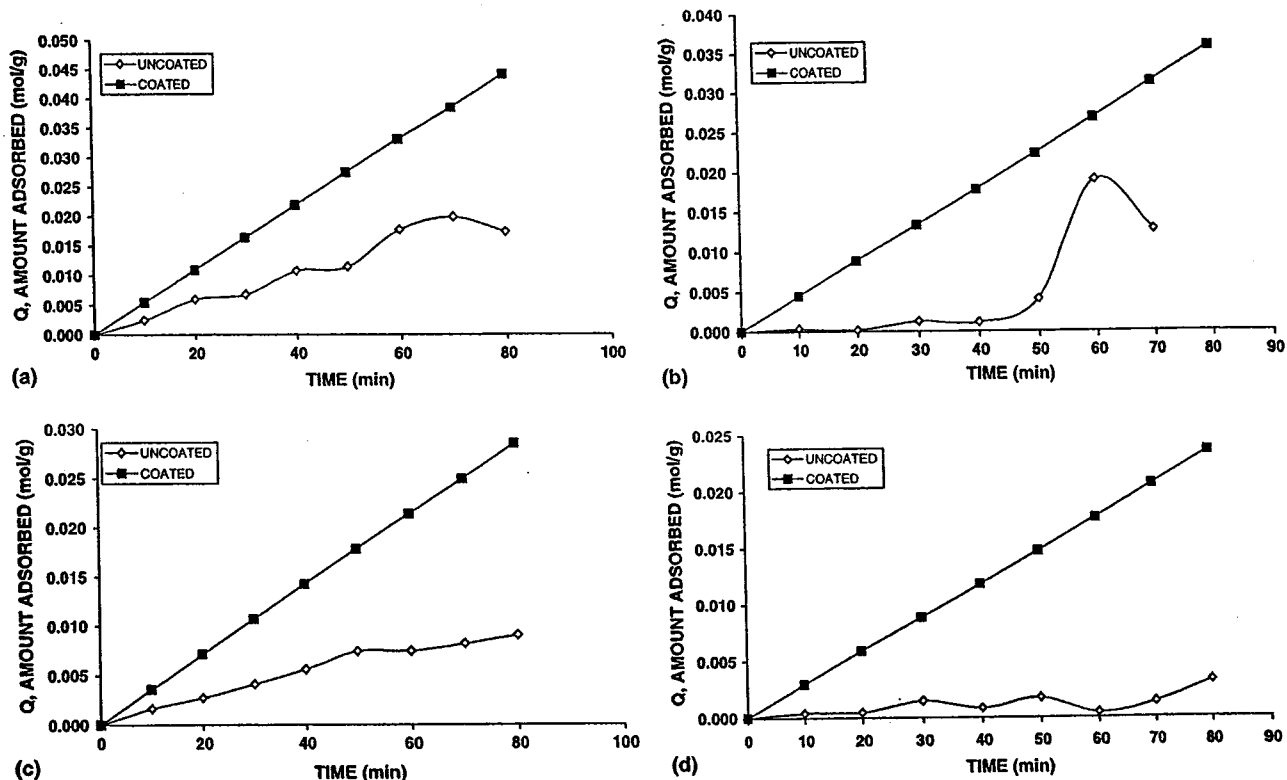


Fig. 7. Comparison between coated and uncoated zeolite at (a) 30 °C; (b) 100 °C; (c) 200 °C; and (d) 300 °C.

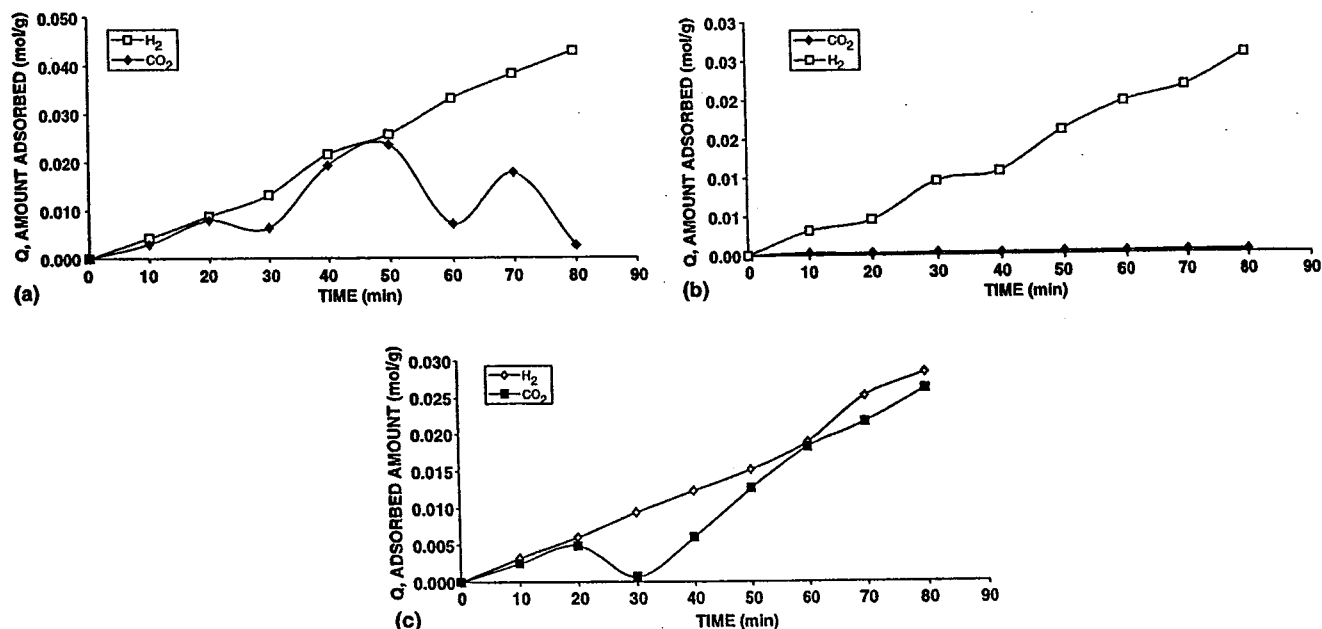


Fig. 8. Amount of hydrogen and carbon dioxide adsorbed on coated zeolite at temperature (a) 30 °C; (b) 100 °C; and (c) 200 °C.

the Pd/ $\gamma$ - $Al_2O_3$  was uniform, with pore size of less than 20 nm and the metals were highly dispersed in the alumina

matrix. The zeolite that was coated with Pd/ $\gamma$ - $Al_2O_3$  resulted higher hydrogen adsorption compared to the uncoated

zeolite. In a binary gas system, H<sub>2</sub> gas maintained higher adsorption on coated zeolite compared to CO<sub>2</sub> gas even at high temperature condition. In fact, Pd/ $\gamma$ -Al<sub>2</sub>O<sub>3</sub> coated zeolite was proven to perform best at higher temperature.

#### Acknowledgments

The authors acknowledge the short term grant from USM/MOSTE to enable the completion of this work.

#### References

- [1] Argonne National Laboratory, Hydrogen transport membrane (HTM) for separation of pure hydrogen at high temperatures, 2004 [online], accessed on May 2005.
- [2] H.I. Chen, J.D. Shiau, C.Y. Chu, T.C. Huang, *Separation and Purification Technology* 32 (2003) 247–254.
- [3] T.D. Chen, L. Wang, H.R. Chen, J.L. Shi, *Materials Letters* 50 (2001) 353–357.
- [4] B. Delmon, J.T. Yates, *Recent Advances and New Horizons in Zeolite and Technology*, Elsevier Science, New York, 1996, pp. 272–273.
- [5] E. Diaz, S. Ordonez, A. Vega, J. Coca, *Microporous and Mesoporous Materials* 70 (2004) 109–118.
- [6] B.C. Gates, *Catalytic Chemistry*, John Wiley & Sons, Inc., New York, 1991.
- [7] M. Kajiwara, S. Uemiya, T. Kojima, E. Kikuchi, *Catalysis Today* 56 (2000) 65–73.
- [8] C.K. Lambert, R.D. Gonzalez, *Materials Letters* 38 (1999) 145–149.
- [9] D. Lee, L. Zhang, S.T. Oyama, S. Niu, R.F. Saraf, *Journal of Membrane Science* 231 (2004) 117–126.
- [10] S. Lowell, J.E. Sields, *Powder Surface Area and Porosity*, Chapman and Hall, 1991.
- [11] R.I. Masel, *Principals of Adsorption and Reaction on Solid Surfaces*, John Wiley & Son, Inc., 1996.
- [12] Y. Wang, Y.S. Lin, *Journal of Sol-Gel Science and Technology* 11 (1997) 185–195.

## DEVELOPMENT OF PALLADIUM-ALUMINA MEMBRANE USING SOL-GEL TECHNIQUE

N.N.N. Mustafa\*, M.R. Othman and A. L. Ahmad

Chemical Engineering School, Engineering Campus, Universiti Sains Malaysia, Seri  
Ampangan, 14300 Nibong Tebal, Pulau Pinang, Malaysia  
Email: nknorfauziah@hotmail.com

### ABSTRACT

High selectivity poses serious challenge to inorganic membrane developers in the past and present research setting. The difficulty in acquiring the required selectivity remains to be the focal component in ceramic membrane research, along with development of an inorganic composite palladium-alumina membrane that is structurally stable, characterized by high hydrogen permeation and flux. The sol-gel process from alkoxide as starting material to prepare for unsupported and supported palladium-alumina membrane and the results of membrane characterization are presented in this paper. The effects of PVA and palladium content on the changes of the pore structure after drying and sintering process are as well delineated to ensure sufficiently good membrane can be produced and re-produced before investigation of actual selectivity can be pursued.

**Keywords:** Palladium, Alumina, Membranes, Sol-Gel method

### 1.0 INTRODUCTION

Many techniques are applied to prepare the membrane, including CVD (Chemical Vapor Deposition), PVD (Physical Vapor Deposition), Sol-Gel, etc. Among this techniques, the sol-gel technique has been found to be most convenient technique to obtain nanoporous ceramic membranes with high purity products, uniform and controlled pore size distribution (from 0.5~several 10 nm), which can be formed at relatively low temperature (about 400-600°C) and it is an easy method to synthesis membrane [H.P. Hsieh, 1996, Q. Fu et al., 1999, H.A. Rangwala et al., 1993, A.F.M. Leenars et al., 1985, X.R. Huang et al. 1997]. Alumina is a ceramic material, and this material has compact crystal structure, strong chemical bonding and they are more stable. Ceramic membranes have been known for years and used in many different applications depending on their numerous advantages, stability at high temperatures and pressure resistance, good chemical stability, high mechanical resistance, long life and good defouling properties. Those advantages not only make the membrane very suitable for separation application, but also for reaction enhancement [H.P. Hsieh, 1996]. Palladium and its alloys, platinum, nickel and the metals in groups 3 to 5 of the periodic table are all permeable and have affinity towards hydrogen to a certain extent. Hydrogen permeable metal membranes made of palladium and its alloys are the most widely studied due to their high hydrogen permeability, chemical compatibility with many hydrocarbon containing gas streams, and infinite high selectivity hydrogen separation [J. Deng et al., 1995, M. Kajiwara et al., 2000, Y. Wu et al., 2004]. This research is focused on modified alumina membranes by metal, which are designed to combine some advantages of alumina and palladium membranes.

### 2.0 EXPERIMENTAL PROCEDURE

Aluminum secondary butoxide ( $\text{Al}(\text{OCH}(\text{CH}_3)\text{C}_2\text{H}_5)_3$ ) are used as the precursor of alumina, butanol ( $\text{CH}_3(\text{CH}_2)_3\text{OH}$ ) as a solvent and nitric acid ( $\text{HNO}_3$ ) is used for peptization to form a highly dispersed, stable colloidal solution. The alumina sols are prepared by adding aluminum secondary butoxide and butanol to deionized water while

heating to a temperature of 90°C and continuously stirred high speed using magnetic stirrer.

The stock palladium solutions were prepared by dissolving varying weight of palladium chloride (PdCl) in separate beakers of 100 ml into deionized water before adding a small amount of hydrochloric acid to peptize the solution. The solution was stirred and heated around 70-80°C for 1 hour. Then, palladium chloride solution and PVA solution were mixed with alumina sol and the mixture was stirred rigorously. The range of palladium chloride concentration employed in this work was within 0-8 volume percent. This solution was stirred for 2 hours to ensure complete mixing. Nitric acid (HNO<sub>3</sub>) was added to suspension to further peptize and stabilize the sol particles. The alkoxide: water: HNO<sub>3</sub> molar ratio used in this work was 1:100:0.07. The hydrolysis was performed at room temperature and the suspension was peptized for about 24 hours at range temperature 85-95°C under reflux conditions. After that the colloidal suspension was steadily cooled to room temperature to produce stable colloidal sol. An adequate amount of sol was further dried in oven at 100°C for 4 hours to evaporate water and most of butanol, until gellation was obtained. After drying, the samples were then sintered at 500°C-1000°C for 16 hours to form unsupported  $\gamma$ -alumina membrane.

To prepare supported palladium-alumina membrane, a palletized porous  $\alpha$ -alumina support was dipped into the colloidal suspension. Then, the coated pellet was dried and sintered at temperature of 500°C-1000°C for 16 hours to produce supported Pd-alumina membrane. The viscosity of the solution, the TGA analysis of alumina gel, FTIR analysis of Pd/alumina wet gel, the morphology of the films by scanning electron microscopy (SEM) and evolution pore diameter with respect to thermal variation are discussed in this work.

### 3.0 RESULT AND DISCUSSION

#### 3.1 The Reaction of Gel During Sintering

##### 3.1.1 Thermogravimetric Analysis (TGA)

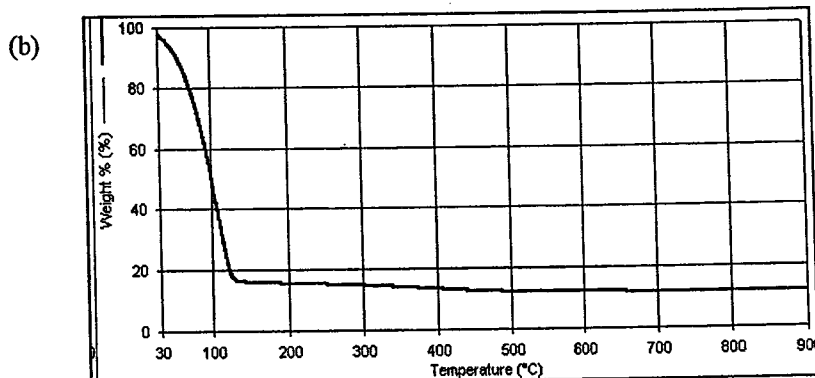
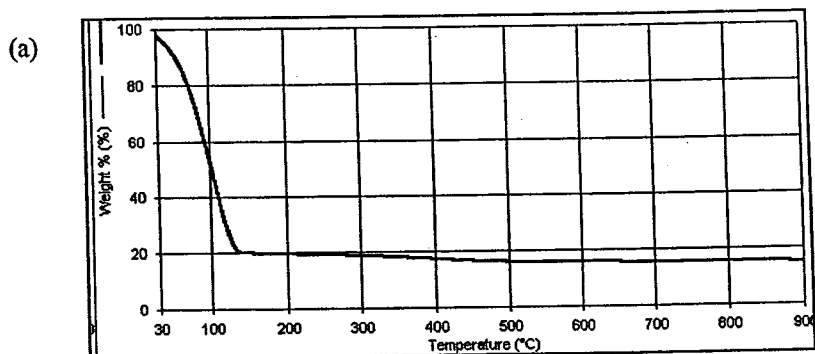


FIG. 1: Thermogravimetric analysis curves; (a) alumina wet gels; (b) Pd/alumina wet gels. The gels were heated in nitrogen stream at a rate of 10°C/min.

The weight loss of alumina and pd/alumina during heat treatment was measured by TGA. The samples were heated in nitrogen stream to 100°C and held at this temperature for 30 min in order to remove all physically adsorbed water before heating up to 900°C at a rate of 10°C min<sup>-1</sup>, and the result shown in Figure 1. Thermogravimetric curves (TGA) shows a drastic weight loss in the alumina and pd/alumina of about 80% from 30°C to 130°C, and gradual weight loss occurs from 130°C to 600°C, after which no subsequent weight loss was observed at temperatures over 600°C. This weight loss was a result of evaporation of residual alcohol and water during the formation of the oxide phase and the pyrolysis of the surfactant and residual organics (copolymer) such as PVA. The TGA curves for the alumina and Pd/alumina indicate that a substantial portion of the copolymer is pyrolyzed at 130°C but that copolymer is not completely removed until 600°C. The above results imply that during the sintering process the organic groups begin to decompose from 130°C and decompose completely around 600°C.

### 3.1.2 Fourier Transform infrared Analysis (FTIR)

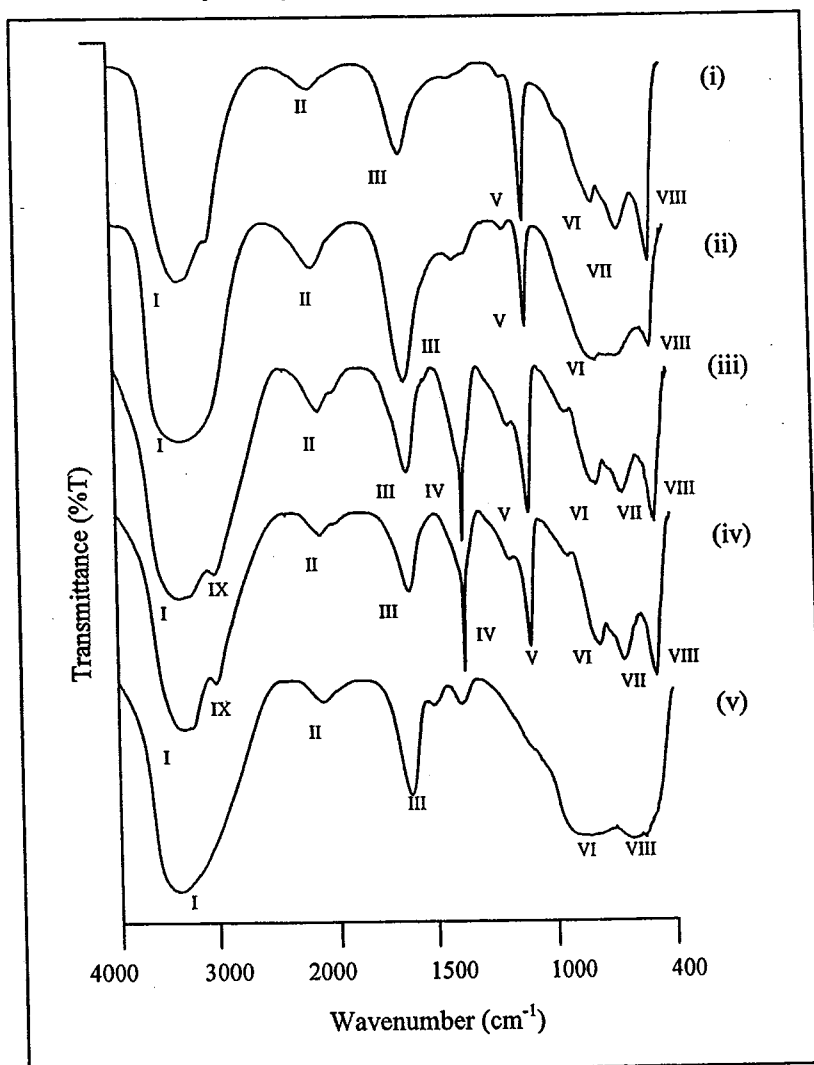


FIG 2: Infrared absorption spectra (FTIR) of Pd/alumina membrane at different stages of processing; (i) Pd/alumina boehmite sol; (ii) Pd/alumina wet gel (iii) Pd/alumina film dried in an ambient air; (iv) Pd/alumina films heating at 130°C; (v) Pd/alumina film after heating at 600°C.

The FTIR spectra in Fig. 2 display the corresponding chemical changes, which occur during heating of Pd/alumina films treated at various temperatures. The results obtained for alumina and Pd/alumina samples are identical and show no significant effect that merits discussion. The FTIR spectrum of Pd/alumina wet gel shows broad O-H stretching vibration (associated) at 2700-3540  $\text{cm}^{-1}$  (groups of water) {I}, CC stretching vibration at 2100-2140  $\text{cm}^{-1}$  {II}, C=C stretching vibration (Me-C=C); Me= heavy element, group with a heavy element directly attached to C=C at 1565-1650  $\text{cm}^{-1}$  {III}, CH<sub>3</sub>-metal groups due to CH<sub>2</sub> rocking vibration at 700-900  $\text{cm}^{-1}$  {VI} and C-C skeleton vibration at 490-595  $\text{cm}^{-1}$  {VIII} observed throughout the various film processing stages. Peaks related to the copolymer, C-H wagging vibration at 610-690  $\text{cm}^{-1}$  {VII}, N-H and C-H deformation vibration (Al-CH<sub>3</sub> bonds) at 1020-1100  $\text{cm}^{-1}$  {V} (appeared in the sol, wet gel, film dried in ambient air and heating at 130°C), C-H deformation vibration (mostly two equal intense bands) at 1365-1385  $\text{cm}^{-1}$  {IV} and C-H stretching vibration at 3070-3100  $\text{cm}^{-1}$  {IX} appeared in the films dried in an ambient air and heating at 130°C. This peaks disappeared after heating at 600°C indicating that this is a good processing temperature for Pd/alumina film because the copolymer is fully removed and Al<sub>2</sub>O<sub>3</sub> network undergoes no further chemical changes and becomes stable.

### 3.2 The Structure and Morphology of Alumina Films

#### 3.2.1 Scanning Electron Microscopy Analysis (SEM)

Figure 3 shows SEM images of a pd/ $\gamma$ -Al<sub>2</sub>O<sub>3</sub> supported membrane surface sintered at 600°C snapped at different magnification and direction. From the Fig. 3a and 3c, it can be seen that the film is even, smooth and compact. The film without PVA illustrated by Fig.3(b) resulted in certain degree of cracks, micro-bumps and micro-holes. The cross-sectional image of supported membrane shown in Fig. 3(d) demonstrates that the upper pd layer was successfully coated and fused onto the alumina porous pellet/support.

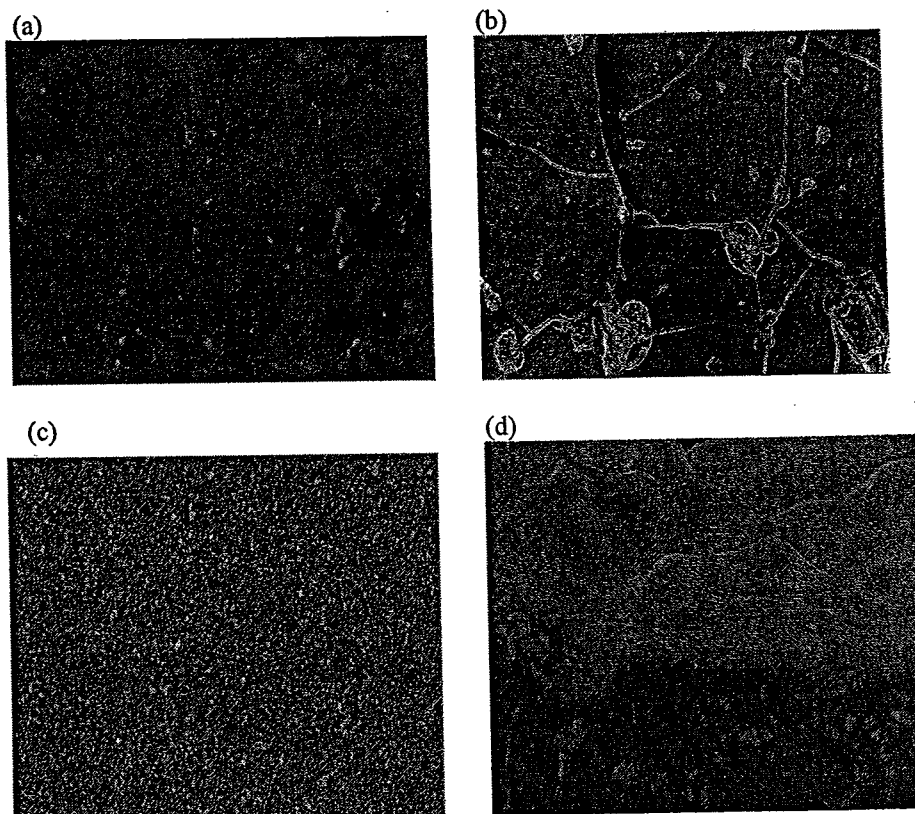




FIG. 3: Scanning electron micrographs of the supported Pd/alumina sintered for 16 hrs at max. temperature, 600°C using temperature-programmable Carbolite Furnace; (a) Supported Pd/alumina films surfaces containing PVA at 1000 x magnification; (b) Supported Pd/alumina films surfaces without PVA at 1000 x magnification; (c) Supported Pd/alumina films surfaces containing PVA at 10 000 x magnification; (d) cross-sectional image of supported membrane at 1000 x magnification.

### 3.2.2 Nitrogen Adsorption

The effect of sintering temperature on BET surface area and average pore size of Pd/alumina composite and alumina membrane are illustrated in the following figure. The BET surface area and pore volume are both decreasing with increase in sintering temperature. This is due to the collapse of the pores with shrinkage of the material structure. However, the pore diameter of both Pd/alumina and alumina decreases with increase in sintering temperature.

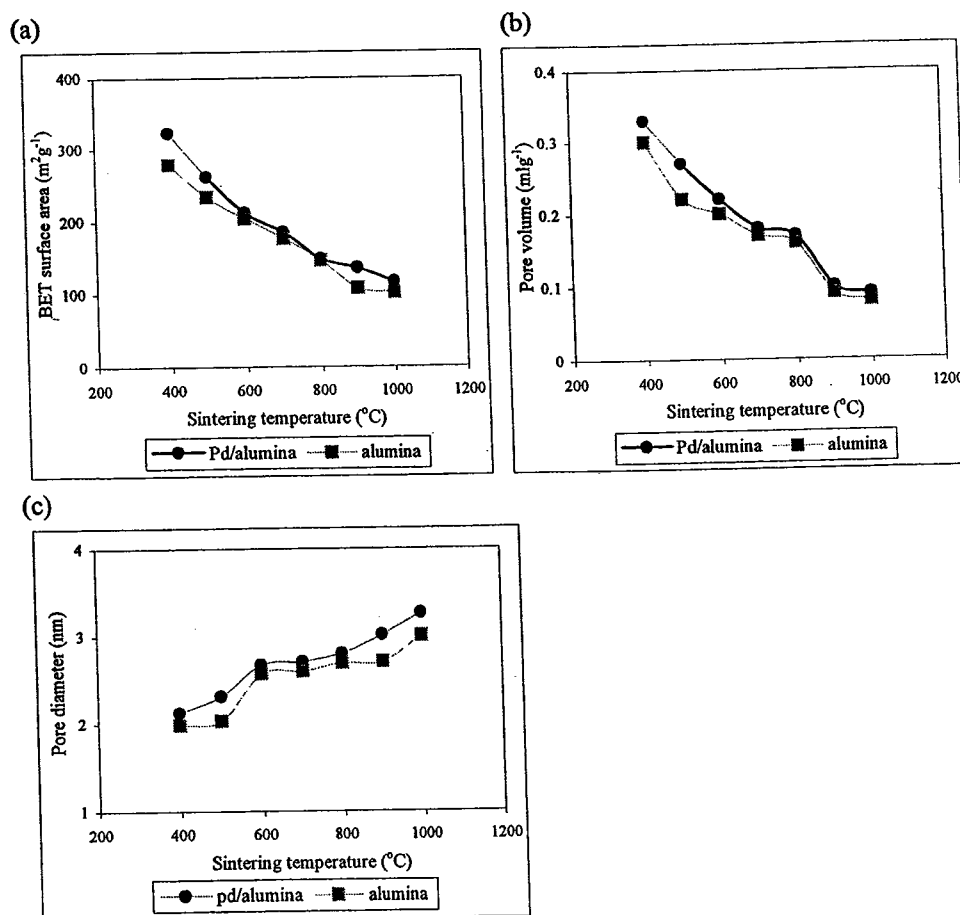


FIG. 4: (a) The BET surface area; (b) pore volume; and (c) average pore diameter of unsupported membrane as a function of sintering temperature.

The BET surface area, pore volume and pore diameter of Pd-alumina composite appears to be greater than alumina at all sintering temperature. Further scrutiny of the figure demonstrates that the BET surface area, total pore volume and average pore diameter remained almost constant between 600-800°C. This happens because the boehmite sols transformed during dehydration at 600°C and 800°C to  $\gamma$ -alumina. Prolonged heat treatment at 900-1000°C, results in the formation of transition aluminas ( $\delta$

and  $\theta$ ) and change in particle morphology [K.L. Yeung et al., 1997]. Further heating at temperature higher than 900°C, would result in the collapsing of the pores with corresponding decrease in surface areas and densification would occur [K. Haas-Santo et al., 2001 and Y. Wu et al., 2004]. The color of the nanocomposites also changed from brown, to grey brown, yellow-brown up to black, as the membrane progressively heated, indicating the growth of the finely dispersed palladium particles and the change of the surface state of the membrane.

### 3.2.3 Effect of Binder (PVA) on the sol viscosity and pore diameter

From the figure 5, it is shown that additional binder in the sol mixture increases the viscosity of the solution. This is due the fact that more particles underwent binding with each other causing increase in viscosity [K.S. Seshadri et al., 2003]. The resulting pore diameter of the finally sintered membrane demonstrates interesting findings that deserves due attention. As more PVA was added at 2% level, the pore diameter seems to increase initially. And then the pore diameter drops down progressively to below 3nm as the PVA level was increased to 8%. This is in contrast view of many researches in the past that correlates increase of pore size with increase in PVA addition. The reason for such trend to occur is probably due to the presence of finely dispersed palladium particles that bind cohesively and more effectively to each other and other suspended solids compared to that of solution without these palladium particles. This correlation would be further probed in the near future work in order to be able to understand the underlying mechanisms that are presence in the system.

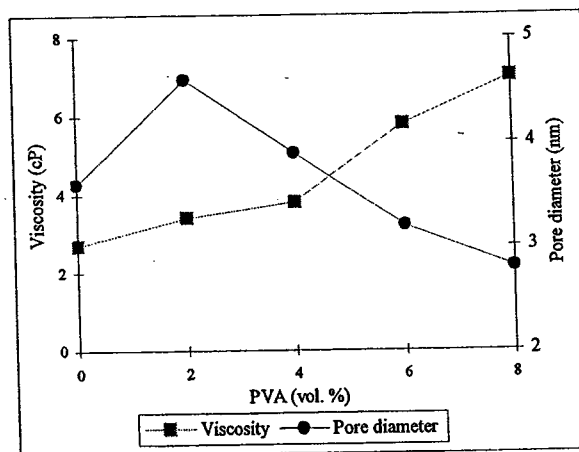


FIG. 5: Viscosity of sol and pore diameter of membrane as a function of percentage of PVA content in sol.

### 3.2.4 Effect of Palladium addition on BET surface area and pore diameter

Figure 6 shows the effect of palladium content in the preparation of pd/alumina membrane on the BET surface area and pore diameter of the membrane. It shows that, when palladium content was increased, surface area and pore diameter was decreased. The palladium precursor added to the alumina sol seemed to affect the interactions among the colloidal particles during gelation. When heated to higher temperature the palladium particles precipitated from the alumina network and grow to larger sizes in the encapsulating matrix. The small particles located along the pore channels would thereby reversibly lead to a decrease in the surface areas and pore diameter [Y. Wu et al., 2004].

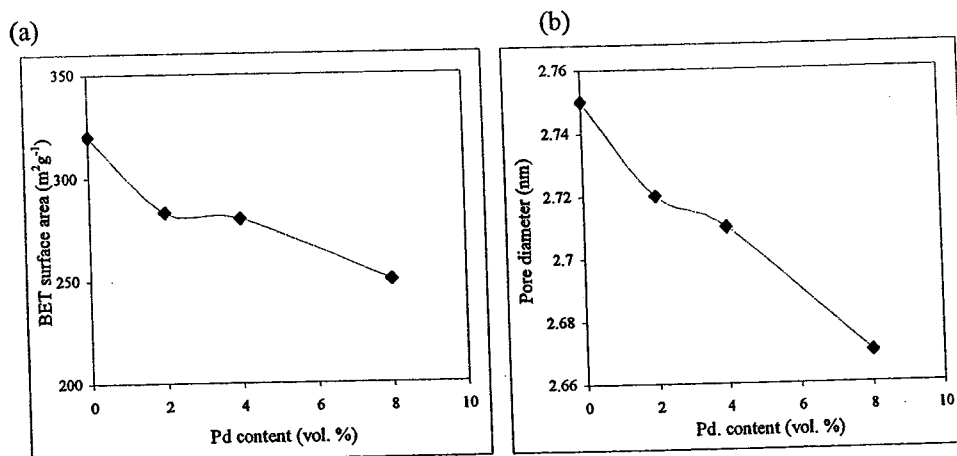


FIG. 6: (a) The BET surface area; and (b) pore diameter membrane as a function of Pd content (vol %).

### 3.0 CONCLUSION

The characteristics of the membranes, as judged by SEM and nitrogen adsorption show that the Pd-alumina membranes are uniform, with pore size of less than 4 nm. This will not result if palladium is not properly dispersed in the membranes. FTIR and TGA characterization shows that 600°C is a good processing temperature for the Al<sub>2</sub>O<sub>3</sub> and Pd/alumina film to form stable structures. The surfactant and residual organics appeared to be completely removed and Al<sub>2</sub>O<sub>3</sub> network undergoes no further chemical changes.

### ACKNOWLEDGEMENT

The authors acknowledge the research grant provided by Universiti Sains Malaysia Penang that enables the production of this article.

### REFERENCES

- A.F.M. Leenars and A.J. Burggraaf (1985), "The Preparation and Characterization of Alumina Membranes with Ultrafine Pores", *Journal of Colloid and Interface Science* 105, 27-40.
- H.A. Rangwala and J.E. Taylor (1993), "High Temperature Separation of Hydrogen Using Novel Ceramic Membranes", Final Report, Alberta Research Council, Devon, Alberta.
- H.P. Hsieh (1996), "Inorganic Membranes for Separation and Reaction", *Membrane Science and Technology Series*, 3.
- J. Deng and Z. Cao and B. Zhou (1995), "Catalytic Dehydrogenation of Ethanol in a Metal-Modified Alumina Membrane Reactor", *Applied Catalysis A: General* 132, 9-20.

- K. Haas-Santo, M. Fichtner and K. Schubert (2001), "Preparation of Microstructure Compatible Porous Supports by Sol-Gel Synthesis for Catalyst Coating", *Applied Catalysis A: General* 220, 79-92.
- K.L. Yeung, J.M. Sebastian and A. Varma (1997), "Mesoporous Alumina Membranes: Synthesis Characterization, Thermal Stability and Nonuniform Distribution of Catalyst", *Journal of Membrane Sciences* 131, 9-28.
- K.S. Seshadri, M. Selvaraj, R. K. Moorthy, K. Varatharajan, M. P. Srinivasan and K.B Lal (2003), "Role of Binder in The synthesis of Titania Membrane", *Bull. Mater. Sci.*, vol. 26, No. 2, 221-225.
- M. Kajiwara, S. Uemiya, T. Kojima and E. Kikuchi (2000), "Hydrogen Permeation Properties through Composite Membranes of Platinum Supported on Porous Alumina", *Catalysis Today* 56, 65-73.
- Q.Fu, C.B. Cao, and H.S. Zhu (1999), "Preparation of Alumina Films From a New Sol-Gel Route", *Thin Solid Films* 348, 99-102.
- X.R. Huang, G.L. Meng, Z.T. Huang and J.M. Geng (1997), "Preparation of Unsupported Alumina Membrane by Sol-Gel Techniques", *Journal of Membranes Science* 133, 145-150.
- Y. Wu, Y. Zhang and L. Zhang (2004), "Effects of Finely Dispersed metallic palladium on microstructure and properties of nanocomposites produced by sol-gel technique", *China Particuology*, vol. 2, no. 1, 19-24.

### Contemporary Technologies for CO Reduction from Mobile and Stationary Sources

M.R. Othman, N.N.N. Mustafa and A.L. Ahmad  
School of Chemical Engineering  
Universiti Sains Malaysia, Engineering Campus,  
14300 Nibong Tebal,  
Seberang Perai Selatan,  
Pulau Pinang.

#### Abstract

Two-thirds of the carbon monoxide emissions come from the combustion of fossil fuels, with the largest contribution coming from mobile sources. The present technologies employed to control the emission of CO effectively include catalytic converters that convert CO to CO<sub>2</sub>, a more efficient combustion engine that can curb the CO emission from its exhaust system, the use of cleaner fuel such as compressed natural gas or liquefied petroleum gas in replacement for diesel, and the use of fuel cell in replacement for the current fossil fuel based combustion engine system. The use of fuel cell is the most favorable since the products constitute only electricity, water and moderate amount of heat. Nevertheless, fuel cell performance degrades substantially in the presence of CO in the H<sub>2</sub> feed stream. The objective of this paper is to highlight the importance of pt/pd ceramic membrane in increasing the performance of fuel cell and reducing the CO emission from mobile and stationary sources.

#### Keywords:

CO, Fuel cell, Pd membrane, Pt membrane, ceramics.

#### 1.0 Carbon Monoxide

Carbon Monoxide (CO) is a colorless, odorless, tasteless and poisonous gas produced through incomplete combustion of organic compounds such as wood coal, kerosene, gasoline, etc. In pristine atmosphere, the average concentration of CO is 0.1 ppm, which comes from natural sources, such as methane oxidation, forest fire, and oceanic microorganism production. Today, the concentration of CO in the atmosphere is increasing at an alarming level due to the frequent use of fossil fuel combustion by human to generate energy. CO is mass produced from leaking chimney in coal power plant and WGS reactor, back-drafting from kilns/furnaces, unvented kerosene and gas space heater, kerosene space heater, millions of personal automobile, or millions of individuals' cooking grills, gas stoves and cigarettes smoking.

Internal combustion engines from gasoline powered motor vehicles contribute approximately two-thirds of the CO in the atmosphere. Table 1 gives the composition of car exhaust gases from an Otto combustion engine. Even though CO comprises about 2% (by volume) from the total exhaust gases, emissions from millions of vehicles on the road has exacerbated the environmental problem.

Table 1: Average exhaust gas composition of an Otto engine.

Exhaust gases	Composition (vol %)
N <sub>2</sub>	74 %
CO <sub>2</sub>	12 %
H <sub>2</sub> O	10 %
CO	2 %
NO <sub>x</sub>	0.5 %
CH <sub>x</sub>	0.1 %
SO <sub>2</sub>	60 ppm (0.006 %)
H <sub>2</sub>	0.4
Pb, P, Si	Traces
O <sub>2</sub>	1.0 %

With the increasing public concern over the deterioration of air quality, regulatory bodies have made significant efforts towards improving vehicular emission standards. The air quality guidelines for CO legislated by Malaysia and United States are given in Table 2.

Table 2: Ambient Air Quality Standards, Malaysia & United States.

	Malaysia		United States	
	ppm	g/m3	ppm	g/m3
Carbon Monoxide(CO)	9	10	9	10
8-hr avg	30	35	35	40

1.1 *The health effects of Carbon Monoxide*

When human breathes air containing carbon monoxide, it is absorbed through the bloodstream and then the CO immediately displaces oxygen from the blood and bonds with the hemoglobin to form carboxyhemoglobin (COHB). CO can cause adverse health effect as minor as flu or the start of a cold, headache, dizziness, nausea and fatigue to as acute as severe headaches, mental confusion, vomiting, vision loss, hearing impairment and eventual unconsciousness. Continuous inhalation of CO can cause memory loss, permanent brain damage, coma and eventually death [1].

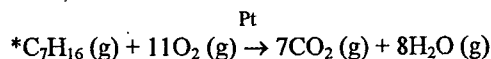
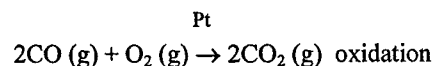
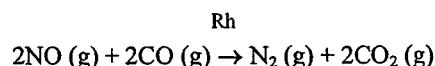
2. **Technology for CO Control**

2.1 *Catalytic Converters*

A catalytic converter is a device that is incorporated into the exhaust system of a car. Inside the converter is a ceramic or metallic substrate with an active coating incorporating alumina, ceria and other oxides and combinations of the precious metals - platinum, palladium and rhodium to convert CO to CO<sub>2</sub>. Since 1970's, CO emission level has been controlled using oxidation catalysts. The catalysts could reduce CO emission by up to 80% during that time. In the early 1980's, automakers introduced more sophisticated converters, plus on-board computer chips and oxygen sensors to help optimize the efficiency of the catalysts. In today's passenger cars, the catalysts are capable of reducing more than 90% carbon monoxide emitted by internal combustion engines over their lifetimes.

Palladium and platinum have been used as catalysts in the chemical and petroleum industries to promote the water-gas shift reaction and steam reforming reaction. Platinum combined with rhodium catalyze the oxidation of carbon monoxide (CO) and hydrocarbons (HC) to carbon dioxide (CO<sub>2</sub>) and water while at the same time reducing NO<sub>x</sub> to nitrogen.

Beside Pt and Pd, Rh is also used as a catalyst in the catalytic converter. The reaction that takes place in the converter can be summarized as follows:



\* C<sub>7</sub>H<sub>16</sub> (g) represents the unburnt hydrocarbon

2.2 *Improved internal combustion engine*

In year 2001 Malaysia planned to adopt the so-called Euro-1 standard on motorcycle smoke emissions in an attempt to curb air pollution. New two-stroke engine motorcycles that only emit up to eight grams of carbon monoxide per kilometer of usage (g/km), 4 g/km of hydrocarbon, and 0.1 g/km of nitrogen oxide were allowed to be manufactured or imported. For four-stroke engines, the allowable limit was 13 g/km of carbon monoxide, 3 g/km of hydrocarbon and 0.3 g/km of nitrogen oxide.

In order to accommodate the more stringent emission standard requirement, the two stroke engine motorcycle models will have to be improved either by improving the combustion process or fitting its exhaust systems with catalytic converters. Meanwhile, four-stroke models will need only slight modifications. The other strategies for helping motorcycle manufacturer to meet lower emissions limits from internal combustion engines include retrofitting catalytic converters and associated engine, improving the combustion process and fuel management, adding air injection or exhaust gas recycling and decreasing the time required for the catalytic converter to reach its full efficiency.

2.3 *Cleaner fossil fuel*

Malaysia has a larger natural gas reserve than its oil reserve. Natural gas is therefore, an attractive source of energy for its people. Recently, a study on motorcycles that used natural gas has been conducted. It was discovered that combustion from natural gas produced cleaner emissions and better performance at full load and top gear of 8500 rpm. Natural gas gave complete combustion with a decrease of 99.6% of carbon monoxide, 72.5% of unburned

hydrocarbon at a speed of 70 km/h. However, there were major setbacks associated with the use of natural gas in gasoline engines. First, the lower calorific value of natural gas burning velocity reduced engine power by at least 15% at maximum load. Second, the life span of the engine was shortened remarkably. Due to these setbacks, more research efforts have been initiated and focused on the use of compressed natural gas, liquefied petroleum gas, propane, oxygenated blends and other reformulated fuels, instead.

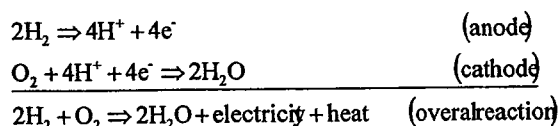
Another strategy to reduce CO pollution is by reducing the consumption on the fossil fuel itself. This can be achieved if the use of personal vehicles is discouraged, while the use of captive fleet vehicles such as LRT commuters, buses, taxis, and delivery vans is encouraged and promoted consistently.

#### 2.4 Fuel Cells

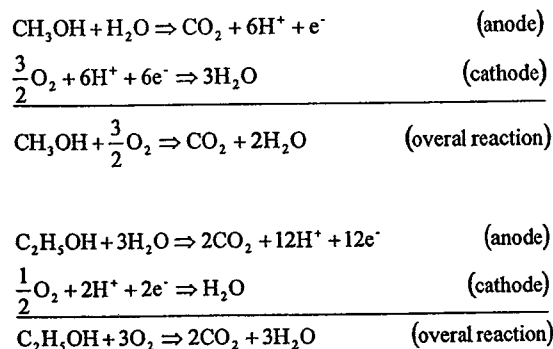
The Industrial Revolution in the nineteenth century and the popularity of automobiles utilizing oil-based combustion engine, which is more than a century old, pollutes both the local and the global environment, demonstrated a proclivity for convenience and a penchant for the creature comforts afforded by the technology. Since the advent of the wheel, man's interest in energy conservation has stoked the imaginations of leading scientists and inspired inventions both practical and bizarre. These advances have necessitated the need to identify affordable energy sources, without relying on fossil fuels and other non-renewable resources. Over the last half-century, the most promising alternative power source has been the fuel cell. Fuel cells have been used in spacecraft since 1960's. After the dwindling manufacturing cost of the cell, the technology can now be used for both electricity generating plants (stationary source) and exhaust free automobiles (mobile source).

A fuel cell is an electrochemical device that utilizes hydrogen and oxygen in the presence of catalysts to produce electricity, heat and water. A fuel cell generates current by transforming hydrogen gas into a mixture of hydrogen ions and electrons in the anode. The anions are transferred to the cathode through proton exchange membrane while the electrons are conducted to the current collector and a load to do work. Upon completing the circuit, electrons travel to the cathode and combine with oxygen and anions to produce water.

Fuel cells have received accolades with increasing interest among scholars, scientists and venture capitalists for many years, for they are able to accompany or perhaps, replace the combustion heat engines of the past and present. Several kinds of fuel cell already exist, some in the form of prototypes and others as niche products. Fuel cells in general are defined by the type of electrolyte used in the system. These include Proton Exchange Membrane Fuel Cell (PEMFC), Alkaline Fuel Cell (AFC), Phosphoric Acid Fuel Cell (PAFC), Molten Carbonate Fuel Cell (MCFC) and Solid Oxide Fuel Cell (SOFC). If hydrogen is used as fuel and supplied in the cathode and oxygen in the anode, the reaction scheme that takes place in the fuel cell system is as follows [2]:



Fuel cell is also defined by the type of fuel used, such as Direct Methanol Fuel Cell (DMFC) or Direct Alcohol Fuel Cell (DAFC). If methanol and alcohol are used as fuel respectively and supplied in the cathode and oxygen in the anode, the reaction scheme that takes place is as follows:



#### 3.0 Membrane technology

Recently, PEM fuel cells have become more cost effective for application under 25 kW than the other types of fuel cells and perform best when pure hydrogen is used as the fuel. However, when hydrogen containing CO, even in a very minute level of CO (as small as 100 parts per million) is fed into the

fuel cell, it causes serious poisoning to the surface of catalyst, blocking the sites that hydrogen needs for reactions. This has decreased the voltage drastically. CO has been known to exhibit strong tendency to adsorb and preferentially oxidize on the surface of the catalyst, eventually dwarfing the overall performance of the fuel cell. An ideally diffusive membrane layer, if used to improve the fuel cell performance, should be able to perform at least 2 functions simultaneously. First: to block CO from poisoning the catalyst, and second: to facilitate transport of only H<sub>2</sub> onto the catalyst surface in order to oxidize the fuel completely into electrons and protons in the anode side.

Presently, reliable high temperature membranes with the desired separation efficiency for hydrogen from gas mixtures are not available commercially. It only exists as a bench scale product for laboratory research. Historically, palladium membrane is used to catalyze dissociation/adsorption process of H<sub>2</sub> to H<sup>+</sup>. The H<sup>+</sup> diffuses readily into the membrane while the heavier CO molecules diffusion is hindered. Then, reassociation/desorption process of H<sup>+</sup> to H<sub>2</sub> takes place at the other side of the membrane. Although palladium has been used, platinum is also capable of catalyzing similar process and it performs at a faster rate. The use of platinum however, is limited by the economic factor due to the platinum price that is highly expensive.

#### 4.0 CO conversion and selectivity

The capacity of CO conversion and selectivity determines the effectiveness of the membrane being used in the fuel cell or other applications that requires elimination/reduction of CO from the exhaust stream. Currently, platinum and/or palladium have been found to tolerate CO and exhibit high selectivity for hydrogen. The use of these metals together with ceramic support can potentially block CO and other contaminants that exist with H<sub>2</sub> in order to generate higher fuel cell power.

In the previous work, high selectivity of CO oxidation over platinum on alumina ceramic was successfully achieved. Using 1% or less CO in the hydrogen rich fuel processor gas, the level was significantly reduced to only a few ppm of CO [3]. Figure 2 shows the activities of the catalyst as a function of temperature for a dry gas composition of 1% CO, 1% O<sub>2</sub>, 65% H<sub>2</sub> and a trace amount of He. The conversion of CO was a maximum at temperature of 170°C with 80% conversion. At this temperature, the selectivity was about 50% as shown in Figure 3.

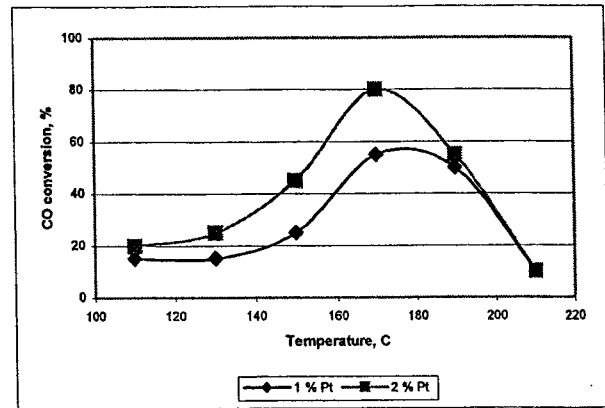


Figure 1: carbon monoxide conversion as a function of temperature for 1 and 2 % Pt on supported on Al<sub>2</sub>O<sub>3</sub>.

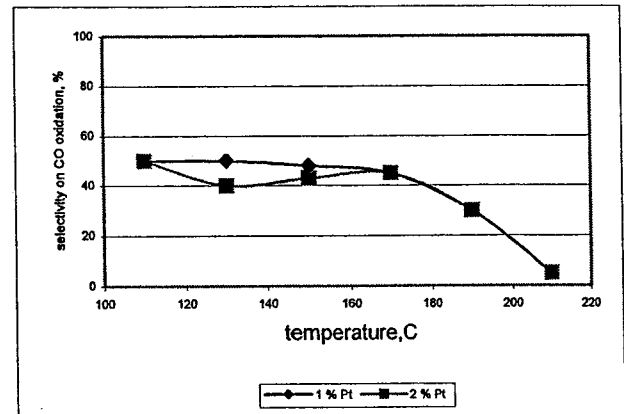


Figure 2: carbon monoxide selectivity as a function of temperature for 1 and 2 % Pt on supported on Al<sub>2</sub>O<sub>3</sub>.

#### CONCLUSION

Carbon monoxide is harmful and a very dangerous gas to human and living creatures. Most of CO that exists in the ambient air is derived either from the internal combustion engines in automobile or industries. The contemporary technology known to be able to eliminate CO completely from both mobile and the stationary sources is fuel cell. But, the performance of the fuel cell may be set back by the presence of CO in the hydrogen enriched feed stream. The use of pt/pd ceramic membrane can be effective in preventing CO from poisoning the catalysts in the fuel cell system. At the same time, the membrane can also be used to



JABATAN BENDAHARI  
UNIT KUMPULAN WANG AMANAH  
UNIVERSITI SAINS MALAYSIA  
KAMPUS KEJURUTERAAN  
SERI AMPANGAN  
PENYATA KUMPULAN WANG  
TEMPOH BERAKHIR 31/12/2006

DEV AND CHARACTERIZATION OF PLATINUM-PALLADIUM CERAMIC MEMBRANES FOR FUEL CELL

Tempoh Projek: 15/12/2004 - 14/11/2006

DR MOHD ROSLEE OTHMAN

304\_P/KIMIA\_6035128

JUMLAH GERAN:-

NO. PROJEK:-

PANEL:- JIFENDEK

PEVAJA:-

Yol

Peruntukan (a)	Perbelanjaan sehingga 31/12/2005 (b)	Tanggungan semasa 2006 (c)	Belanja Semasa 2006 (d)	Jum. Belanja 2006 (c + d)	Jumlah Belanja Tekumpul (b+c+d)	Baki Peruntukan Semasa 2006 (a-(b+c+d))
110006 GAJI KAKITANGAN AWAM	6,500.00	0.00	0.00	0.00	0.00	6,500.00
210006 PERBELANJAN PERJALANAN DAN SARA	2,100.00	0.00	0.00	0.00	0.00	2,100.00
230006 PERHUBUNGAN DAN UTILITI	200.00	0.00	0.00	0.00	0.00	200.00
260006 BAHAN MENTAH & BAHAN UNTUK PENYEL	7,692.00	0.00	0.00	0.00	0.00	7,692.00
270006 BEKALAN DAN ALAT PAKAI HABIS	1,492.00	9,330.10	0.00	5,299.00	14,629.10	(13,137.10)
290006 PENYELENGGARAAN & PEMBAIKAN KECIL	0.00	0.00	0.00	3,803.51	3,803.51	(3,803.51)
296006 PERKHIDMATAN IKHSAS & HOSPITALITI	1,000.00	160.00	0.00	391.00	551.00	449.00
	18,984.00	9,490.10	0.00	9,493.51	18,983.61	0.39
Jumlah Besar	18,984.00	9,490.10	0.00	9,493.51	18,983.61	0.39